

**Zeitschrift:** IABSE reports = Rapports AIPC = IVBH Berichte  
**Band:** 999 (1997)

**Rubrik:** Poster sessions

#### **Nutzungsbedingungen**

Die ETH-Bibliothek ist die Anbieterin der digitalisierten Zeitschriften auf E-Periodica. Sie besitzt keine Urheberrechte an den Zeitschriften und ist nicht verantwortlich für deren Inhalte. Die Rechte liegen in der Regel bei den Herausgebern beziehungsweise den externen Rechteinhabern. Das Veröffentlichen von Bildern in Print- und Online-Publikationen sowie auf Social Media-Kanälen oder Webseiten ist nur mit vorheriger Genehmigung der Rechteinhaber erlaubt. [Mehr erfahren](#)

#### **Conditions d'utilisation**

L'ETH Library est le fournisseur des revues numérisées. Elle ne détient aucun droit d'auteur sur les revues et n'est pas responsable de leur contenu. En règle générale, les droits sont détenus par les éditeurs ou les détenteurs de droits externes. La reproduction d'images dans des publications imprimées ou en ligne ainsi que sur des canaux de médias sociaux ou des sites web n'est autorisée qu'avec l'accord préalable des détenteurs des droits. [En savoir plus](#)

#### **Terms of use**

The ETH Library is the provider of the digitised journals. It does not own any copyrights to the journals and is not responsible for their content. The rights usually lie with the publishers or the external rights holders. Publishing images in print and online publications, as well as on social media channels or websites, is only permitted with the prior consent of the rights holders. [Find out more](#)

**Download PDF:** 16.01.2026

**ETH-Bibliothek Zürich, E-Periodica, <https://www.e-periodica.ch>**

## **Poster Sessions**

## A New Test for Stud Connectors in Ribbed Slabs

**P.G.F.J. (Pieter) VAN DER SANDEN**

Civil Engineer

Eindhoven University

Rosmalen, The Netherlands

**J.W.B. (Jan) STARK**

Professor of Steel Structures

Delft University

Rijswijk, The Netherlands

**H.H. (Bert) SNIJDER**

Professor of Steel Structures

Eindhoven University

Utrecht, The Netherlands

**H.W. (Wim) BENNENK**

Professor of Concrete Structures

Eindhoven University

Koudekerk aan den Rijn, The Netherlands

### Summary

A new push test was developed to investigate the behaviour of headed studs in ribbed slabs. The main reason was that the standard push tests are not suitable for the validation of numerical models. A series of tests with the new test set-up was carried out and evaluated. The test set-up and some test results are briefly described.

### 1. Introduction

The behaviour of a composite steel-concrete beam is essentially influenced by the properties of the longitudinal shear connection. In present practice the resistance of shear connectors placed in the ribs of composite slabs are related to the resistance of a connector in a solid slab by means of one reduction factor. It is now generally agreed that this method is not satisfactory.

A research project was started to develop a numerical model for the simulation of the behaviour of a headed stud connector in the rib of a composite slab. It appeared that in the standard Eurocode 4 push tests as normally used, the boundary conditions were not unique. Therefore, a new push test suitable for the validation of the numerical model, was developed.

### 2. Tests: specimens, measurements and results

Contrary to the standard test procedure just one rib was tested (see Fig. 1). All loads and boundary conditions were carefully monitored. This included all support reactions (see Fig. 1), the internal forces in the stud ( $N_z$ ,  $M_x$  and  $M_z$ ) and the difference between the displacements of the concrete rib and the foot of the stud. This is essential for the validation of numerical models.

In total 22 tests were carried out. The parameters which were varied are: the steel sheeting (with and without sheet, with and without embossments, 'thin' and 'thick' sheet), the geometry of the

rib, the place of the stud within the rib, the welding technique (through deck welded stud and stud placed in a precut hole in the sheet), the concrete strength and the hogging reinforcement.

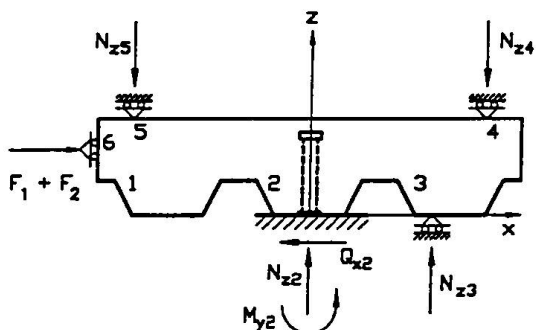


Fig. 1 New test set-up

Most results confirmed the general behaviour known from standard push tests as described in Eurocode 4. Also, new ideas were gained which resulted in an improved insight in the behaviour. It appeared that the steel sheeting had a significant influence on the behaviour. As well a larger thickness of the sheet as the presence of embossments increased the failure load. Both the failure modes 'tension shear failure of the stud' and 'concrete cone' were observed.

Analyzing all results some postulations about the behaviour could be made. One of them is that, for through deck welded studs, the behaviour for both failure modes is initially the same. At the moment that a crack originated at the rear side of the stud the behaviour became different, which finally resulted in a completely different failure mode.

Normally it is accepted that through deck welded studs in comparison with studs in precut holes, have higher failure loads. The new push test showed the contrary. This is probably caused by the fact that the concrete in front of the stud is completely restrained. For this reason it was found that the behaviour was quite different, although the failure mode is finally the same.

Although perhaps obvious, at small slip the headed stud connection transferred the load by stud bending and by a couple of normal forces: one in the stud and one in the rib at the rear side of the stud. The test results showed that, prior to the occurrence of the maximum shear load, the full plastic moment of the stud was exceeded. Besides the plastic deformations of the stud, other non-linear phenomena were observed: buckling of the sheet, cracking of the concrete, crushing of the concrete, punching of the stud through the concrete, sliding of the concrete over the sheet and plastic deformations of the sheet caused by riding over. Most of them occurred at small slip already.

### 3. Conclusions

The results of the new push test are suitable for the validation of numerical models. The numerical model should be able to take complicated non-linear phenomena as described into account. Once the numerical model is able to predict the behaviour of the new push test, a powerful tool is available to determine design formulae for composite beams.

### 4. References

Van der Sanden, P.G.F.J., 'The behaviour of a headed stud connection in a 'new' push test including a ribbed slab.' Tests: Main report, BKO-report 95-15 and Tests: Background report, BKO-report 95-16. Eindhoven University of Technology, March 1996.

The test results included: the shear force-slip relation, the load at first cracking of concrete, the place of the first crack (front side or rear side of the stud) and the failure mode. Material properties of the stud, the sheet and the concrete were determined.

## Connection Characteristics for Joints between Hollow Core Slabs and Slim Floor Beams

**Matti V. LESKELÄ**  
Ph.D. (Civ.Eng.)  
University of Oulu  
Oulu, FINLAND

Matti Leskelä, born 1945, received his PhD in 1986 and has been carrying out research into composite structures from the early 1980's. His latest work has concerned problems of partial interaction and various shear connections in composite structures such as slim floors, composite slabs and concrete filled steel tubes.

### Summary

Hollow core slabs become part of a composite flooring when they are supported on beams. When slabs are integrated with slim floor beams, a system of multiple longitudinal shear interfaces will form in which the webs of the hollow core slabs also become a shear interface. The load-slip characteristics of the connection interfaces are described so as to give an impression of their role in finite element modelling, and their typical behaviour as observed in the calculation is explained.

### 1. Introduction

In slim floor structures, hollow core slabs (HC slabs for short) supported on beams inevitably become a part of a composite system when grouted joints are used. Although it is a conservative assumption to neglect this interaction in beam design, it should be allowed for when designing the slabs, as it has been shown by experimental and theoretical research that the vertical shear resistance of the slabs is considerably reduced as compared with the maximum resistance of the slabs on non-flexible supports. The real structural system includes various longitudinal shear interfaces with highly non-linear characteristics, and the stiffness of the joints will decrease considerably during loading of the system, causing then a reduction in the composite interaction rate.

#### 1.1 Discretization into layered beam elements

In order to discretize a typical system, as in Fig. 1, into beam elements, four layers of elements are required, which should be connected appropriately by coupling elements that model the behaviour of the shear interfaces (i1) to (i4), as described below.

#### 1.2 Description of interfaces

Shear interfaces develop mainly through balancing of the longitudinal normal forces due to the bending moment in the composite cross-section, the forces to be balanced being the compressive force at the top hulls of the HC slabs, which serve as flanges to the beam, and the tensile force at the beam section. The behaviour of the top hulls of the HC slabs is similar to that of the concrete slab in contemporary composite beams, but the method of transferring the compressive force to the beam is more complex. With reference to Fig. 1, the interfaces to be distinguished are: (i1) concrete bonding to the concrete or steel surface, (i2) connection of a reinforced or unreinforced top concrete layer to the beam through a cracked or uncracked vertical interface, (i3) connection between the top and bottom hulls of

the slab units, and (i4) connection of the bottom hulls of the HC slabs to the beam. The problems arising due to the composite behaviour are related to the forces transferred through interface (i3), in which the web ribs of the slabs serve as shear connectors between the hulls.

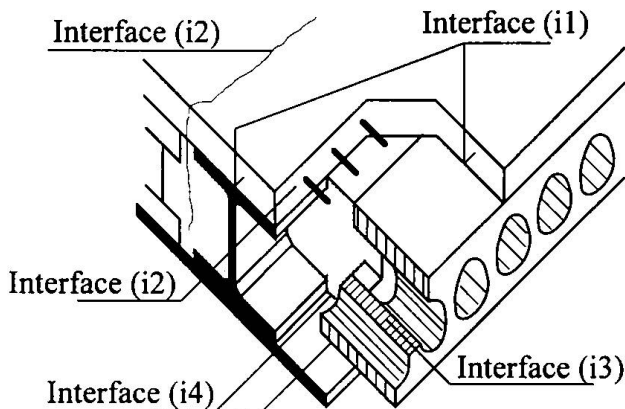


*Fig. 1 General view of the various longitudinal shear interfaces activated in a slim floor in which HC slabs are integrated in the system*

## 2. Connection characteristics

It is evident from Fig. 1 that if interface (i2) is inefficient, the majority of the force transfer from the top hull of the slab to the beam body must happen through (i3). This is always the case in structures with no reinforcement at interface (i2). The deformability of the system may be described in terms of the load-slip properties of the shear interfaces, of which (i1) and (i3) are characterized as non-ductile in the sense that the load drops considerably after the peak load is reached, and the slip required for reaching the peak load is quite small, normally much less than 1 mm. Independent of any transverse reinforcement at interface (i2), it should be characterized as ductile, as no sudden unloading will normally occur, and the same is also valid for (i4). The non-ductility of interface (i3) is critically reflected in the ability of the decking to bear loads, as a failure in the webs normally means collapse of the whole slab.

### 2.1 Methods to enhance behaviour of slabs

The considerable reduction in the vertical shear resistance of HC slabs is attributable to the transverse shear stresses in their webs, and any effective means of reinforcing the slabs must reduce the transverse shear stresses [1]. There are two methods for doing this, re-routing of the longitudinal shear forces and strengthening of the critical interface (i3). The practical importance of these measures is well demonstrated by the parametric studies carried out by finite element calculations, in that reinforcement of the top concrete across the beam normally means an enhancement of some 20 to 30 % and filling of the voids at the slab ends to a length equal to the depth of the voids approximately the same degree of improvement.

## 3. Reference

[1] Leskelä, M.V. and Pajari, M., "Reduction of the Vertical Shear Resistance in Hollow Core Slabs when Supported on Beams". Concrete 95, Conference Papers, Volume One, CIA and FIP (559-568), Brisbane, Australia 1995

## Interlayer Bond Deterioration under Repeated Shear Load

Non-reinforced interlayer connections in an interlayered concrete composite slab under repeated shear load

**Ludovit NASCH**  
Principal R.W., Civil Eng.  
USTARCH - SAV  
Bratislava, Slovak Republic



Ludovit Nasch, born 1938, received his civil engineering degree in 1962 from the Slovak Technical University (SVST), and his CSc. in 1978 from the Slovak Academy of Sciences, where he works at the Institute of Construction and Architecture (USTARCH) in the department of mechanics.

### Summary

Non-reinforced interlayer connections, as they are known from the concrete composite elements, has been investigated experimentally under both, monotone increasing and repeated loading. The purpose of our research was not only to obtain the limiting stress values (or the respective interlayer displacements) at the rupture, but also to investigate the energy dissipation during the whole process of interlayer bond deterioration. Due to the repeated loading *the quick data acquisition and storing technique* has been used.

### 1. Specimens, loading, experimental set-up, and instrumentation

In this part of the research project made at the Institute of Construction and Architecture of the Slovak Academy of Sciences, two families of specimen, (Figure 1), were experimentally analysed under both, monotone and repeated loading. The first of the families (where the overall breaking mechanism was aimed at) comprise the full size 1200 x (70+170) x 6000 mm, (breadth x thickness x length) specimens based on the precast, prestressed wide planks KAPPA, produced by the ZIPP Ltd. - Bratislava. The second family of which only we will speak further, consists of the smaller size 200 x 200 x 600 mm three layer specimens, where the importance of such parameters as the interface roughness, the normal stress intensity, the cube strength, and the workability of the concrete, changes of the concrete mix, etc., to the overall behaviour of the interlayer connection can be investigated more readily. The surface roughness *left-as-vibrated, roughened by the sheep-leg roller* (as used for the KAPPA planks), and *trawled by the wooden lath trowel*, and three levels of the normal stress intensity (*0,0; 0,1; and 0,4 MPa*) has been chosen for analysis. The Hydopuls - Schenck loading apparatus was used to load the specimen placed appropriately between the upper cross beam and the loading piston of the loading machine. Both loading types were displacement controlled; *the monotone increasing load* by the constant loading piston velocity of 1/100 mm per second, and *the repeated loading* by the sinusoidal motion of the loading piston. Up to  $2,0 \times 10^6$  loading cycles with the 14 Hz frequency were imposed on the specimen. The piston's lower and upper position were so adjusted, to have

the upper loading force at the required level, and the lower value of the loading force to be approx. 10 or 15 kN. Altogether nine IWT 302 inductive gauges were used to measure changes of the length base across the interlayer connection, (channels 1-4), the vertical interlayer slip, (channels 6-9), and the loading piston position, (channel 10). The loading force intensity was acquired from the channel 5.

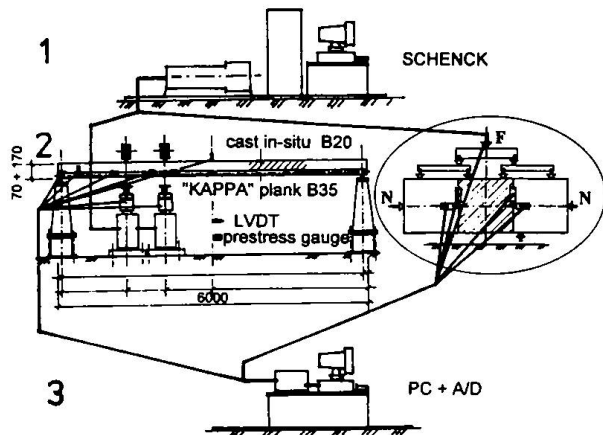


Figure 1

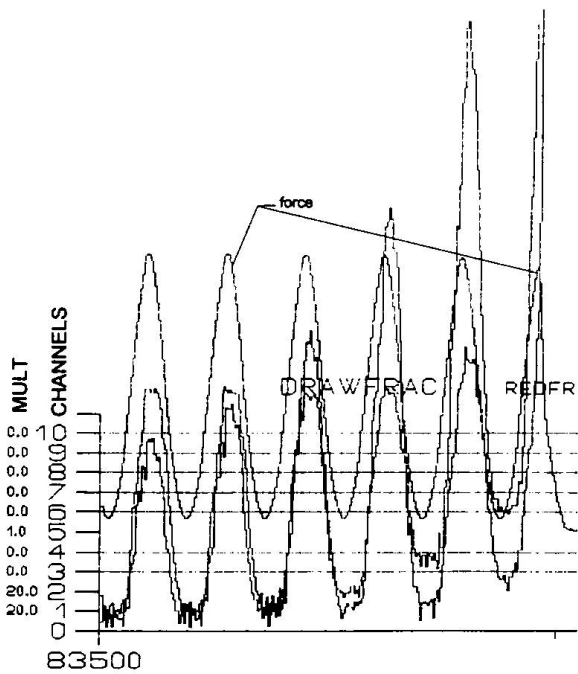


Figure 2

interlayer *adhesion* only, (accounted for in the fracture mechanics), but also the *mechanical interlock* due to the surface roughness, and the *friction* due to the normal stress intensity, together with the manufacturing conditions, play the main, if not the decisive role.

#### References

1. Nasch, L.: Behaviour of interlayer connections between the old and new concrete. In: Proceedings of the First Slovak Conference on Concrete Structures, STU, Bratislava, Sept. 1994, pp. 100 - 107.

**Acknowledgement** The financial support of the VEGA, grant No. 2 / 1264, is gratefully acknowledged.

## 2. Results and discussion

On the Figure 2 we can see selected primary data as acquired during the last 6 cycles (from approx. 14000) before final rupture of the second interlayer connection of the 25/VI three layer specimen (surface roughness *left as vibrated*, and  $\sigma_n = 0,4$  MPa). The whole experiment has been scanned with the sampling frequency of 600 Hz, and so the vertical line segments creating any of the depicted curves are, in this case, the 1/600 sec. apart. Length between the numbered ticks on the vertical axis equals 1/100 mm for the displacements, and 20kN for the loading force. We can see (alike the data for different normal stress, and interface roughness, and monotone load, published elsewhere, [1] ) the significant increase of the measured displacements in the pre-critical part of the diagrammed data. There is an increase of displacements across the connection plane between 12 and 13  $\times 10^{-2}$  mm for the last 100 cycles, (6 to  $10 \times 10^{-2}$  mm for the last 10 cycles) without any significant loss of the connection's stiffness, as well as the energy accumulated during the loading phase. It should be reminded at this place, that the crack opening of about 1/100 mm is discernible by the naked eye. On the ground of the experimental evidence could be stated, that not the

## Connection of New and Old Concrete with Bonded Reinforcement Bars

Dr. Erich K.R. WISSE

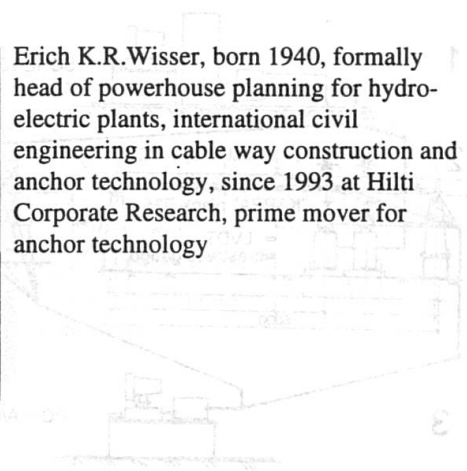
Dr. techn., Struct. Civil Eng.

Hilti Corporation

Schaan, Princ. of Liechtenstein



Erich K.R. Wissner, born 1940, formerly head of powerhouse planning for hydroelectric plants, international civil engineering in cable way construction and anchor technology, since 1993 at Hilti Corporate Research, prime mover for anchor technology



### Summary

In most cases connection of new and old concrete is performed by extending the reinforcement, often by means of post-installed bonded bars. New systems suitable of use on site have been developed, tested and introduced worldwide by Hilti Demolition and Fastening Technology, based on Eurocode 2, Design of Concrete Structures. Now engineers have a tested method to solve such problems as bridge renovation, retrofitting of industrial buildings, enhancement of earthquake resistance, etc.

### 1. Background Information

To get a monolithic behaviour of concrete structures cast in several parts it is necessary to establish continuity of the existing reinforcing. This can be accomplished either through cast-in-place starter bars or much more often by means of post-installed bonded rebars. Design rules for this applications have not been available up to now.

### 2. New connection systems

Following observation of jobsite working methods and on basis of experience with adhesive products, two connection systems were developed:

#### 2.1 Rebar connection with HIT-HY 150

A hole is drilled close to a cast-in rebar and cleaned of dust. Adhesive is injected from the back of the hole to the surface using a dispenser. The rebar is then inserted. Owing to the thixotropic formulation of the adhesive, rod insertion can be accomplished vertically downwards, horizontally or vertically upwards.

As a hybrid system, the adhesive HY-150 combines the benefits of resins (fluidity, fast curing, strong compound) with those of cements (insensitive to humidity, post-hardening, heat-resistant) and exhibits the same behaviour as cast-in rebars.

## 2.2 Rebar connections with HVU

A hole is drilled close to a cast-in rebar and cleaned of dust. A foil cartridge is inserted in the hole and the rod driven through the cartridge with a hammer drill. This modern resin gains full load capacity in a shorter time, also at temperatures lower than 0°C, has a matrix of high compression strength and shows no creep.

### 3. Design Concept for Rebar Connections

In cooperation with Prof. Marti [4] design rules were elaborated based on the safety concept of Eurocode 2 [1] and three failure modes:

- Limit of rebar utilisation
- Limit of adhesive bond utilisation
- Limit of concrete bond utilisation

The basic anchorage length (steel fully utilised) derived from tests ([2], [3]) corresponds with the European codes. Also, the splice length in beams show good conformity, given that the appropriate application-specific rules of EC2 are applied to the basic anchorage length (fig. 2).

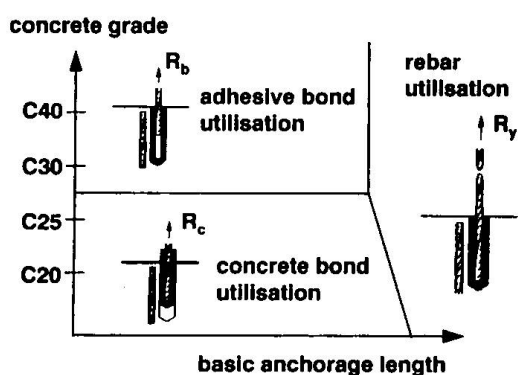


*Fig. 1 Design Concept*

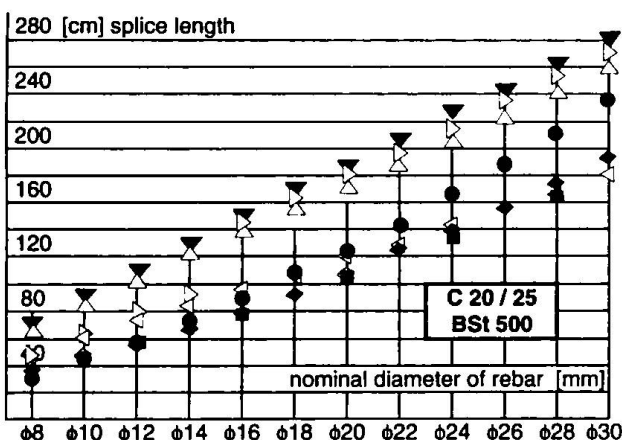


Fig. 2 Comparison of splice length in a beam at different European codes

	EU	GB	D	A	CH	HIT-	
	EC 2	BS	DIN	ÖN B	SIA	HY	HVU
		8110	1045	4200	162	150	
	▼	△	▷	◆	◀	●	■
φ8	75	69	52	37	48	30	[cm]
φ10	94	86	66	46	60	44	
φ12	113	103	79	55	72	58	58
φ14	132	120	92	65	84	74	
φ16	150	138	144	78	96	88	78
φ18	169	155	162	91	108	108	
φ20	188	172	180	106	120	122	104
φ22	207	189	198	121	132	144	
φ24	226	206	216	138	144	166	132
φ26	244	224	235	155	156	188	
φ28	263	241	253	173	168	212	164
φ30	282	258	271	192	180	236	[cm]

The pull-out and beam tests verify that the two systems HIT-HY150 and HVU, result in a load-slip relationship nearly identical with that of cast-in-place reinforcing bars. For this reason they are ideally suited for the connection of new with old concrete.

- [1] ENV 1992-1-1, Eurocode 2: Design of Concrete Structures
- [2] Marti P.: Anchoring Concrete Reinforcement using Hilti HIT-HY150, Report no. 93.327-1, 1993
- [3] Marti P.: Anchoring Concrete Reinforcement using HVU, Report no. 93.327-2 and 3
- [4] Hilti: Rebar Fastening Guide, Fastening Technology Manual B2.2, 1994

## A Design Method for Glass-Adhesive-Glass Composite Structural Elements

**Andrew PYE**  
 Postgraduate Civil Engineer  
 University of Bath  
 Bath, UK

Andrew Pye, Born 1972, 1995  
 gained a first degree in civil  
 engineering at the University of  
 Bath, 1996 postgraduate engineer  
 in the School of Architecture and  
 Civil Engineering at the University  
 of Bath. Researches into bonded glass  
 in load bearing structures.

**Dr Stephen LEDBETTER**  
 Director  
 Centre for Window and Cladding Techn.  
 Bath, UK

Stephen Ledbetter, Born 1953,  
 gained a first degree in civil engineering  
 at Dundee University and a doctorate  
 at Bristol University, appointed Director  
 of CWCT 1990. Researches into  
 all aspects of cladding and the building  
 envelope.

### Summary

The use of architectural glass in long span or high load applications is limited by the slenderness of glass plates which leads to excessive deflection. However, by using composite glass-adhesive-glass beam sections it is possible to carry greater loads, over longer spans with less deflection, Pye and Ledbetter (1997). This paper outlines current work at the University of Bath that will enable the quantitative design of T-beams fabricated from flat plates of toughened glass with a thin adhesive joint at the web-flange interface.

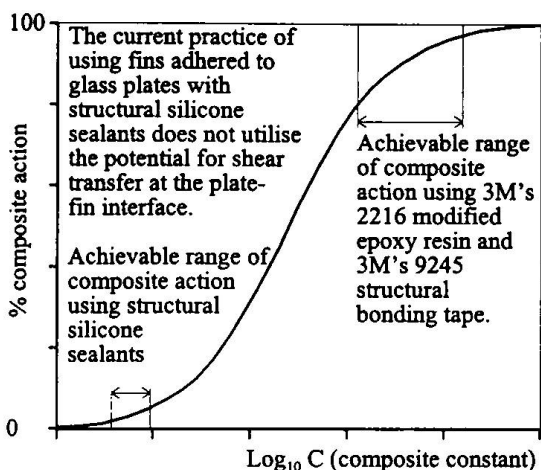
### Composite Model

The authors have developed an expression which describes the behaviour of a thick-thin-thick composite with a flexible core, Equation (1). This demonstrates that the current practice of using fins to strengthen glass plates does not utilise the shear transfer at the plate-fin interface, Figure 1. It also demonstrates the increased degree of composite action which is possible using the adhesives that have been selected for this work. These are 3M 2216 B/A grey epoxy adhesive and 3M structural bonding tape 9245. The first is a flexible, two part, room temperature curing structural adhesive. The second is a new material that is applied as a tape and is heat cured to develop structural strength.

$$S_0 \frac{d^4 y}{dx^4} - CS_1 \frac{d^2 y}{dx^2} = \frac{d^2 M}{dx^2} - CM \quad (1)$$

$S_0$  is the stiffness of the equivalent layered section  
 $S_1$  is the stiffness of the equivalent monolithic section  
 $x$  is the distance along the beam  
 $y$  is the deflection perpendicular to the span  
 $C$  is the composite constant  
 $M$  is the moment

The degree of composite behaviour is controlled by the composite constant, C, which is a function of the adhesive shear modulus, glass Young's modulus and the cross section geometry. However, in most practical designs it is the choice of the core material and joint dimensions that offers the greatest scope for improving composite action.



$$\text{percentage composite action} = \frac{\delta_C - \delta_L}{\delta_M - \delta_L} \times 100$$

$\delta_C$  deflection of the composite section  
 $\delta_L$  deflection of the equivalent layered section  
 $\delta_M$  deflection of the equivalent monolithic section

*Figure 1 Comparing the performance of a glass-adhesive-glass T-beam constructed using a structural silicone sealant and a modified epoxy resin. Based upon equation (1).*

## Failure Mechanisms

The failure of a glass T-beam may be by one of the five mechanisms listed in Table 1. After having determined and appropriately factored the necessary loads and material properties, the occurrence of each mechanism must be checked

In addition to the composite failure mechanisms the glass may also fail because of very localised high stresses such as those generated by a stone impacting upon the glass. Fortunately it is possible to design against these types of failures by either over-designing the glass plates or by introducing a sacrificial layer.

A potential problem in assessing the performance of wide-flanged beams is that the full width of the flange does not work compositely with the web because of shear lag effects. By strain gauging the flange during physical testing the authors have quantified this behaviour and shown that it would be possible to approach the problem by determining an effective width as is currently practised with steel and concrete structures.

### Failure Mechanism

Glass bending failure

Glass shear failure

Lateral torsional buckling

Adhesive shear failure

Adhesive tensile failure/glass plucking failure

### Assessment

- Equation (1) may be developed to yield the maximum tensile glass stress and while this is below the surface compression of the toughened glass failure will not occur.
- The maximum shear stress may be determined in the same manner as steel sections. This must be less than the shear capacity of the glass. However, initial results from a series of punching shear tests conducted to determine the shear capacity of glass indicate that a glass shear failure is unlikely in most realistic support conditions.
- The distribution of compression stresses must be such that the section is stable. It is possible to design to a reduced moment capacity by considering the slenderness of the beam, position of restraints and distribution of load. Assessing the reduced capacity has been based upon a combination of physical testing and finite element modelling.
- This is dependent upon the ability of the adhesive to yield and redistribute stresses. It is also sensitive to the rate of loading. Difficulties arise in quantifying the complex elasto-plastic behaviour. Current work is based upon a combination of physical testing and finite element modelling.
- There may be a cohesive failure which is a function of the adhesive, an adhesive failure which is a function of the adhesive and the primer or a plucking failure which is a function of the glass. All of these mechanisms may be easily prevented by suitable joint detailing and increasing the adhesive contact area..

*Table 1 A summary of the failure mechanisms of glass-adhesive-glass T-beams.*

## Conclusion

It is possible to predict the performance of composite glass-adhesive-glass T-beams and by applying a similar methodology it would be possible to assess the performance of other sections such as I's,  $\pi$ 's and boxes. However, the current process of determining critical stresses is complex and would need to be presented in a simplified manner if it were to be used in practice.

## References

Pye, A, and Ledbetter, S, (1997), 'The engineering of composite glass beams', ICBEST - 97, Bath.

## Monotonic Behaviour of Fastening Systems for Sandwich Panels

**Federico M. MAZZOLANI**  
Full Professor of Struct. Eng.  
University of Naples  
Naples, Italy

**Gianfranco DE MATTEIS**  
PhD Student of Struct. Eng.  
University of Naples  
Naples, Italy

**Raffaele LANDOLFO**  
Research Assistant, PhD  
University of Naples  
Naples, Italy

### Summary

The influence of connecting system on the structural behaviour of sandwich diaphragms in pin-jointed steel frames is investigated in this paper. The importance of connections on the global response of the whole system has been evidenced through experimental as well as numerical analyses. Detailed tests on different sandwich panel connection typologies allow to set up an analytical model able to predict their monotonic performance. Such a model is useful to characterise the behaviour of connection when accurate global non-linear analyses are required.

### 1. Introduction

Light-weight curtain wall systems are more and more used in both industrial and civil buildings, where they can cooperate with the steel skeleton, giving rise to a composite action like a diaphragm action. Nowadays, the interest is therefore concentrated in the evaluation of their contributing effect on the structural behaviour of the building. Depending on the adopted connecting system, such panels may, in fact, provide a remarkable increasing of both lateral stiffness and ultimate strength of bearing steel frames subjected to horizontal loads. The linear analysis for infilled frames, as it is suggested in the present code (EC3-Part 1.3), allows to take account for the skin effect in terms of both strength and initial stiffness. Nevertheless, it does not allow to assess the actual ductility resources of the system as well as its dissipative capacities. The interaction between steel cladding panels and structural framing system has been analysed within a general research project, sponsored by ECSC and developed through the cooperation between University of Naples and Italian Consortium CREA. With regards to the sandwich panels, experimental, theoretical and numerical activities have been performed [1].

### 2. The influence of connecting systems

Numerical as well as full-scale experimental analyses on different sandwich panel typologies connected each other and to the external frame by means of different kinds of connecting systems have emphasised that the contribution of the connections to shear flexibility of the panel is generally prevalent and plays a fundamental rule on the overall behaviour of infilled frames [1,2]. In addition, it has been shown that the actual behaviour of shear diaphragms, as the shear load increases, is more and more non-linear, depending on the behaviour of the adopted connecting system, being the major source of non-linearity just concentrated in connection elements. In order to develop an accurate analysis, the complete shear load-lateral displacement relationship should be therefore determined. The aim can be pursued by means of adequate non linear numerical tools. The proper structural characterisation of connections becomes therefore the starting point for the correct interpretation of the response of steel shear walls.

### 3. The behaviour of connections

The actual behaviour of connecting systems has been investigated by means of experimental tests [3,4]. Sandwich panels with trapezoidal, embossed as well as plane external sheets has been tested. Besides, a special panel with an internal steel reinforcing profile has been considered. The analysis have concerned both panel-to-panel connections and panel-to-external frame connections. With reference to the former, screwed connections and bonded connections, using glue and biadhesive bands has been analysed. Riveted and welded connections have not been taken into account. The *riveted connections*, in fact, have not a good behaviour under cyclic loads because they present a brittle mechanism of fracture, while the *welded* ones are not applicable owing to the very thin thickness of panel sheets.

The collapse mechanisms have found obviously to be strictly related to the connection typology. As regard to *screwed connections*, the sheeting resistance is demonstrated as the weak point of the joint, being the collapse always characterised by a large holeovalisation. The connection for corrugated sheets have shown a bad performance due the impossibility to connect both sheets on the two sides. On the contrary it is to emphasise the good behaviour of reinforced panel connections which allow to rely on both strong resistance and stiffness.

As far as *bonded connections* are concerned, the collapse phenomenon has been characterised by the slipping between the two opposite parts of the specimens, which follows a more or less sudden disjunction. In particular the connections with *biadhesive band* has provided a too low ultimate load, which makes the good ductility qualities useless. The *glued* bonded connections has instead shown a good ultimate strength value, joined to a very high brittle behaviour.

Based on the previous experimental results, two panel typologies have been selected for testing panel-to-external frame connecting system: the embossed sheet one and the flat sheet with reinforcing cold-formed profile. As far as connecting system typologies are concerned, only screwed connections using self-tapping screws have been considered.

The collapse of connection was characterised by a large holeovalisation, with bearing and tearing of the sheets. The maximum load value is found to be strictly depended on the number of resisting sheets, as well as on their thickness. The corresponding load-slip curves are typical for this failure mechanism, showing the great displacement capacity as consequence of sheet holeovalisation.

### 4. Further development

In order to develop accurate global non-linear analyses contemplating the diaphragm effect of sandwich claddings, a mechanical model able to predict the monotonic behaviour of connection typologies should be set up. Such a model could be based upon mechanical properties of connections as pointed out from experimental test results and generalised by using a simple appropriate analytical formulations.

### References

- [1] Mazzolani, G. De Matteis, R. Landolfo: "The stiffening effect of cladding panels on steel buildings: the ECSC research project in progress", in Proceedings of European Workshop on Thin-Walled Structures, Krzyzowa, Poland, September 1996.
- [2] Mazzolani, G. De Matteis, R. Landolfo: "On the shear flexibility of corrugated shear panels" STEEL STRUCTURES, Journal of Singapore Structural Steel Society, December 1995.
- [3] F.M Mazzolani, G. De Matteis, R. Landolfo: "Shear tests on sandwich panel connections" - Cost C.1 Workshop, Praga, October, 1994.
- [4] Mazzolani, R. Delponte, G. De Matteis, R. Landolfo: "Experimental analysis on sandwich panel-to-external frame connecting systems", 4th Cost - C1 Seismic Working Group Meeting , Anacapri (NA), 5-6 ottobre 1995.

## Long Term Behaviour of Composite Concrete Structures

**Olivier BERNARD**

Research Engineer

Swiss Fed. Inst. of Technology

Lausanne, Switzerland

**Eugen BRÜHWILER**

Professor

Swiss Fed. Inst. of Technology

Lausanne, Switzerland

### Summary

The numerical simulation of the widened Javroz bridge deck demonstrates that it is essential to consider the early age behaviour of the composite deck consisting of new and old concrete layers. Actually, internal stresses mainly due to restraint of thermal shrinkage may decrease the strength of these hybrid structural elements and affect their durability. The most effective measure to limit the early age damage is to decrease the maximum temperature of the new concrete during hydration by a system of cooling pipes.

### 1. Introduction

The 45 year-old Javroz bridge in Switzerland, a 170m long concrete arch bridge spanning 90m, will be improved to account for future traffic needs. The existing deck slab will be modified by an additional concrete layer and larger cantilever slabs (fig.1). The challenge being to restore a service life comparable to that of a new structure. The long term behaviour and thus the durability of the modified slab must therefore be studied by considering the composite action of the new section consisting of two concrete layers of different ages.

According to [1], the adherence between old and new concrete layers decreases continuously, and the hybrid system may fail after 17 - 20 years of service. This can be explained by the fact that the influence of the early age behaviour of the new concrete is usually disregarded, and the only criterion considered is the short term adhesive strength between the two materials.

### 2. Description of the domain studied

During the lifespan of hybrid structural elements, three stages can be distinguished (fig.2). First, during *hardening of the new layer*, the effects of cement hydration must be considered to determine the internal stress state mainly due to restraint of thermal shrinkage caused by the old concrete support. These internal stresses are at the origin of cracking of the new concrete layer which may affect strength and durability. To evaluate this effect, the *initial damage coefficient*

$\alpha$  can be defined as  $\alpha = \left( 1 - \frac{\text{resid. strength}}{\text{init. strength}} \right)$  ; small reduction of  $\alpha$  (curve  $\alpha_2 < \alpha_1$ ) leads to

a significant extension of lifespan. Secondly, during *service life*, effects of temperature variation as well as dynamic and fatigue action due to traffic loading are superimposed to the initial stress state and play a major role in damage propagation. Finally, *failure* of the hybrid system is determined according to ultimate state criteria.

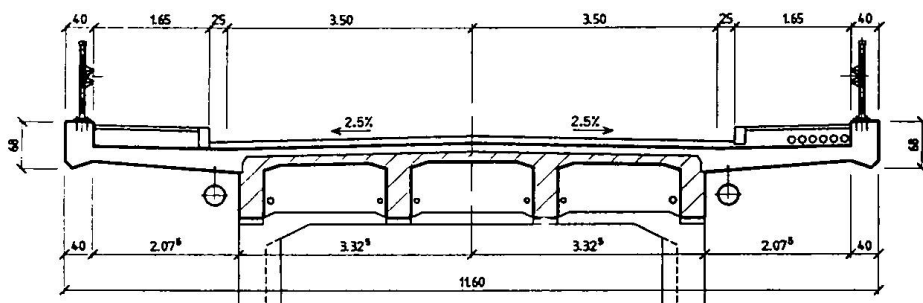


Fig. 1 Cross section of the widened Javroz bridge deck

### 3. Analysis of early age behaviour of a hybrid concrete bridge deck

The early age behaviour of the modified bridge deck is analysed by a numerical study [2]. The initial stress state and the likelihood of crack formation are determined [3], taking into consideration both the hydration heat release and variable environmental conditions.

For three different construction sequences, the initial state of internal stresses is obtained in terms of parameters such as cement content, temperature of fresh concrete, duration of cure, thickness and modulus of elasticity of the new concrete. The results show that reducing the cement content by 50 kg/m<sup>3</sup> has the same effect of avoiding early age damage of the hybrid deck as pouring of fresh concrete the temperature of which has been lowered by 5°C. The most effective measure is to decrease the maximum temperature of the new concrete during hydration. Numerical simulation shows that a system of pipes for cooling water placed in the new concrete layer allows for sufficient temperature decrease to reduce significantly internal stresses (fig.3). Without specific measures, the coefficient  $\alpha$  is 0,75 600 hours after pouring the new concrete. Comparatively, with the use of cooling pipes in the young concrete, this coefficient is reduced to 0,30.

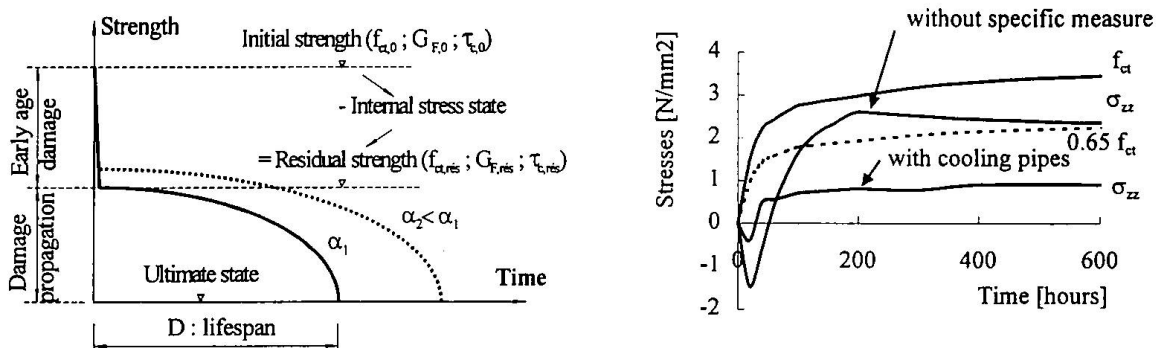


Fig. 2 Damage curve of composite concrete structures

Fig. 3 Evolution of out of plane stress  $\sigma_{zz}$  in the cantilever slab versus tensile strength  $f_{ct}$

#### References :

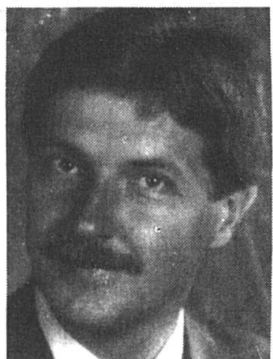
- [1] Wittmann F.H., Proceedings of the 2<sup>nd</sup> Bolomey Workshop on Adherence of Young on Old Concrete, Sion, Aedificatio Publishers, 1994.
- [2] Bernard O., Brühwiler E., Comportement au jeune âge du tablier formé de vieux et de nouveau béton - Remise en état et élargissement du pont sur le Javroz, EPFL-MCS Report n° 95.36.01, Lausanne, December 1996.
- [3] Intron SME, Module MES/2.5D of Finite Element Modules for Materials Science and Structural Engineering, User's manual - version 3.0, Yverdon, Switzerland, 1995.

## Health and Safety Monitoring of Composite Structures

Helmut WENZEL

Dr.-Ing.

Vienna Consulting Eng.  
Vienna, Austria



Helmut Wenzel is a member of WC V of IABSE. He earned a PhD in Bridge Construction from the University of Vienna in 1978 and is the Managing Director of VCE, with offices in Vienna, Taiwan and Korea. Dr. Wenzel also teaches Bridge Design and Construction at the University of Vienna.

## SUMMARY

Structures show a typical dynamic behaviour which may be addressed as „**Vibrational Signature**“. Changes in a structure such as all kinds of damages leading to decrease of load-carrying capacity have effects on the dynamic response. This suggests the use of the dynamic response characteristic for evaluation of structural integrity. Monitoring or measurements of the dynamic response of structures makes it possible to get very fast knowledge of their actual condition.

## 1. THE BRIDGE MONITORING SYSTEM BRIMOS

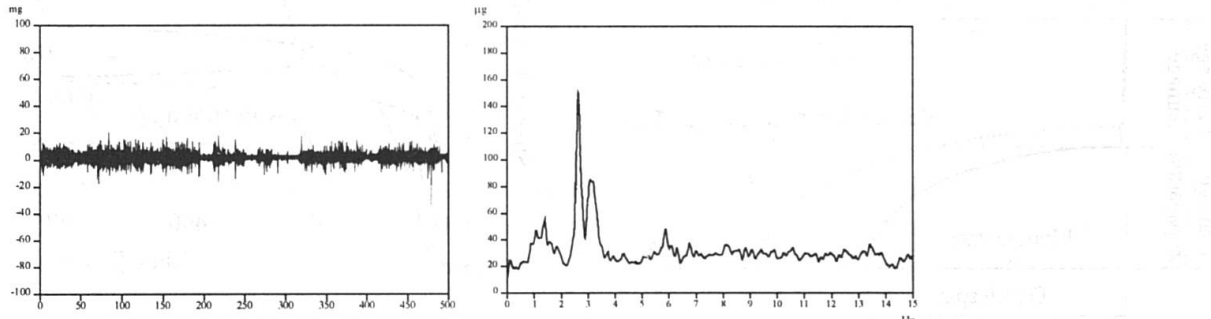


Figure 1 : Typical signal and spectrum of the Nordbrücke in Vienna (composite structure)

For the purpose of „System Identification“ a monitoring set-up was created, that enables quick an efficient recording as well as signal processing and report generation. The basis is the measurement of acceleration in a well determined layout of relevant locations of a structure. This provides data for the FFT analysis to generate the desired spectra. In addition data of the actual displacement of the structure is collected by infrared laser to gather information on the static behaviour and its relation to the dynamic action.

## 2. DATA PROCESSING

The collected data are processed to provide an informative report, which shall contain information on the signals itself in the desired units, the power spectrum of the readings, raw and smoothened, the drift of the readings and the relevant displacements. In a further step the readings of the various locations are combined to get an averaged spectrum and the related displacements. This is the basis for the animation of the Eigenform of the structure and the visualisation of it.

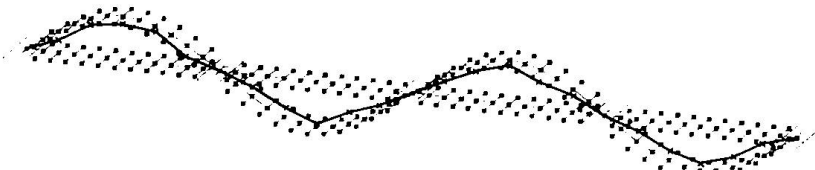
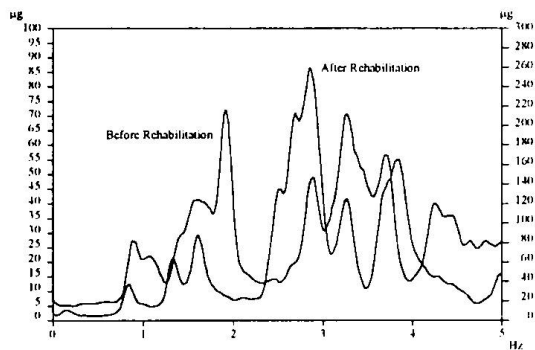


Figure 3 : First Eigenform calculated and measured of the Nordbrücke in Vienna

## 3. CONCLUSION

Due to the fact, that this bridge was monitored during 3 different stages, before, during and after the rehabilitation, valuable information was gained about the influence of the state of the structure on the response spectrum. From this basis it is tried to develop further tools to assess the quality of structures using data from dynamic monitoring.



## Time-dependent Response of Composite Structures

**Franc SAJE**

Assist. Prof., Dr.  
University of Ljubljana  
Ljubljana, Slovenia

Franc Saje, born 1941, obtained his Civil Eng. degree in 1965 and Ph.D. degree in 1990 from the University of Ljubljana.

**Joze LOPATIC**

Teaching Assist., M.Sc.  
University of Ljubljana  
Ljubljana, Slovenia

Joze Lopatic, born 1963, received his Civil Engineering degree in 1987 and his M.Sc. degree in 1990 from the University of Ljubljana.

### Summary

The paper deals with the procedure of numerical computational analysis of time-dependent response and redistribution of internal forces of a composite plane beam structure due to the rheology of material. Concrete creep is taken into account according to the linear theory of creep. The influence of concrete ageing and shrinkage is, similarly to the influence of concrete creep, considered by the adequate constitutive law of material.

### 1. Introduction

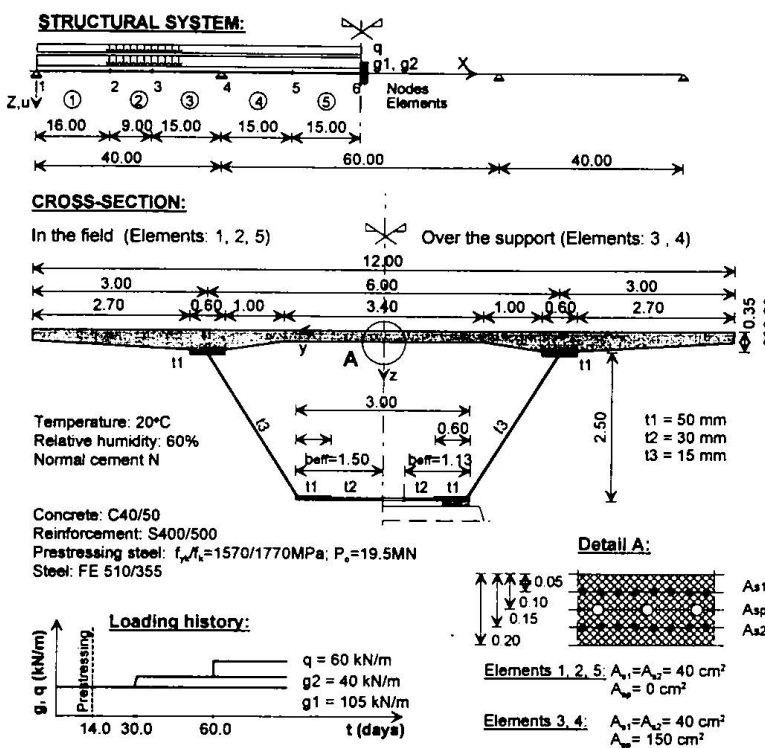
In order to make an adequate computational simulation of the behaviour of composite structures within time, it is necessary to consider also the influence of the rheology of material as well as the influence of cracks on the time-dependent response of the structure. Due to the rheology of material some extreme stresses appearing in the structure during the construction can decrease significantly after a certain time, but their influence on the strains or displacements of the structure often remains to a large extent the same. For this reason also the influence of gradual construction and the building technology have to be considered in the numerical simulation of the time dependent stress-strain relationship of structures.

### 2. Response of the Structure to the External Load

The time dependent response of the composite structure is simulated on a computer by using the finite element method. The geometrical nonlinearity of the structure is considered with adequate kinematic equations of the structure [1]. Physical nonlinearity and the rheology of material are taken into account using the adequate constitutive laws of materials. The influence of cracks on the behaviour of composite structures is taken into account by way of the constitutive equations of cross-sections [2, 3]. The time-dependent behaviour of the concrete according to the linear theory of concrete creep is modelled in the accordance with the well known constitutive law of concrete in its integral form. For the reinforcing steel, prestressing steel and profile steel of composed structures, a bilinear stress-strain diagram is taken into account.

The constitutive equations of the cross-section as the relationships between the internal forces, the elongation and the curvature of the element axis are obtained by the integration of the stresses through the whole composite cross-section consisting of concrete, reinforcing steel, prestressing steel and profile steel [2]. Bernoulli-Navier hypothesis is considered.

### 3. Computational Example



A composite bridge presented in Fig. 1 with spans of 40.0 + 60.0 + 40.0 m was analysed with the prepared software for the prediction of the behaviour of structures. The analysis takes into account concrete ageing, shrinkage and creep, relaxation of the prestressed steel and the influence of gradual construction. A part of the obtained results is presented on figures 2 and 3.

Fig. 1: Computational example - composite box girder

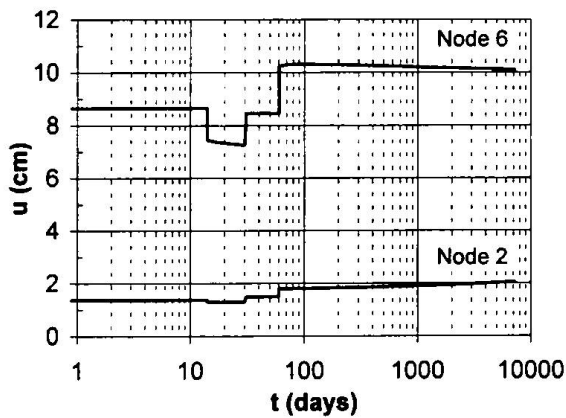


Fig. 2: Deflections time-history

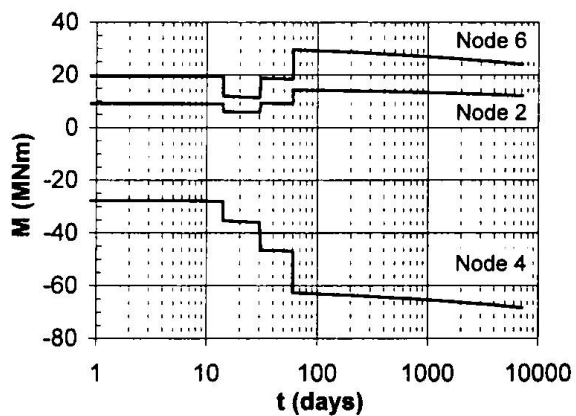


Fig. 3: Bending moment time-history

### 4. References

1. Banovec J., An efficient finite element method for elastic-plastic analysis of plane frames, Nonlinear Finite Element Analysis in Structural Mechanics, Springer-Verlag, Berlin, 1981, pp 385-402
2. Saje F., Viscosity of plane concrete structures, Ph.D. Thesis, University of Ljubljana, 1990
3. Lopatič J., Time dependent response of reinforced concrete structures by arbitrary stress level, Ph.D. Thesis in preparation, University of Ljubljana, 1997

## Study of Behaviour of Concrete Beams Strengthened by Steel Plates against Shearing Force

**Hidehiko ABE**

Dr. Professor

Ashikaga Institute of Technology  
Ashikaga, Japan

born in 1931, received his doctoral degree in 1974 from Tokyo Univ. He has investigated fatigue of steel materials and behaviour of composite structures.

**Akinori NAKAJIMA**

Dr. Associate Professor  
Univ. of Utsunomiya  
Utsunomiya, Japan

born in 1954, received his doctoral degree in 1983 from Tohoku Univ. He has investigated stability of structures and behaviour of composite structures.

### Summary

The paper presents an experimental and analytical study of concrete beams strengthened by vertically encased steel plates to increase the capacity against the shearing force. It was found that if such plates were properly arranged, the shearing capacity could be effectively increased and be applied to actual bridges, where the beam depth is severely restricted. The authors also developed a new FEM method of nonlinear two-dimensional rigid body-spring system, which proved to be useful to examine the behavior of such composite beams analytically in detail.

### 1. Introduction

The depth of beams in a concrete bridge is often severely restricted because of the clearance under the bridge or the depth of end parts of beams is curtailed by almost half to provide hinge-supports in a cantilever-type bridge. Occasionally, the shearing resistance in these parts is not large enough to prevent local damages in a long service period or under increased loading condition. The authors have developed a method for strengthening against the shearing force in which steel plates are vertically encased in the case of newly constructed bridges and they are attached on outer faces by studs and adhesive in the case of existing bridges.

The authors conducted a series of experiment, using various test specimens and also examined their elasto-plastic behavior by a new analytical method of two-dimensional rigid body-spring system, which was developed by the authors.

### 2. Experiment

The test setup and an example of the specimens (Model A-1) is shown in Fig. 1. Steel plates with studs are encased, which are separated at the center to prevent them from resisting the bending moment. A sufficiently thick steel plate with studs is attached also on the lower side. The amount of reinforcing bars was minimized, so as to investigate mainly the effect of steel plates. Several specimens were made for the test, in which the thickness of encased steel plates and the pattern of arrangement of the studs were varied. In addition to uni-axial strain gauges, tri-axial ones were installed to measure the distribution of shearing stresses in the plates.

In result cracks occurred in all the specimens at the central portion due to bending moment, and also large cracks occurred diagonally between the end supports and the loading points. Fig. 2 shows an example of cracks of concrete and the distribution of maximum and minimum principal stresses in the encased web plate at the maximum load. Fig. 3 shows an example of distribution of the shearing stress in the web plate. The stress appeared higher at the mid-depth. Comparing the results of fracture of the specimens, it seems that the studs located near the upper and lower edges act more effectively than those located in the mid-depth region.

### 3. Analytical Investigation

The concrete and steel portions are respectively divided into triangular elements. Adjoining elements and studs are connected with each other by springs in the two directions, parallel and perpendicular to each side of elements. The springs are provided with peculiar nonlinear characteristics, in order to examine the plastic behavior of the beam. Fig. 4 indicates an example to show how fracture or yield develops in the beam.

### 4. Conclusions

As the result of experiment and analysis the following conclusions are drawn:

- 1) The steel plates with studs encased at the end portions of concrete beams are effective for strengthening against shearing force and the studs arranged near the edges are more effective.
- 2) The analytical method of FEM of two-dimensional rigid body-spring system, which was developed by the authors, are useful to accurately account for the mechanism of fracture of such composite structures, which can not be detected in details by experiments.

**Acknowledgment:** The authors would like to express their gratitude to Mr. Masaki Toba and Mr. Katsuhiko Nakai for their cooperation in the experiment and analysis.

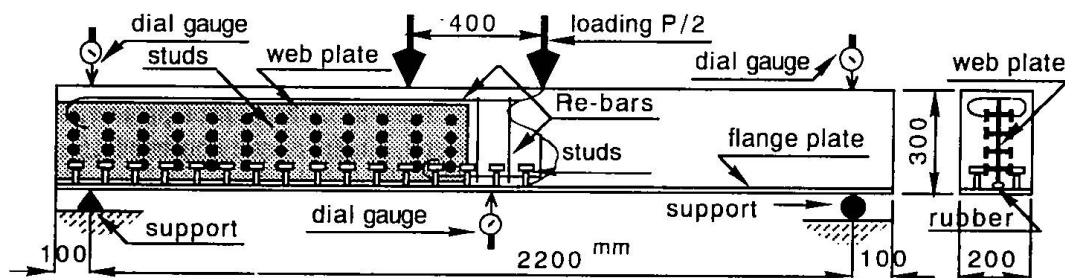


Fig. 1 Setup for test and a specimen (Model A-1)

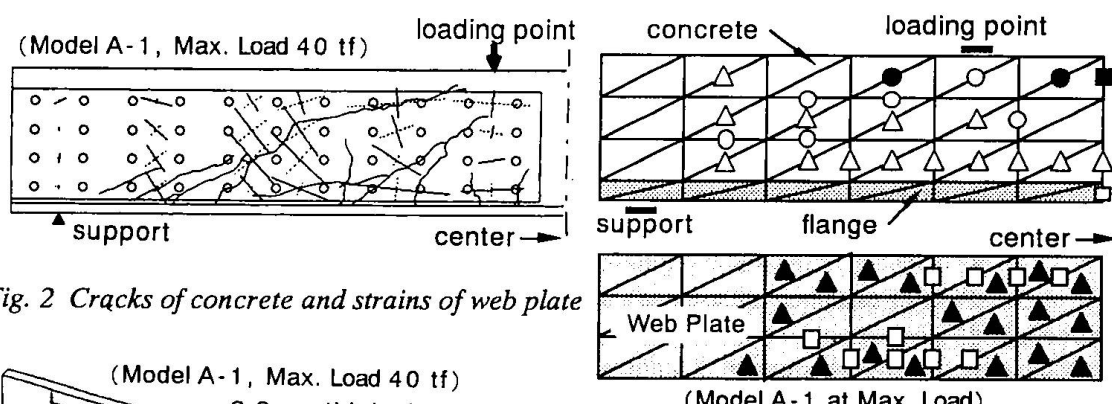


Fig. 2 Cracks of concrete and strains of web plate

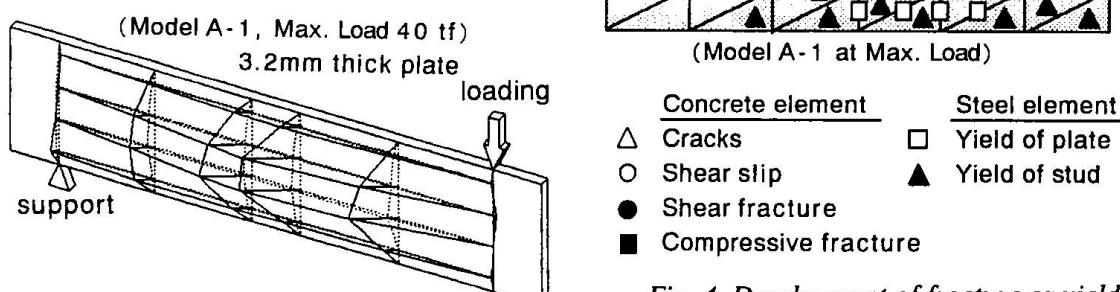


Fig. 3 Distribution of shearing stress in web plate

Fig. 4 Development of fracture or yielding of concrete and web plate

## Composite Cylinders Subjected to External Pressure

**C. Douglas GOODE**

Dr. Eng.

Secretary/Treasurer ASCCS  
Draughton, Skipton, England



Douglas Goode, born 1930, spent 6 years as an engineer with Sir Robert McAlpine & Sons Ltd then 28 years at The University of Manchester, retiring in 1990.

### Summary

Nine tests on cylinders with a composite, steel-concrete-steel, wall subjected to external pressure are described. The results show the advantage of this form of construction.

### 1. Composite Construction

The unpublished research reported in this paper was commissioned by Tecnomare SPA of Italy as part of their study to develop vessels to resist high external pressure for hydrocarbon production in deep water. It was carried out by the University of Manchester, England, and consisted of testing nine cylinders with steel-concrete-steel walls with a hemispherical dome at one end. Such vessels are relatively insensitive to initial imperfections and fail, after the steel skins have yielded, by strength breakdown of the filler material. Previously published reports describe the theory and show it is a faithful guide to the actual structural behaviour and strength.

### 2. Tests

The objectives of the tests were:

1. To compare the experimental pre-collapse behaviour and failure pressure with theoretical predictions.
2. To examine the cylinder/hemisphere interaction.
3. To study the effect of a penetration through the cylinder wall.
4. To measure the change in radial deformation with time under sustained pressure and the effect of sustained pressure on the ultimate strength.

All nine shells tested were cylinders, with an outside diameter ( $D_o$ ) of 495 mm and steel skin thickness ( $t_o=t_i$ ) of 2.00 mm ( $f_y = 297 \text{ N/mm}^2$ ; except TEC 6 where, for the inside skin,  $t_i = 1.91 \text{ mm}$ ,  $f_y = 260 \text{ N/mm}^2$ ), with a hemispherical dome as closure at one end (the steel in the skins of the dome was thinner 1.25 mm to 1.4 mm and of lower strength). The strength of the concrete filler varied, cube and cylinder strength is given for each cylinder in Table 1. The cylindrical portion was 1000 mm (approx.  $2D_o$ ) except for TEC 6 where it was 683 mm. TEC 5, 6, 7 & 8 had penetrations, formed of steel tubes 108 mm outside diameter, through the cylinder wall. In TEC 9 the pressure was sustained for 38 days at  $6 \text{ N/mm}^2$ , causing yield of the inside skin. The test failure pressure ( $p_{fx}$ ) is compared with the simple limit theory failure pressure ( $p_f$ ) in Table 1.

Shell	Wall thick. $h_{av}$ mm	cube $f_{cu}$ N/mm <sup>2</sup>	cylinder $f_c$ N/mm <sup>2</sup>	Test $p_{tx}$ N/mm <sup>2</sup>	Theory $p_f$ N/mm <sup>2</sup>	$p_{tx} / p_f$
TEC 1	23.1	49.7	42.2	7.6	8.28	0.92
TEC 2	23.2	49.4	45.4	8.6	8.29	1.04
TEC 3	22.0	47.0	41.1	7.5	7.93	0.95
TEC 4	20.3	48.0	43.3	7.2	7.68	0.94
TEC 5	23.0	50.2	40.8	8.6	8.29	1.04
TEC 6	22.8	52.3	42.5	9.6	7.90	1.22
TEC 7	20.6	46.8	43.8	7.8	7.68	1.02
TEC 8	23.1	52.0	44.9	8.6	8.42	1.02
TEC 9	22.9	56.8	46.6	9.1	8.65	1.05
Average (excluding TEC 6)						1.00

Table 1. Test results compared with theory

The failures occurred with an inward facing lobe, about 600 mm long and 220 mm wide, in the cylinder portion of the shell and were not affected by the dome or penetrations or the sustained pressure. The higher strength achieved by TEC 6 is attributed to its shorter length ( $L/D_o = 1.38$ ), with the restraint provided by the stiffer dome and closed end enhancing its strength.

Theoretically failure is assumed to occur when the maximum principal stress in the concrete  $\sigma_1$  (which will be the circumferential stress near the inside skin) reaches:  $\sigma_1 = \sigma_{uniax} + 3 \sigma_3$  where  $\sigma_{uniax}$  is the uniaxial strength of the concrete (taken as 0.75  $f_{cu}$  to compare with tests, though 0.67  $f_{cu}/\gamma_m$  should be used in design) and  $\sigma_3$  is the minimum principal stress (the radial stress in the concrete at the interface with the inside skin).

The simple limit state failure pressure is given by:

$$p_f = 2 [ t_o f_{yo} + t_i f_{yi} + (h_{av} - t_o - t_i) (0.75 f_{cu} + 6 t_i f_{yi} / (D_o - 2 h_{av} + 2 t_i)) ] / D_o$$

Table 1 shows that this theory is a reasonable predictor of ultimate strength. The detailed results show that the elastic/plastic theory was a good predictor of pressure/deformation behaviour and of ultimate strength. These results are particularly satisfying in view of the unexpectedly high yield stress of the steel. This had the effect of bringing the steel yield pressure close to the failure pressure thus causing stresses in the concrete filler to be approximately 70% of the cube strength when the steel skin first started to yield. The domes, which had a similar total wall thickness as the cylinder, were stronger than the cylinders even though the strength of the steel skins in the domes was less than half the strength of the skins in the cylinder. There were no problems at the cylinder/dome intersection; the failure zone was in the cylinder, except for TEC 3 where the failure lobe encroached into the dome. Creep of the concrete filler during the sustained pressure test on TEC 9 caused the initial deformation to increase by 25% after one day and by 70% after 38 days under a pressure that was 70% of the predicted failure pressure; the ultimate strength was not affected by the cylinder being subjected to sustained pressure.

Penetrations through the composite shell wall, with a diameter up to 22% of the main cylinder diameter, gave no cause for concern either at the design working pressure or at failure. In no case did the penetration initiate failure or reduce the shell's strength.

A more detailed description of this work and references to other research on composite cylinders under external pressure is available at the poster presentation.

## The Safety of Composite Sub-Sea Structures

**C. Douglas GOODE**

Dr. Eng.

Secretary/Treasurer ASCCS  
Draughton, Skipton, England



Douglas Goode, born 1930,  
spent 6 years as an engineer with  
Sir Robert McAlpine & Sons Ltd  
then 28 years at The University of  
Manchester, retiring in 1990.

### Summary

This paper discusses the safety of sub-sea structures which are subjected to external water pressure comparing the use of a 'depth margin' with the standard 'load factor' approach and the advantages of composite construction for this situation.

### 1. Safety

There have been some significant, and costly, failures of offshore structures in the North Sea during tow-out or commissioning (Frigg, during tow-out Oct. 1974 and Sleipner 'A', Gandsfjord near Stavanger, 23 Aug. 1991<sup>(1)</sup> ). Although inadequate design and/or construction defects may have played a part in the sinking of these structures it is the author's opinion that an inappropriate loading philosophy was the major cause.

Vessels subject to water pressure due to depth are currently designed by applying a load factor to the design depth pressure. The design depth should allow for the tidal range and the expected maximum wave height over the design life. The sea-water pressure is usually considered a dead load ('permanent action' in Eurocode 4 terminology) with load factors of between 1.2 and 1.4 applied to this pressure when considering the ultimate limit state. Norwegian designers use 1.2 for temporary loads during construction (1.3 for permanent work), China uses 1.2, Australia 1.25, Eurocode 4 uses 1.35, and in the UK 1.4 is applied to dead loads. This approach gives a low safety margin for shallow depths and excessive safety (overdesign) for deep depths.

A more appropriate method would be to add a 'depth margin' to the design depth to allow for inaccurate modelling of the actions and uncertainties in the profile of the sea-bed, for sea-bed vessels, or accidental excursion into deeper water for submersibles and then multiply this by a small load factor (to allow for uncertainties in the assessment of the effects of the actions). The choice of values for these will depend on the accuracy with which the tidal range, storm surge and wave height have been assessed; the author considers an 80 m depth margin desirable when these are not well known decreasing to say 50 m when they have been well assessed. In both approaches partial safety factors would also be applied to the materials, or in the USA and Australia 'capacity reduction factors' to the equations, to obtain the 'safe' resistance of structural members to the action effects at the ultimate limit state.

Table 1 compares these two approaches to safety philosophy for various design depths from 67 m (the depth to the probable failure point on Sleipner 'A') to 2 km (recognising that oil exploration

is being carried out in 2 km water depths), when 80 m is used for the 'depth margin' with a load factor of 1.10. This shows that at 67 m design depth a structure designed using the 'depth margin' approach would be designed for a pressure twice that of the 1.2 load factor and that they would give the same ultimate design pressure at 880 m depth. Comparing with a load factor of 1.4 shows the 'depth margin' approach gives safer structures until a design depth of 293 m is reached. At 1000 m the vessel would have to descend a further 400 m before reaching the ultimate pressure when the load factor of 1.4 is used; this does seem excessively safe.

Design depth (m)	pressure (N/mm <sup>2</sup> )	'depth margin' 80 m load factor of 1.1	load factor of 1.2	load factor of 1.4
		$p_{ult}$ (N/mm <sup>2</sup> )	$p_{ult}$ (N/mm <sup>2</sup> )	$p_{ult}$ (N/mm <sup>2</sup> )
67	0.68	1.63	0.81	0.95
100	1.01	2.00	1.21	1.41
<b>293</b>	2.96	<b>4.14</b>	3.55	<b>4.14</b>
500	5.05	6.44	6.06	7.07
<b>880</b>	8.89	<b>10.67</b>	<b>10.67</b>	<b>12.44</b>
1000	10.10	12.00	12.12	14.14
2000	20.20	23.11	24.24	28.28

Table 1. Depth margin and load factor approach compared at ultimate limit state pressure ( $p_{ult}$ )

## 2. Composite Construction

Cylinders subjected to external pressure, such as occurs in sub-sea vessels, are sensitive to geometrical and material imperfections which can lead to instability failure before the material strength of the vessel is reached. The thinner the wall thickness the worse is this situation; and vessels designed for shallow depths will have thin walls. This is where composite construction (a steel-concrete-steel wall) has advantages over all steel construction<sup>(2,3)</sup>. The composite requires a thicker wall, which is stiffer and so not prone to instability, yet cheaper for the same strength; less steel is used as the concrete carries a proportion of the load (the proportion depending on the percentage of steel). At failure of the composite wall the steel will be at yield and the concrete, being subject to triaxial compression, exceeds its uniaxial strength. Failure of the composite cylinder invariably occurs where the wall thickness is thinnest and so it is better to base the resistance of the cylinder on an estimate of the thinnest wall thickness, calculated allowing for construction tolerances, rather than the nominal thickness shown on the drawing.

## 3. References

1. NEW CIVIL ENGINEER, "Failure of sealed wall scuttles 115M gas rig", New Civ. Engr, 1991, 22/29 Aug., pp 4-5. (Also NCE 1991, 5 Sept., pp22-23).
2. GOODE C D "The design of double-skin composite structures", Third Int. Conf. on Steel-Concrete Composite Structures, Fukuoka, Japan. Proc., 26-29 Sept. 1991, pp. 605-610.
3. MONTAGUE P, NASH T and GOODE C D, "Large steel-concrete composite cylinders under external pressure", Proc. Instn Civ. Engrs. Structs & Bldgs, 116, May 1996, pp 174-185.

## Creep and Shear-Lag Effects in Composite Beams with Flexible Connection

**Luigino DEZI**

Professor

University of Ancona  
Ancona, Italy

**Graziano LEONI**

Dr. Eng.

University of Ancona  
Ancona, Italy

**Angelo Marcello TARANTINO**

Research Assistant

University of Ancona  
Ancona, Italy

### 1. Problem statement

In modeling steel-concrete composite beams, two kinematical aspects should be considered: the deformability of the shear connection and the non-uniform distribution of the longitudinal displacements in the slab (shear-lag). The deformability of the shear connection allows a slip at the beam-slab interface, increasing the global flexibility of the structure, while the shear-lag effect implies a non-uniform distribution of stresses in the slab. Furthermore, the behaviour of the composite beam is strongly influenced by the concrete time-dependent effects [1]. Although the effects of creep, connection deformability and shear-lag have been extensively examined in literature, their interaction is not completely known.

For this purpose, a general analysis for composite beams has been developed to encompass shear-lag effect, flexible shear connection, creep and shrinkage of the concrete [2]. Starting from the definition of a suitable displacement field which takes into account slipping at beam-slab interface and slab shear deformation, a global balance condition is obtained by means of the virtual work principle. By assuming a linear elastic behaviour for steel beam and shear connection, and a linear viscoelastic behaviour for the concrete slab, the problem is governed by a coupled system of four integral-differential equations. The unknowns of the problem are the functions describing beam deflection, axial displacements of the steel beam and the concrete slab, and intensity (along the beam axis) of the shear-lag effect introduced by means of a suitable shape function for the shear warping of the slab cross section (depending on the point of the cross section only). In particular, the shape function is a quadratic function constant on the slab depth, null at the beam-slab interface and satisfying conditions ensuring local equilibrium at the slab free edges.

Given the generality of the creep function adopted, a closed form solution cannot be achieved for the system. In order to obtain an accurate numerical solution, the system is solved by introducing two discretizations: one for the time interval, which permits solving the integral-differential problem by a step-by-step procedure considering a set of simpler differential problems, and the other for the beam axis in order to apply the finite differences method.

### 2. Principal results

An extensive numerical parametric analysis, carried out for beams with different geometry and subjected to different restraints and load conditions, has made it possible to obtain some information on the complex time dependent behaviour of composite structures. In particular, the time evolution of the shear-lag and the mutual influence between shear-lag and connection deformability have been studied in detail. For the sake of brevity, only results related to an isolated case (but which can be qualitatively extended to a wide class of composite structure) are reported here.

Fig. 1 shows the numerical results obtained for a two-span continuous beam. The creep analysis was performed with the CEB creep function [3] by considering the following values for concrete strength and relative humidity:  $f_{ck}=30 \text{ MPa}$  and  $\text{RH}=50\%$ . The solution at loading time  $t_0=28 \text{ days}$  (elastic solution) is compared with the viscoelastic solution ( $t_\infty=25550 \text{ days}$ ). Furthermore, results obtained taking into account the shear-lag effect (curves denoted by SL) are compared with those obtained under the classical hypothesis adopted for composite beams with flexible shear connection, namely preservation of plane cross section for the steel beam and the concrete slab considered separately (curves denoted by P). The most important results are summarised in the sequel.

1. The beam axis deflections notably increase as a consequence of the time-dependent behaviour of the concrete, while they are less sensitive to the shear-lag effect (Fig. 1a).
2. The shear-lag effect, as is well known, strongly modifies the stress distribution in the slab only in the neighbourhood of the intermediate support, by significantly increasing the value which would be obtained by assuming the plane cross section hypothesis for concrete slab and steel beam (Fig. 1b).

- Influence of the shear connection stiffness ( $\rho$ ) on shear-lag is shown in Fig. 1c, where the elastic values of the stresses  $\sigma_{SL}$  and  $\sigma_P$  at the intermediate support cross section are compared. Increasing  $\rho$ , shear-lag stress  $\sigma_{SL}$  increases more than  $\sigma_P$  as shown by the dashed curve related to the ratio  $\sigma_{SL}/\sigma_P$ . The coupling between the shear-lag effect and the shear connection stiffness is thus evident.
- Fig. 1d shows the influence of creep on the shear-lag effect. The time evolution of the ratio between  $\Delta\sigma$  and  $\sigma_{SL}$  (see Fig. 1b) is reported for three different values of the shear connection stiffness. Such a ratio permits defining the slab effective width  $b_{eff}$  (adopted by the principal technical codes, e.g. ENV 1994-2) as

$$b_{eff} = \frac{1}{\sigma_{SL}} \int_{-b/2}^{b/2} \sigma_c dx = b - \frac{\Delta\sigma}{\sigma_{SL}} \int_{-b/2}^{b/2} f(x) dx$$

where  $b$  is the real value of the slab width and  $f(x)$  is a function depending on the cross section only. It is evident that such a ratio, even if it depends on the  $\rho$  value, remains almost constant in time showing a substantial uncoupling between creep and shear-lag effect.

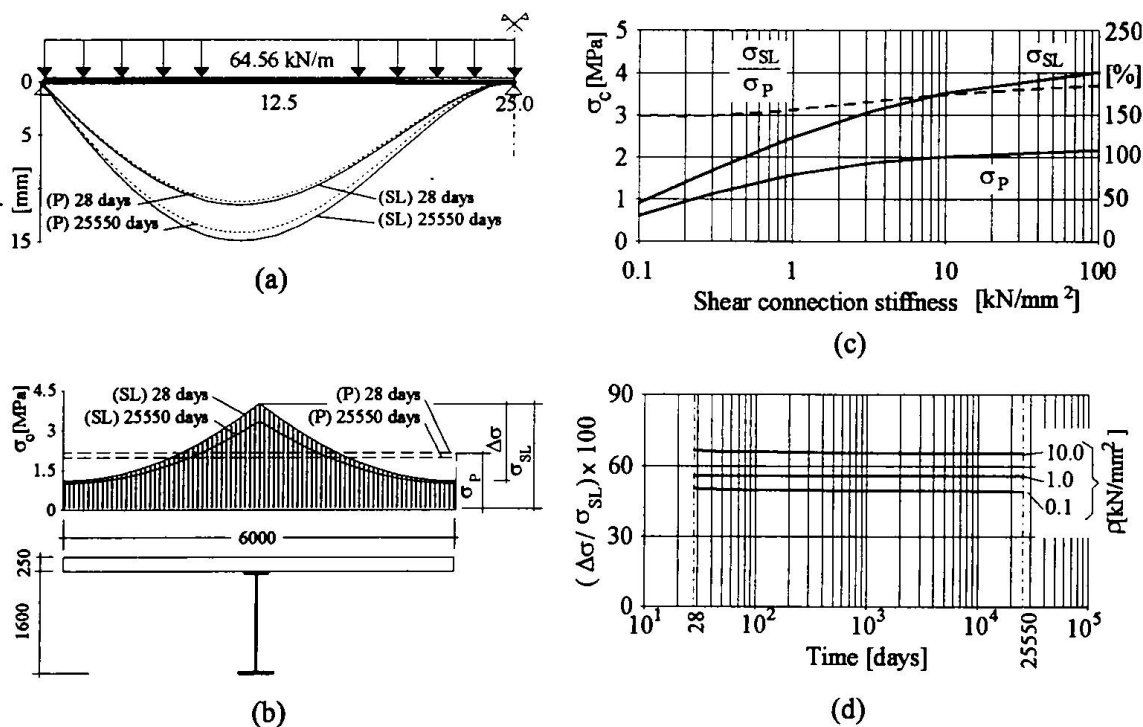


Fig. 1. (a) Influence of shear-lag and concrete creep on the beam deflections. (b) Concrete creep effect on the slab stress distribution. (c) Influence of the shear connection stiffness on the shear-lag effect. (d) Influence of the concrete creep on the shear-lag effect.

### 3. References

- 1 Dezi, L., and Tarantino, A.M. (1993), "Creep in composite continuous beams. I: Theoretical treatment." *J. Struct. Engng. ASCE*, 119(7), 2095-2111.
- 2 Dezi, L., Leoni, L., and Tarantino, A.M. (1997), "Time dependent analysis of shear-lag effect in composite beams." (Submitted for the publication on *J. Struct. Engng. ASCE*).
- 3 "CEB FIP model code 1990." (1988). *C.E.B. Bulletin d'information n. 190*, C.E.B. F.I.P. Comité Euro-International du Beton, Paris, France.

## Calculation of Stresses for Composite Structures

**Biljana DERETIC-STOJANOVIC**

Assist. Prof.  
Univ. of Belgrade  
Beograd, Yugoslavia

B. Deretic-Stojanovic, born 1955,  
received her doctor's degree 1992 from  
Belgrade Univ. Yugoslavia.

### Summary

The calculations of the stresses for the statically indeterminate composite structures as general, are presented. The approximate methods EM and AAEM and exact method are applied. The stresses, for the example of statically indeterminate composite structures due to uniformly distributed load and the shrinkage of concrete are determined. Using the limiting concrete creep functions the upper and lower limits of the stresses are determined.

### 1. The exact method (TM)

The cross section of the composite structures contain concrete (b), prestressing steel (p), steel member (n) and reinforcing steel (m). Concrete is considered as a linear viscoelastic material. The relaxation of the presstresing steel is taken into account.

$$\sigma_b = E_{b0} \hat{R}'(\varepsilon - \varepsilon_s), \quad \sigma_p = E_p \hat{R}_p \varepsilon \quad (1.1)$$

Other kinds of steel: steel member (n) and reinforcing steel(m) obey Hook's law :

$$\sigma_k = E_k \varepsilon \quad k=n,m. \quad (1.2)$$

The exact method, established by Lazic , using linear integral operators, is applied. Starting from the integral stress-strain relationship the expressions for stress and strain, in the exact method, are derived without mathematical negligence. Calculation of statically indeterminate composite structures is same as calculation of the corresponding structures whose material is homogeneous and elastic except that in composite structures we solve integral equations.

### 2. The approximate methods (AAEM, EM )

The algebraic stress-strain relationship for concrete contain two independent parameters: the reduced creep coefficient  $\varphi(t, t_0)$  and the aging coefficient  $\chi = \chi(t, t_0)$  (AAEM). When  $\chi=1$  the same equations represent the EM method.

$$\begin{aligned} \sigma_b &= E_{b0} \zeta_b (\varepsilon - \varepsilon_s) - \rho_b \sigma_b, \quad \sigma_b = \sigma_b(t_0, t_0), \\ \zeta_b &= \frac{1}{1 + \chi \varphi_r}, \quad \rho_b = (1 - \chi) \varphi_r. \end{aligned} \quad (2.1)$$

When the relaxation of prestressing steel is introduced, the algebraic stress-strain

relationship for the prestressing steel may be written as:

$$\sigma_p = E_p \zeta_p \epsilon \quad (2.2)$$

Calculation of statically indeterminate composite structures is same as calculation of the corresponding structures whose material is homogeneous and elastic.

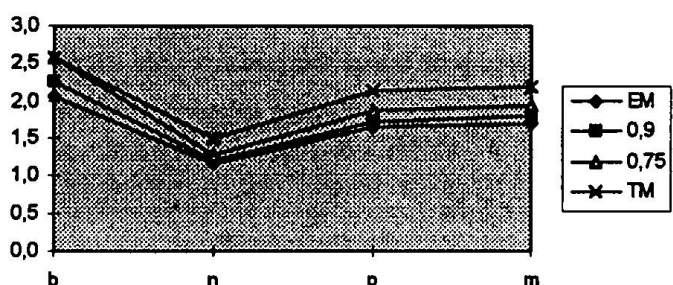
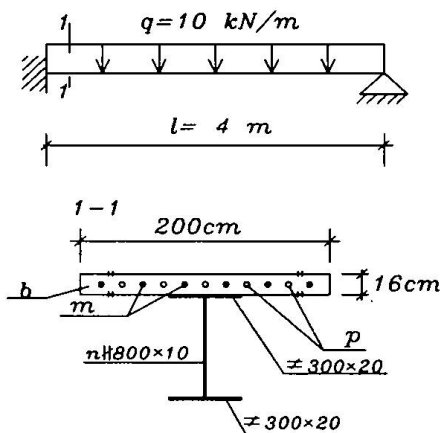
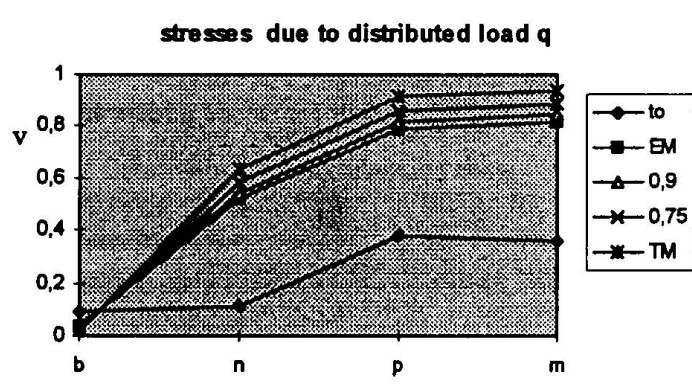
The redistribution of stresses for the example of composite structures due to uniformly distributed load and the shrinkage of concrete is calculated. Values of stresses are shown on the graphs 1,2 as follows.

Data: Concrete (b)  $E_b = 30 \text{ GPa}$ ,  $\varphi_b = 3,5$ ,  $\epsilon_s = -30 \cdot 10^{-5}$

Prestressing steel (p):  $E_p = 210 \text{ GPa}$ ,  $F_p = 100 \text{ cm}^2$ ,  $\zeta_p = 8\%$

Steel member (n):  $E_n = 200 \text{ GPa} = E_s$

Reinforced steel (m) :  $E_m = 200 \text{ GPa}$ ,  $F_m = 80 \text{ cm}^2$



### 3. Conclusion

The redistribution of stresses for the composite section during in time, occurs due to viscoelastic properties of concrete and relaxation of prestressing steel. Stresses of concrete are reduced and stresses of steel parts are increased. Using the concrete creep function of the aging theory in the exact method and the hereditary function in the EM method the upper and the lower limits of the stresses are determined. We choose the aging coefficient  $\chi$  in the AAEM method to lie within these limits. As we can see in graphs this conditions for the values of coefficient  $\chi$  from 0,75 to 0,9 are fulfilled.

## Stochastic Long-Term Analysis of Composite Girders

**Katsuhiko TAKAMI**  
 Associate Professor  
 Yamaguchi University  
 Ube, Japan

Katsuhiko Takami, born 1955,  
 received his Dr. Eng. from Kyusyu  
 University, Japan in 1986.

**Sumio HAMADA**  
 Professor  
 Yamaguchi University  
 Ube, Japan

Sumio Hamada, born 1944,  
 received his Ph.D from the University  
 of Alberta in 1972.

### Summary

The creep properties of concrete significantly influence the long-term behavior of steel-concrete incomplete composite girders. In this paper, a stochastic creep analysis based on the First-Order Second-Moment Method are carried out considering the uncertainties of creep properties. The results are compared with those obtained from the Monte Carlo simulation. The effect of variability of material properties on the long-term behavior of incomplete composite girders are exhibited.

### 1. Introduction

The creep properties of concrete significantly influence the long-term behavior of steel-concrete incomplete composite girders. In the design of those structures, the deterministic creep coefficient, such as the ACI-209 model, the CEB-FIP-90 model is utilized to estimate long-term effects. These creep properties are subjected to some amount of variability. Therefore, it is not so easy to correctly predict the long-term behavior of these girders. In this study, a stochastic creep FEM analysis based on the First-Order Second-Moment Method are carried out considering the uncertainties of creep properties. The results are compared with those obtained from the Monte Carlo simulation.

### 2. Stochastic FEM Analysis based on the F.O.S.M

The incomplete composite girder in this FEM analysis consists of a concrete beam element, a steel beam element and a continuous spring element which connects concrete and steel. Using the age adjusted effective modulus method in constitutive low on the concrete, the creep stiffness equation of the incomplete composite girder is expressed as following.

$$[K]\{U\} = \{F\} + \{G\} \quad (1)$$

where

$[K]$ :creep stiffness matrix of composite beam,  $\{U\}$ :creep displacement vector  
 $\{F\}$ :external force vector,  $\{G\}$ : creep force vector

The sensitivity displacement is derived from Eq.(1) as

$$[K] \frac{\partial \{U\}}{\partial X_i} = - \frac{\partial [K]}{\partial X_i} \{U\} + \frac{\partial \{G\}}{\partial X_i} \quad (2)$$

$(i = 1 \sim m)$

where  $X_i$  is probabilistic variables such as the relative humidity, affecting creep behavior of concrete. The value  $m$  is the number of the probabilistic variable. The variances of deflection and stress of the concrete slab and steel beam can be evaluated from Eq.(2).

### 3. Calculation and Results

The CEB-FIP-90 model has adopted as a creep coefficient, which mainly consists of 4 terms of the relative humidity, the mean compressive strength of concrete, the notational size of member and the age of concrete. Besides the creep coefficient the aging coefficient and the modulus elasticity of concrete at loading time also effect the age adjusted effective modulus in the analysis. In this study, the relative humidity, the compressive strength of concrete at the age of 28 days, the modulus of elasticity of concrete and the aging coefficient are regarded as probabilistic variable. The data of those values are the mean value and the coefficient of variation which represents the scatter. Other data are deterministic values.

The numerical calculations are carried out for the simple composite beam shown in Fig.1. The following numerical values are adopted: span length  $L=40m$ ; modulus elasticity of steel  $E_s=2.1 \times 10^5 \text{ MPa}$ ; uniformly distributed sustained load  $p=54.145 \text{ kN/m}$ ; rigidity of connector  $Q_z=0.4 \text{ kN/mm/mm}$ ; loading time and final time for creep analysis is 14days, 10000days, respectively; mean relative humidity  $RH=60\%$ ; mean compressive strength of concrete at the age of 28days  $f_{ck}=30 \text{ MPa}$ ; mean aging coefficient  $\chi=0.76$ ; mean modulus elasticity of concrete  $E_c=2.85 \times 10^5 \text{ MPa}$ .

The comparisons of the variance of creep deflection and creep stress of concrete at the mid span are shown in Fig.2 and Fig.3 between this study and Monte Carlo simulations, where the number of sampling calculation is 1000, and every coefficient of the variation of relative humidity, compressive strength of concrete, aging coefficient, and modulus elasticity of concrete ranges from 10% to 40%. Results of this study show good agreements with those from Monte Carlo simulations.

### 4. Conclusion

The present paper expresses the incomplete composite analysis including the scatter of material properties of long-term behavior, which results in good agreement with the results evaluated from the Monte Carlo method.

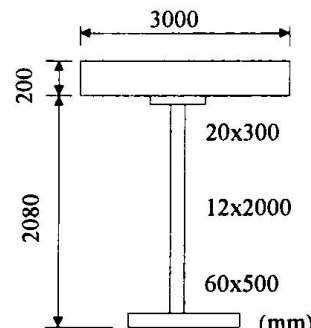


Fig.1 Cross Section

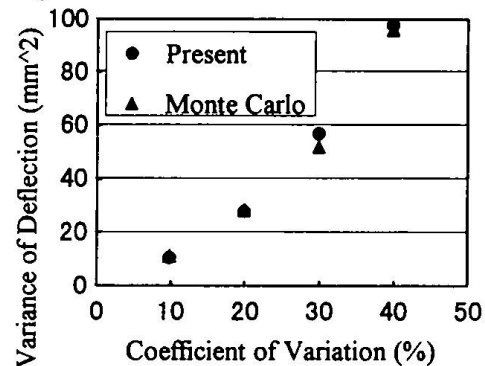


Fig.2 Comparison of Result(a)

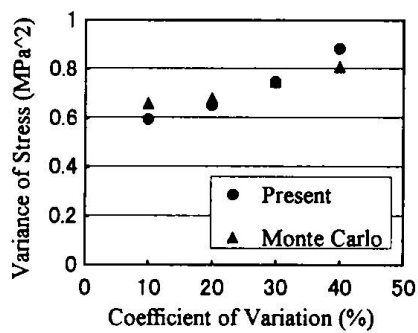


Fig.3 Comparison of Result(b)

## Design and Tests of New Steel-Concrete Slabs

**Eduard AIRUMYAN**  
PhD., Head of Laboratory  
CNIIPSK named Melnikov  
Moscow, Russia

He was born 1936,  
received his PhD degree  
in 1973 in the Central  
Research Institute of  
Structures in Moscow.

**Oleg BOYKO**  
Dipl. Eng., Director  
EXERGIA Co Ltd.  
Lipetsk, Russia

He was born 1959,  
graduated from the State  
Institute of Building  
engineers in Odessa

### Summary

Results of analysis and full-scale tests of new deck and roof slabs, designed as composite steel-concrete structures are presented. The new system of anchors was used for connection of steel load-bearing profiled sections and concrete, filled in their. Shear bond resistance of the anchor connectors and strength of the slabs were researched with tests.

### 1. Composite deck -slab

New structure of composite steel-concrete deck slab was worked out with CNIIPSK(Moscow) and EXERGIA Co (Lipetsk). The slab is consisted of profiled steel sections like cassettes, manufactured from galvanised steel sheet of thickness from 0,8 to 1,2 mm with cold-forming. Depth of section's wall -300 mm, flange width-110 mm, length-up to 13 m. Sections are supported with their walls on deck beams and connected each other with edge folds of flanges using seaming machine. The sections are fixed to beams with screws, nails or welded studs. The sheeting of sections is used as permanent shuttering and work reinforcement of the composite deck. Concrete of strength classes from B20 to B40 is located into sections with layers of thickness from 80 to 110 mm. Lightweight concrete is accepted to use with unit mass not less than 1800 kg/m<sup>3</sup> and compressive strength not less than 17 MPa.

Composite behaviour between steel sections and concrete is ensured ( after it became hard) by corrugated steel strips of width from 30 to 50 mm as transverse pieces of cold-formed profiled sheets of thickness 0,8-1,0 mm with trapezoidal waves ( Fig. 1) The strips are located along each section and fixed to its wall with pop-rivets or weld spots. Except concrete sound-proofing or heat insulation layers can be located within depth of the slab.

### 2. Analysis of the slab

Ultimate desing moment for bending composite slab are calculated as for reinforced concrete structure with external reinforcement assuming full interaction between steel sections and concrete, provided Eurocode 4 and Building Standard of Russia. Safety factor of steel section as main reinforcement is assumed equal 0,7 .Results of analysis of slabs with sections from steel of thickness 0,8-1,0 mm and concrete of different classes are as given in Table.

### 3. Testing

Standard full-scale test of new composite slab was carried out to control analysis results.

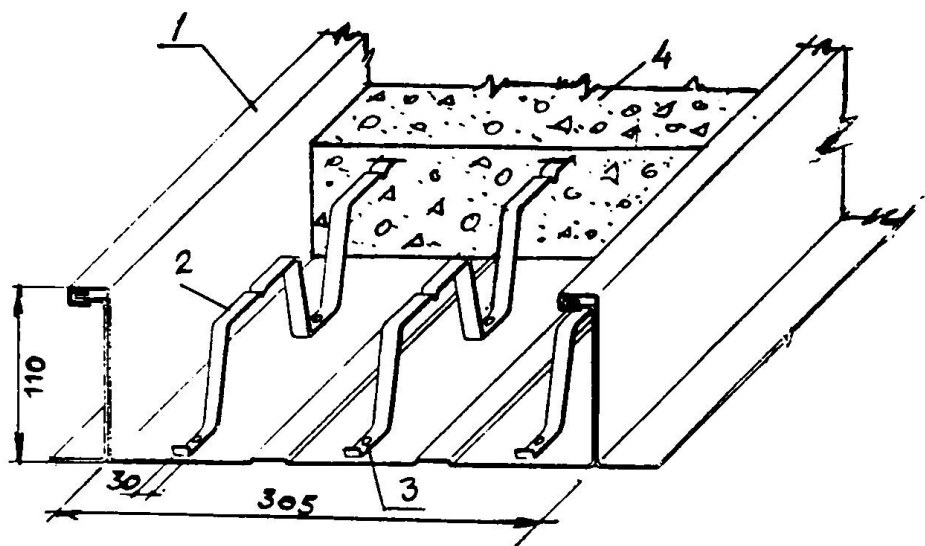


Fig. 1. Anchor connectors in composite slabs  
 1 - steel section; 2 - anchor; 3 - pop-rivet or weld spot; 4 - concrete

The specimen was represented a simply supported slab with length of 4,1 m, width of 0,9 m and span of 4 m. Thickness of steel sections was of 1,0 mm. Corrugated sheet anchors with width of 30 mm, wave depth of 44 mm and thickness of 0,8 mm are fixed with pop-rivets to the sections, which was filled in with concrete completely. Cubic concrete compressive strength was 20-20,6 MPa (cubics). Two equal concentrated line loads  $P$  were applied at thirds of the span. The deflection of the slab at the middle of its span was equal 7,3 mm when  $P=10$  kN, relative movement between the sections and concrete at the ends of the specimen was less than 0,3 mm. Ultimate failure moment on the slab was equal 20,5 kNm (with calculation of its weight).

Recomended maximum span of the new slab is up 4,0 or 5,5 m without or with a temporary support at the middle of the span accordingly during packing of wet concrete.

Thickness, mm		Ultimate desing moment ( kNm) on 1 m of slab width for concrete classes				
concrete	section	B15	B20	B25	B30	B40
80	0,8	10,6	10,8	11,1	11,2	11,3
	0,9	11,7	12,0	12,3	12,4	12,6
	1,0	12,8	13,2	13,6	13,7	13,9
110	0,8	14,1	14,3	14,6	14,7	14,8
	0,9	15,7	15,9	16,3	16,4	16,5
	1,0	17,2	17,6	18,0	18,1	18,3

Table 1. Results of analysis of the slabs

## Arch Bridge Crossing the Brno-Vienna Expressway

### Jiri STRASKY

Professor of Civil Engineering  
Technical University of Brno  
Brno, Czech Republic

Jiri Strasky, born 1946,  
received his engineering  
and Ph.D. degree from the  
Technical University of  
Brno. He is a Registered  
Engineer in both California,  
USA and the Czech Republic.

### Ilja HUSTY

Partner  
Strasky Husty and Partners  
Brno, Czech Republic

Ilja Husty, born 1950,  
received his engineering degree  
from the Technical University of  
Brno. He is a Managing Director  
of Strasky Husty and Partners,  
Consulting Engineers.

### Summary

A composite arch bridge formed by a steel tube in-filled with concrete that supports a cast-in-place concrete deck of a trough cross section is described in terms of the architectural and structural solutions, static function and process of construction. Results of the static and dynamic tests are compared with the results of the static and dynamic analysis.

### 1. Architectural and Structural Solution

A new 67.50 m span steel-tube arch bridge carries local road traffic across the new Brno-Vienna Expressway in the Czech Republic. In evaluating the angle of skew of the crossing, it was determined that using only one arch as the load-bearing member would be the most aesthetically and structurally preferable solution. The arch is formed in a circle with a radius of 74.75 m by a single steel tube with a diameter of 900 mm and a thickness of 30 mm in-filled with concrete. Internally, the steel tube is stiffened by diaphragms at a distance of 2 m. The arch is fixed in concrete foundations on each side of the expressway - see Fig. 1. The arch supports a slender trough-shaped cast-in-place concrete deck using edge girders in the shape of New Jersey barriers which serve as stiffening girders as well as safety barriers. The deck is post-tensioned by cables situated at the edge girders and in the deck slab.

The deck is connected to the arch by steel struts situated perpendicular to the axis of the arch at a distance of 6 m. These steel struts, which are connected to the stiffening diaphragms of the steel arch tube, are of a small box-cross section and are also filled with concrete. To guarantee the stability of the arch not only in the vertical direction but also in the transverse direction, these struts are triangular in shape; the width of the triangle is always constant, but the length is variable. In the middle of the bridge, the arch is fix-connected directly with the deck. The first and last side spans, which are relatively long, are supported by inclined cast-in-place concrete struts that are pin connected with the deck and with the concrete foundation of the arch. These concrete struts are arranged directly under the edge girders to transfer the loading directly from the edge girders to the foundations, and thus assure the stability of the structure in the transverse direction.

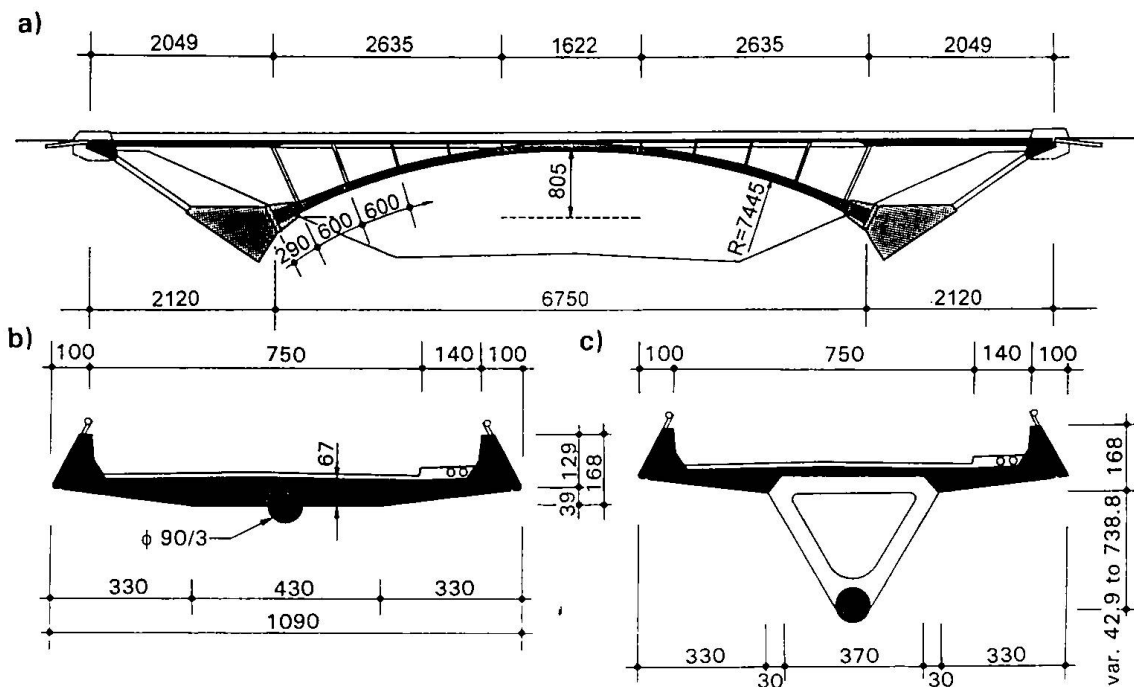


Fig. 1 Structural solution: a) elevation, b) cross section at midspan, c) typical section

## 2. Process of Construction

The steel arch was erected from steel segments with a length of about 12 m. After the erection of the arch, the triangular shaped steel struts were erected. The structure was temporarily supported by hydraulic jacks. Concrete was pumped from the bottom to the top of the arch. To guarantee that there would be no air voids at the top, 3 openings were provided at the top of the arch. After filling the steel tube with concrete, the deck was cast as one unit on traditional scaffolding and post-tensioned. After the deck was post-tensioned, the hydraulic jacks were used to press the arch against the foundation in order to reduce the short-term deformation of the foundation. This operation was repeated after one week.

## 3. Static and Dynamic Analysis

According to the nature of the problem the structure was analyzed as a 2D, 3D frame, and the 3D structure being assembled of the shell and solid elements. Detailed time-dependent analysis was done by our proprietary program TDA using CEB-FIP functions. The design assumptions and quality of the workmanship were checked by static and dynamic loading tests. The bridge was loaded by eight trucks situated in two positions that created maximum bending and torsion in both the arch and the deck. The structure was also tested dynamically. At first the agreement of excited natural frequencies with theoretical values was checked, then the logarithmic decrement of damping and the impact coefficient was determined. The test confirmed our assumptions and good behavior of the structure. The structure was designed by SHP Brno with the collaboration of Fercon Brno and the Technical University of Brno (Dr.Zak, Dr.Navratal and Ing.Hradil). The structure was developed under support of GA 261635.

## The Nevers Bridge: Design of the Steel Concrete Composite Box Girder

### D. POINEAU

Technical Director  
S.E.T.R.A.  
Bagnoux, France

Born 1937. Throughout his carrier he has worked on engineering structures. For about 25 years, specialised in pathology.

### J. BERTHELLEMY

Senior Engineer  
S.E.T.R.A.  
Bagnoux, France

Born 1957, civil engineering degree 1979. He joined SETRA in 1980. Experience in steel and composite bridges and their pathology.

### J-M. LACOMBE

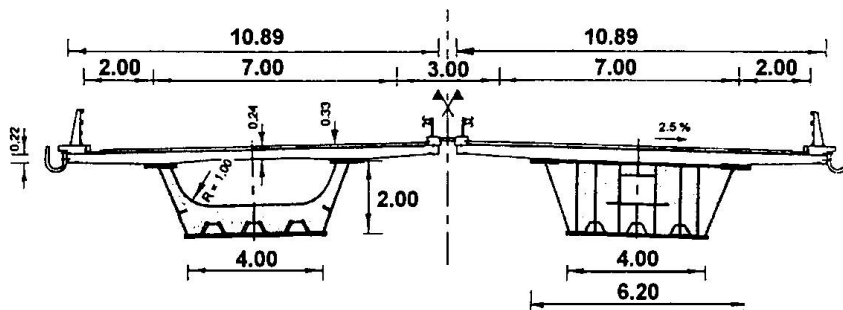
Senior Engineer  
S.E.T.R.A.  
Bagnoux, France

Born 1959, civil engineering degree 1983. He joined SETRA in 1984. Experience in concrete and composite bridges, and in pathology.

### 1. General design of Loire crossing bridge for a road by-passing Nevers.

The Nevers Bridge built between 1992 and 1995 was designed by *SETRA*. It is composed of two independent composite box girders, each one 420 meters long. *J. Richard-Ducros* for the steel structure and *Dalla Vera* for other civil engineering works were the contracting companies. For a more complete description of the bridge, see the article "Cracking control in the concrete slab of the Nevers composite bridge" in the same book.

The alignment of the Loire crossing is straight, and with a small 6 degrees skew angle between the river and the bridge. But every unmechanic skew alignments of bearings is avoided for the structure. This type of composite bridge was economically competitive.



*Cross section of the steel-concrete composite box girders (half standard and half on pier).*

### 2. Decisive advantages of a composite box girder solution.

When the Nevers bridge was designed, the use of plate girders was regarded as less expensive than the use of box girders for steel concrete composite bridges, box girders requiring more fabrication time.

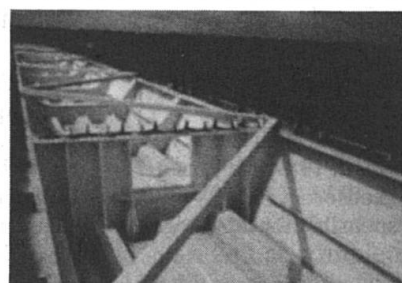
In order to tide over this handicap,

- We designed the steel box with modest outer dimensions to make fabrication, and erection easy. In addition, shear lag and local buckling would make too wide flanges inefficient.
- The alignment of the Nevers box girders is straight, which allowed us to incline webs without geometrical difficulties that appear with highly curved bridges. If webs were vertical, bottom flange would be much too wide to be efficient. Inclined webs reduce the bottom flange width in a favorable way. In addition, the width between upper flanges is free to be optimised. The goal is to reduce distortion solicitation in the intermediate cross frames due to fatigue loads at the connection point between steel and concrete.

- We realized that transport and welding in site of the elements were often in fact the reasons for an overestimated cost of a box-girder solution when compared with the plate-girder solution. The Nevers bridge segments were small enough to be transported in one piece by road. Sections could be fabricated in the full width at the shop, and the best economy was achieved because longitudinal welding on site was avoided all the long of the bridge at the middle of the box.



*Transport of segments*



*Diaphragm on pier*

Composite box girders have however several advantages over plate girders which make their use attractive. The following advantages were decisive for the choice of the Nevers bridge structure :

- A neater appearance since the stiffening can remain invisible in the box.
- All places outside of the bridge are avoided where water could be caught in a trap. Most of the common causes of corrosion disappear which increases the service live and reduces the maintenance costs.
- Because of the low renewing rate of oxygen, the inside of a composite box is usually exposed to far less risk of corrosion than the outside. Very light colors were chosen for painting the steel inner surfaces of the Nevers boxes. This facilitates inspection because corrosion points or eventual fatigue cracks will be easier to detect in the future.

In order to reduce maintenance costs an important point is to avoid birds flying inside the box using smallest openings, birds droppings being very corrosive.

- The width of the box girder plates, especially the bottom plate width, allows large span to depth ratio, to cross the clearance to be allowed for hydraulic, which reduces scale and cost of the road embankments at each end of the bridge.
- Very high torsional rigidity: In closed box girders, torque is resisted mainly by Saint-Venant shear stresses. This is an important advantage for a fatigue sensible structure like a road bridge.

### **3. Important details : temporary bracings and diaphragms on piers.**

The torsionnal stiffness of the box girders is also essential during their construction. Composite box girders only achieve their torsional rigidity after concreting. During erection and concreting, they require temporary bracings.

According to the procedure used by contractors, bracings were only removed on one 20 meters long standard segment just before concreting it, when all other previous concrete segments were hard. This procedure could prevent deformations, that may occur when removing bracings where the deck is not achieved, which dramatically reduces the torsionnal stiffness of an open composite box girder.

Local effects on bearings cause complex states of stress in the supports on piers. We designed a diaphragm on piers to obtain a great rigidity to resist local distortion, and avoid detachment between steel and concrete parts of the composite structure.

## The Øresund Bridge on the Link between Denmark and Sweden

**Henrik CHRISTENSEN**  
Design Manager  
Øresundskonsortiet  
Malmö, Sweden

Henrik Christensen received his civil engineering degree from the Technical University of Denmark in 1987. He joined Øresundskonsortiet in 1994 and is responsible for the bridge design.

**Klaus FALBE-HANSEN**  
Project Director  
ASO Group  
Copenhagen, Denmark

Klaus Falbe-Hansen received his civil engineering degree from the Technical University of Denmark in 1967. He joined Ove Arup in 1968 and is a director of Ove Arup Denmark. He is responsible for the ASO Group's activities.

**Jorgen GIMSING**  
Quality Manager, Design  
ASO Group  
Malmö, Sweden

Jørgen Gimsing received his civil engineering degree from the Technical University of Denmark in 1967. He joined Gimsing & Madsen in 1970 and is managing director of the company. He is technical director in the ASO Group.

### Summary

The Øresund Link being established between Denmark and Sweden is a 16 km toll-funded road and railway crossing. It consists of a 4 km immersed concrete tunnel, a 4 km artificial island and a 8 km long bridge. The bridge includes a 1.1 km cable-stayed high bridge with a navigation span of 490 m and approach bridges each side with typical 140 m spans. The cross section is composite with the upper road deck in concrete and the lower railway deck in concrete on the approach bridges and in steel on the high bridge. The two decks are separated by two parallel steel trusses.

### 1. Introduction

Øresundskonsortiet (ØSK), a company owned jointly and equally by the Danish and Swedish governments, is responsible for the project design and construction of the fixed link. The Link will after its scheduled completion in year 2000, be owned and operated by ØSK.

ASO Group is house consultant to ØSK, responsible for technical services and aesthetics of the bridge. The group consists of Ove Arup & Partners (UK), SETEC (F), Gimsing & Madsen (DK) and ISC (DK). Georg Rotne (DK) is the group's architect.

The contract for the construction of the bridge was signed with Sundlink Contractors HB in November 1995. Sundlink consists of Skanska (S), Hochtief (D), Monberg & Thorsen (DK) and Højgaard & Schultz (DK). The detailed design is carried out for the contractor by a joint venture consisting of COWI (DK) and VBB-VIAK (S). The design of the bridge is based on ASO Group's conceptual and illustrative design for a two-level bridge. The conceptual design is included in the contract in the form of Definition Drawings, which must be followed by the contractor in his detailed design.

### 2. The Bridge

The cable-stayed high bridge (Fig 1) consists of a central navigation span with two side spans each side. Minimum headroom in the main span is 57 m. The high bridge is connected to the artificial island and the Swedish coast at Lernacken via a number of 140 m approach spans. The bridge deck is in two levels with a dual two-lane motorway at the top and a two-track railway at the bottom. The two levels are separated by two parallel Warren type steel trusses.

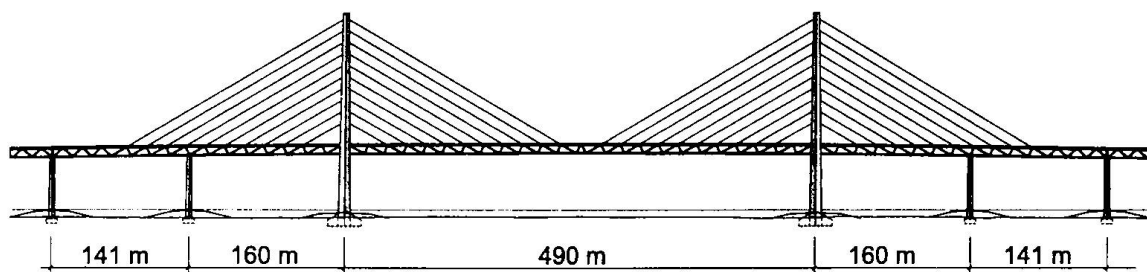


Fig. 1 The cable-stayed high bridge

The steel trusses have a more open bracing ( $45^\circ$ ) than generally used in truss bridges, and vertical members are only installed at truss ends at expansion joints. The 20 m bay length of the truss is constant along the bridge, but the configuration is modified at the cable-stayed spans so that every other diagonal has the same direction as the stay cables. The 490 m main span will at completion be the longest cable-stay supported span in the world carrying both road and heavy rail traffic.

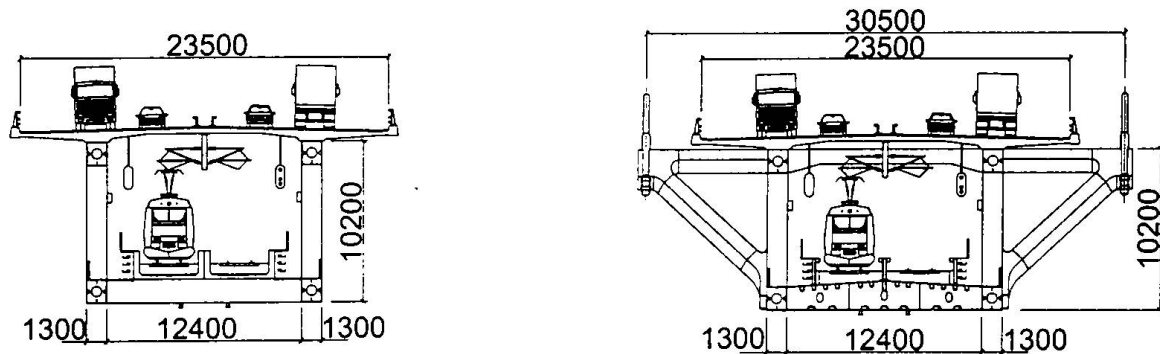


Fig. 2 Cross sections

## 2.1 Details

The trusses are placed 12.4 m apart and are in composite action with the concrete top flange. The transversely prestressed concrete slab has an average thickness of only 0.30 m. Hogging moments in the slab over the supports are transferred to the torsionally stiff upper steel chords. The transfer of tension at the top of the deck to the steel is secured by normal reinforcement anchored to long studs over the webs of the chords. The transfer of normal forces from the truss to the upper deck is concentrated at the nodal points, where 150 mm Nelson studs are provided closely spaced over the 7 m length of the nodes.

On the approach spans, the railway at the lower deck is carried in two concrete trough sections supported on 2.6 m wide transverse steel box beams spanning between the lower nodes. The troughs are in composite action with the chords. The width of the cross beams is determined by the large horizontal forces to be transferred from the truss diagonals to the concrete. The connection between cross beam and concrete is similar to the one described for the upper deck: long studs concentrated at the webs of the troughs to transfer tension from the local hogging moments in the troughs, and short studs concentrated at the outer trough webs to transfer horizontal shear from the steel to the concrete. The troughs are in reinforced concrete. As for the upper deck it was found uneconomic to apply longitudinal prestressing after the shear connection to the steel is made, as a major part of the prestress force would be transferred to the steel. In the cable-stayed spans the concrete troughs are substituted by a shallow steel box between the lower chords, as the advantages of the lighter deck prevailed over the extra cost of the steel.

## Approach to Assessment of Fire Damages: Composite Structures

**Arvind MALHOTRA**  
 Engineer, Arch. Planner  
 HUDCO  
 New Delhi, India



Arvind Malhotra, born 1946 received his Civil Engineering degree followed by post graduation in Town Planning & Business Management. Having varied field experience in Civil Engineering, Urban & Regional Planning, Project Feasibility, Appraisal & Monitoring, for last 28 years.

### Summary

The case study brings out the innovative approach adopted to assess the fire damage which led to a scientific classification of damages and helped to recommend upgradation and retrofitting. The building was restored in a record time with value added remodeling. The availability of the detailed drawings highlighted the needs for proper documentation. Various innovative techniques to strengthen, join, jacket, and retrofit the structures were used. The outbreak of a fire can never be ruled out but it can definitely be minimized and contained. The case study also highlighted the need to stress on Passive measures in the building design and lay out.

### 1. Introduction

Vigyan Bhawan in India, is one of the most prestigious and premier conference centres of Delhi. In April, 1990 a fire broke out in the building, which resulted in severe damages to the building structure and services.

### 2. Approach towards the Restoration

After preliminary assessment of the extent of damage, it was decided to go in for rehabilitation of the main structural elements, for the following reasons.

- 2.1 As it was a composite structure, the impact of fire left different residual strengths of the structural elements, ranging from negligible damage to extensive damage, rehabilitation would be economical and time saving.
- 2.2 A totally new structure would have made it difficult to create the original image of the building, which had its own Historical, Cultural and Architectural features.
- 2.3 Psychologically and Emotionally, it was more conducive for the country at large to have the building renovated as it would also avoid negative publicity. Also the location of the building was in a sensitive VIP area, even controlled demolition would be dangerous.

### 3. Innovative Management Framework

- 3.1 The repair and rehabilitation of this prestigious fire damaged building required an innovative approach which had to transcend beyond the normal Engineering approach. The main features were based on Structural, Aesthetic, Fire safety and Security aspects, as given below :
- 3.2 An apex body was created with representatives of the Administrative Ministry, Construction Agency, User departments, Security and Information services, Architects, Structural Engineer etc.
- 3.3 The opportunity was used not only to restore the current facilities but also to create modern state of art facilities with enhanced value added services in the shortest time.
- 3.4 The National Council for Cement and Building Material (NCCBM), New Delhi was

appointed as consultant to assess the structural damage. They assessed the extent of damage caused to all the RCC elements and determined the residual strength of each element.

3.5 A separate set of Architectural consultants was shortlisted, for not only remodeling the existing building design but also to decrease the risk factors, from both fire and earthquake.

3.6 An exclusive Investigation agency was involved in classifying the damage of structures and also making assessment for their re-use.

#### 4. Damage Assessment Procedure

4.1 Debris Inspection.

4.2 Preparation of Structural arrangement plans at different floors, numbering each column, beam, and slab member.

4.3 Visual inspection of structural members including surface appearance of plaster, colour, Crazing etc., assessment of Structural conditions like spalling, cracks, distortion, delamination etc.

4.4 Recording of visual inspection through spread sheets.

4.5 In-Situ non-destruction test including Ultrasonic Pulse Velocity test, Concrete core tests, Schmidt Hammer tests, etc.

4.6 Laboratory tests, Thermo Gravimetric Analysis (TGA) Differential Thermal Analysis (DTA), X-Ray Diffraction (DRD).

#### 5. Classification based on Intensity and type of Damage

5.1 Superficial repairs, consisting of cement plaster etc.

5.2 General repairs, consisting of cement based polymer, modified mortar/Epoxy mortar.

5.3 Principle repairs, consisting of shotcreting in slabs/beams, structural jacketing, epoxy etc.

5.4 Major structural repairs, consisting of demolition, recasting and strengthening, retrofitting.

#### 6. Lessons learnt

The work was completed in 18 months with an estimated cost of Rs 270 Million, economy was ensured in time and cost.

6.1 A view was taken to entrust the work to the same agency which was earlier responsible for looking after the building. It increased the involvement of the agency and prevented witch hunting.

6.2 Though visually it seemed that the whole structure needed demolition, yet on carrying out scientific inspections it was found contrary to the earlier belief.

6.3 Non-structural elements like doors, windows, AC ceiling, contribute to the fire load and fire spread in the building. Thus a need to be vigilant in their use.

6.4 The faults in the working of Electric and AC installation and fire detection system are one of the primary sources of fire incidence.

6.5 As the building was a composite structure of Brick, RCC, Steel trussed roof, it posed complex problems of design and retrofitting.

6.6 A systematic approach with a multi-disciplinary team is very essential in assessing the fire damage and rehabilitation.

6.7 The silver lining to the dark cloud was capitalized by using the incident as an opportunity for giving better and modern facilities.

6.8 While it is always important to find out the causes of fire, it is more important to take steps at the earliest to remove the image of the Catastrophe. Thus, speed in rehabilitation was prime concern.

6.9 It was found that some materials have theoretically independent properties but when used as composite structures, they behave differently.

6.10 Though the design and structural strength are universal but the valuation has to be based on local understanding and safety factors.

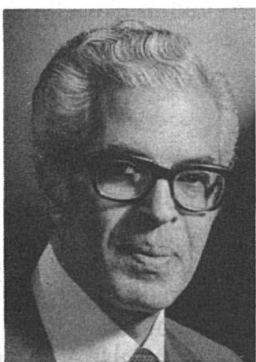
6.11 Passive design options while planning and designing of building are the first safeguard for self containment, not only for fire damage but for any other eventuality like earthquakes.

6.12 Structural fire preventive measures need to be seriously considered in design of buildings. Greater stress should be laid in design by using the thick, well covered structural elements, which afford inherent fire protection of Structures and area available.

6.13 Proper documentation and availability of structural designs of the building enabled the teams to correctly assess the reserve capacities of the structural elements.

## Connection of Steel Beams to Concrete-Filled Tubular Columns

**Hassan SHAKIR-KHALIL**  
 Division of Civil Engineering  
 University of Manchester  
 Manchester, England



Hassan Shakir-Khalil received his BSc and MSc degrees in Civil Engineering from the University of Cairo, Egypt. He obtained his PhD degree from the University of Cambridge, England, UK. He has been researching in the field of concrete-filled tubular columns for the last 15 years.

### Summary

Tests have been carried out on 36 full scale beam-to-column connections. The connections were manufactured by connecting steel beams to concrete-filled tubular columns through either finplate or T-cleat connections. The columns used were either circular or rectangular (CHS & RHS) hollow steel sections. Except for the last eight specimens, all the other test specimens were symmetrically loaded.

### Experimental Work and Numerical Analysis

Table 1 gives a summary of all 36 specimens tested in this experimental investigation. The column tubing of all specimens is 2.8m long, and the column lengths have 15mm thick end plates. The side beams connected to the test specimens of series A-E were symmetrically loaded. However, the eight specimens of series 'F' had either one side beam, or their side beams were unsymmetrically loaded. The webs of the side beams of series A-D were bolted to 10mm thick finplates which had been welded to the columns. Finplates were replaced by T-cleats in series E&F as a result of the large out-of-plane deformations of the RHS walls to which the finplates were welded. Both types of connections are shown in Fig 1.

Figure 2 shows a schematic view of the test rig and test specimen. The rig consists of a base and an upper cross-head connected together by four vertical ties of steel hollow section. The rig is self contained, and the base is securely bolted to the laboratory strong floor. The rig has a head room of about 3m. The loads applied to the side beams by the hydraulic jacks are transferred to the beams through a platform and load cells. The loading platform was used in order to maintain the location of the jacks and at the same time to be able to apply the beam loads at any required eccentricity by simply moving the load cells to the new locations. The beam loads were applied at varied distances from the centre of the column. The beam and column loads,  $P_2$  and  $P_1$ , were increased proportionately, and the beam-to-column load ratio was mainly taken either 1:8 or 1:5.

The rig was originally designed for testing the symmetrically loaded specimens of series A-E, and was thus provided with no lateral bracing. A triangulated, stiff in-plane bracing, not shown in Fig. 2, was therefore welded between the vertical ties in order to ensure the lateral stability of the test rig before testing the unsymmetrically loaded beam-to-column connections of test series F. During the test procedure, all specimens were also laterally restrained at mid-

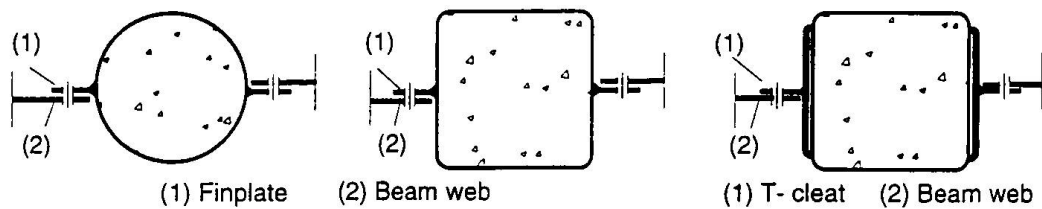


Fig.1 Finplate and T-Cleat Connections

height as shown by '7' in Fig. 2. This lateral restraint was connected at its other end to a stiff bracing system which was securely connected to the strong floor.

The test specimens were provided with electric resistance strain gauges and displacement transducers. The displacements were measured in the plane of loading and also transverse to the loading plane. Displacement transducers were also placed against the column end plates to record the column shortening and end rotations. The strain measurements were carried out over distances equal to three times and twice the lateral dimension of the steel hollow section above and below the finplate/T-cleat positions respectively, an arrangement that was found to be satisfactory.

The ABAQUS software package was used to model the test specimens of series 'F'. It can be seen from the numerical model shown in Fig. 3, that the side beams were not modelled, and neither were the bolt holes in the connection. The T-cleat stem was extended to model the beam, and the numerical model was only used to predict the overall column failure. The boundary conditions at the top of the numerical model were similar to the experimental end conditions in which the top end of the column was fixed in position, and was allowed to rotate freely only in the plane of loading. However, the central nodes at the lower end of the model, and also at its mid-height, were allowed to move vertically, thus allowing for column shortening.

The numerical model has 48 concrete brick elements (C3D20), 96 steel shell elements (S8R) for the RHS steel tube, 16 steel shell elements (S8R) for the T-cleat flanges, 32 steel shell elements (S8R) for the T-cleat stems and 8 rigid brick elements (C3D20) for the end loading plates. In all, the model has 200 elements and 1081 nodes.

Series	Column Size	Type of Connect.	No. of Spec.	Connect. Loading
A	168.3x5CHS	Finplate	8	e2=e1
B	150x150x5RHS	"	8	"
C	219.1x6.3CHS	"	2	"
D	200x200x6.3RHS	"	2	"
E	150x150x5RHS	T-Cleat	8	"
FI	150x150x5RHS	"	4	e2=0.0
FII	150x150x5RHS	"	4	e2<e1

Table 1 Summary of Test Series

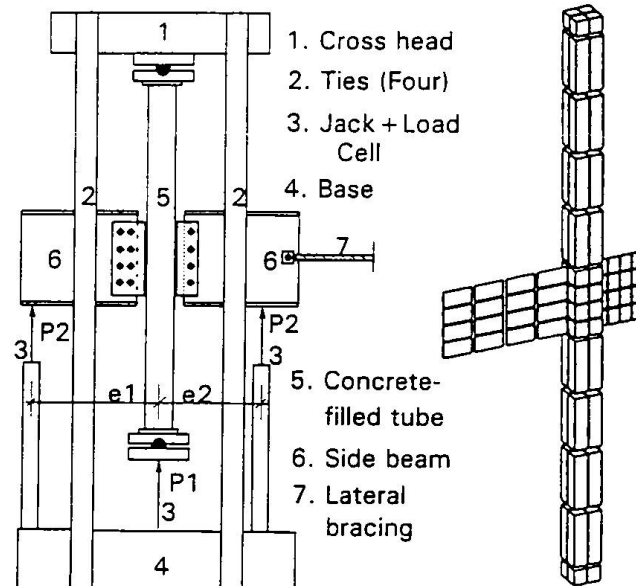


Fig.2 Test Rig and Specimen      Fig.3 Num. Model

Fig.3 Num. Model

## Column-Pile Joints Made of Steel Pipes Filled with Concrete

**Hideaki TAKANO**  
Civil Engineer  
Company Joshin-etsu  
Takasaki, Japan



Hideaki Takano born 1955,  
Complete the Department of  
Junior College Nihon University.

### Summary

For a connection of a column and pile made of concrete-filled steel pipes with different diameters, a simple overlap joint in which a smaller diameter pipe is inserted by the specific length to a larger diameter pipe with concrete filled between them has been proposed as an economical and effective joint system. The experiments indicate that the method to predict the ultimate loads of the present joints has been proposed.

### 1. Test Program

As illustrated in Fig.1, cantilevers of concrete-filled steel pipes (CFSPs) having the present overlap joints are loaded at the top of the column.

### 2. Proposed Model for Prediction of Ultimate Load

Judging from the failure processes of the present joints, it is considered that the bending moment and shear force applied to the column are carried by the couple forces of horizontal bearing pressure and friction developed on the embedded part of the column. Therefore, the authors try to predict the ultimate load of the joints by assuming a load-carrying model illustrated in Fig.2, based on experimental observations of the present tests and finite element analyses previously carried out.

#### 2.1 Balance of moment

From the balance of the moment shown in Fig. 2,

$$M - T \left( \frac{2\sqrt{2}}{\pi} \right) d = - \frac{LP^2}{3(2P - Q)} + (P - Q) \frac{L(5P - 2Q)}{3(2P - Q)} \quad (1)$$

where  $M$  and  $Q$  are bending moment and shear force applied to the column respectively, and  $P$  and  $T$  are resultant forces of bearing pressure and frictional stresses developed on the column respectively. In the above equation, the friction is assumed to be developed on one-fourth the circumference of column on tensile and compressive sides respectively.

#### 2.2 Frictional force at ultimate states

The frictional stresses developed between the column pipe and the concrete filled are assumed to be subject to Coulomb's friction criteria. That is;

$$\tau_{\max} = c + \sigma_n \tan \phi \quad (2)$$

$\tau_{\max}$  : maximum frictional stresses  $\sigma_n$  : normal stresses at the interface

$c$  : cohesion of friction  $\phi$  : friction angle

Then, a resultant force of frictional stresses  $T$  is described as follows;

$$T = c \frac{\pi}{4} d L \frac{P - Q}{2P - Q} + \frac{\pi}{2\sqrt{2}} (P - Q) \tan \phi \quad (3)$$

### 2.3 Bearing pressure at ultimate states

The bearing pressure developed on the column is assumed to be determined by shear capacities of the shear panels which consist of the pile pipe and annular concrete in the overlapped part with the length of  $L$ . Therefore, the bearing pressure is described as follows;

$$P = V_s + V_c \quad \dots \dots \dots (4)$$

where  $V_s$  is a shear capacity carried by steel pipe and  $V_c$  is a shear capacity carried by annular concrete.

The shear capacity of the pile pipe is to be calculated as follows;

When the couple force of bearing pressure is applied to the pile pipe, the tensile force band with the width of  $2/3L$  is assumed to be formed on the lateral panel of the pile pipe in the direction from the center of action of the total bearing pressure on the compressive side to that on the tensile side. At the ultimate states, the tensile force band yields in full. Then,

$$V_s = f_y \cdot 2t \cdot \frac{D'}{\sqrt{\left(\frac{2}{3}L\right)^2 + D'^2}} \left(\frac{2}{3}L\right) \quad \dots \dots \dots (5) \quad \text{where } D' = \frac{\pi}{4} D$$

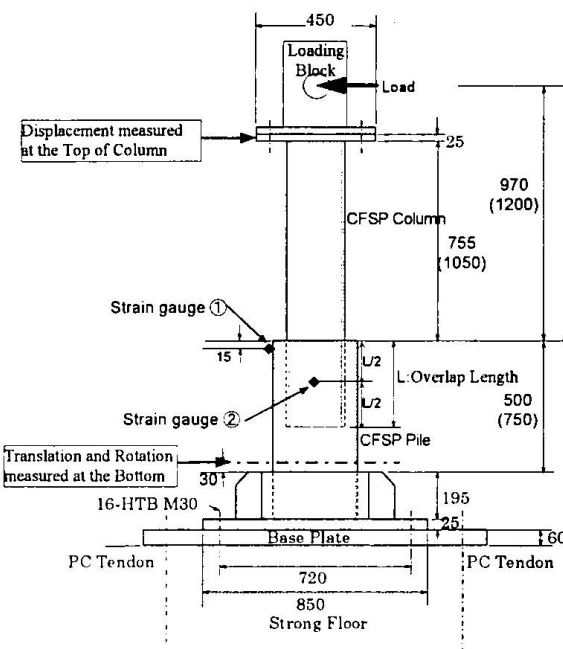


Fig. 1 Description of Test

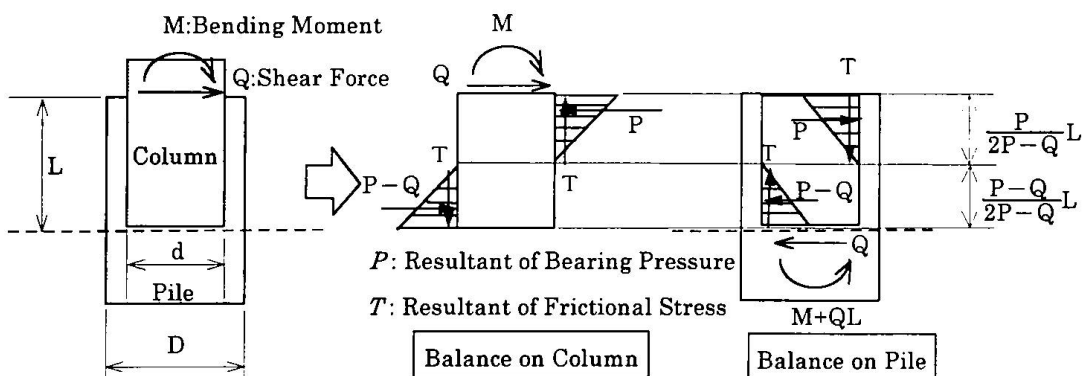


Fig. 2 Load Carrying Model for Predicting Ultimate Loads

On the other hand, because in the experiment the annular concrete was pulled out of the pile pipe, the shear capacity carried by the annular concrete is determined by the resisting force which prevents the concrete from being pulled out.

Therefore, the shear capacity  $V_c$  is;

$$V_c = \frac{3\sqrt{2}}{\pi} \frac{D}{L} \left\{ \frac{\pi}{4} D \cdot [L - (D - d)/2] \cdot c - \frac{\pi}{4} d \frac{L}{2} c \right\} \quad \dots \dots \dots (6)$$

Consequently, the ultimate load can be calculated by solving equation (1) after substituting (3), (4), (5) and (6) into (1).

The calculation yields a satisfactory good approximation to the experimental ultimate loads, though some underestimation occurs.

## Behaviour of the Composite Beam-to-Steel H Column Connection

**Akira MATSUO**

Dr. Eng.

Hiroshima Univ.

Higashi-Hiroshima, Japan

**Yuji NAKAMURA**

Ph.D.

Hiroshima Univ.

Higashi-Hiroshima, Japan

**Rafeek W. SALIB**

Dr. Eng.

Suez Canal Univ.

Port Said, Egypt

**Yoshimasa MATSUI**

Dr. Eng., Civil Engineer

Keisoku Research Consultant

Hiroshima, Japan

### Summary

The main purposes of this paper are to know the behavior of the composite beam-to-steel H column connection and to give the shear yielding and maximum strengths and panel moment  $M_p$ - shear deformation  $\gamma$  relation. The maximum strength is formulated through limit analysis. The panel moment - shear deformation relation is formulated considering the Bauschinger effect and the isotropic and kinematic hardening rule.

### 1. Introduction

It is well known that a concrete slab connected to a steel beam increases the stiffness and strength of the beam. It is also presumable that the concrete slab increases the shear stiffness and strength of the beam-to-column connection. The shear strength and the panel moment  $M_p$ - shear deformation  $\gamma$  relation of bare steel beam-to-column connections are presented(Matsu, 1995). However, the yield strength of the panel with a concrete slab is 20 to 40% larger than the bare steel connection(Nakao, 1984). This paper presents the experimental results and the formulation of the shear strengths and  $M_p$ -  $\gamma$  relation considering the effects of the concrete slab.

### 2. Experimental Plan and Results

The experimental parameters are the shapes(X-type, T-type of frames), member strength(weak beam, weak column), the ratio of the panel yield strength to other members( $R_{py} \approx 0, 0.5, 0.7$ ), aspect ratio( $H_b/H_c = 1.0, 1.5$ ) and displacement ratio( $\delta^-/\delta^+ = 1.0, 1.2$ ).  $\delta^-$  and  $\delta^+$  are the displacements of the loading points of the negative and positive bending beams. For example, the specimen X10B45-10 indicates X-type,  $H_b/H_c = 1.0$ , weak beam,  $R_{py} = 0.45$  and  $\delta^-/\delta^+ = 1.0$ . Experimental results of the 13 specimens are listed in Tab.1, where  $M_{py}^p$  and  $M_{ue}^p$  are the experimental yield and maximum panel strengths respectively. An experimental  $M_p$ -  $\gamma$  relation is shown in Fig.1

### 3. Analytical Strength and $M_p$ - $\gamma$ Model of the Panel

Analytical yield strength  $M_{py}^p$  is obtained by Eq.1 following to Nakao(1987).  $M_{b1}, M_{b2}, Q_c$  and  $V_p$  are negative and positive face moment in the beam, column shear force and an effective volume of the panel.  $M_{py}^p$  predicts the experimental  $M_{py}^p$  fairly well in Tab.1. It is well known that the load carrying capacity of the panel increases after yielding, which is caused by strain hardening effect of the steel plate and direct transmission  $M_p$  of the bending moment from the beam to column through 4 corners of the panel and concrete slab. Changing each parameter in Eqs.2 the ultimate strength of  $M_p$  is given as the minimum value of  $M_p^+ + M_p^-$  (Eqs.2) which is derived from the plastic deformations illustrated in Fig.2. In Eqs.2  $L_c$ ,  $L_b$ ,  $\sigma_{yw}$  and  $t_{wb}$  are the lengths of the column and beam, the yield stress and thickness of the beam web. As an approximate value  $M_p^+ = M_p^- + C_u d$  is also given by neglecting the axial deformations of the beam flanges( $n=0$ ). The total strength of the connection is given by Eq.3. The panel strength when the concrete slab is crashed is given by  $(\tau_y + \tau_u) V_p / 2$ , as the crash of the concrete slab started at an early stage. The compressive strength  $C_u$  of the concrete at the face of the column flange is obtained as follows.

Eqs.2 and 3 are first applied to the specimens which have no panel plate and  $1.4F_c A_c$  is found as the most appropriate value of  $C_u$ , where  $F_c$  and  $A_c$  are the compressive strength of concrete and the area of the flange in contact with the slab. This  $C_u$  is also used for the other cases where the connection has the panel plate. In Tab.1  $M_{uc1}$  and  $M_{uc2}$  correspond to the maximum strengths calculated, considering and neglecting the axial deformation  $\epsilon$  of the beam flanges. Both  $M_{uc1}$  and  $M_{uc2}$  predict the experimental strength well. Judging from Eq.3 in case of  $n=0$  the resisting panel moment corresponding to the current shear deformation  $\gamma$  consists of  $\tau V_p M_s$  and  $Cd$ , where  $\tau$ ,  $V_p$ ,  $M_s$  and  $C$  are the resisting shear stress of the panel, the bending moment transmitted through the 4 corners of the panel and the compressive force of the slab corresponding to  $\gamma$ .  $M-\gamma$  relations are formulated as follows.  $\tau V_p - \gamma$  and  $M_s - \gamma$  relations are separately formulated as two springs connected in series. Each spring is given as a bi-linear type and satisfies the isotropic and kinematic hardening rule (Tsuji, 1988). The compressive force  $C$  to the contraction  $\Delta$  ( $=\gamma d$ ) relation of the slab is followed to Shiga (1988). Predicted  $M-\gamma$  relation is shown in Fig.1.

$$\tau = [M_{b1} + M_{b2} H_b / (H_b + d') - Q_c H_b] / V \quad (1)$$

$$F^M = 2 S a (a+b-c)^2 / b + 2 (1+a/b) (M_{ubf} + M_{ucf}) + 2 a (M_{pbf} + M_{pcf}) / b \quad (2a)$$

$$P_M^+ = [ (S a (a+b-c)^2 (2+k_2(2-H_b/2a))/b + M_{ubf} k_2 Z (2+(nN_{ubf}/2M_{ubf})^2 (1+((H_b+Z)/Z)^2)))/n + 2M_{pbf} a (1+k_2)/b + M_{ucf} (2k_1 + (2k_1-H_b/b)k_2) + M_{pcf} a (2+k_2(2-H_b/a))/b + C_u ((-Z+d')k_2+d')] / (1+k_2(1-H_c/L_b)/k_3) \quad (2b)$$

where  $k_1 = 1+a/b$ ,  $k_2 = k_1 n / (Z - k_1 n)$ ,  $k_3 = 1 - H_b / L_c \cdot H_c / L_b$ ,  $n = eZ / (Hb + Z)\theta$  and  $S = \sigma_{ww} t_w$

$$M_u = (\tau_y + \tau_u) V_p / 2 + M_F + M_{F'} \quad (3)$$

## REFERENCES

1) Nakao M.: Annual conference of AIJ, (1982) 1869-1870, (1983) 1259-1260, (1984) 1565-1566, (1987) 905-906 2) Matsuo A.: IABSE Symposium San Fransisco, (1995) 1435-1440 3) Tsuji B.: Transactions of AIJ, No.270 (1978) 17-22, 4) Inoue K.: Annual conference of AIJ, (1995) 523-524, 5) Shiga T.: Annual conference of AIJ, (1986) 377-378

Tab.1 Experimental and analytical results (unit: tmm)

Specimens	pMyc	pMyc	pMyc/pMyc	pMue	pMuc1	pMuc1/pMue	pMuc2	pMuc1/pMue
X10B45-10	7167	7116	0.993	12021	13221	1.100	12170	1.012
X10B45-12	6333	6944	1.096	12839	13465	1.048	12293	0.957
X10B67-12	10850	10748	0.991	17257	17608	1.020	16436	0.952
X10B00-10	-	-	-	5822	6965	1.196	5914	1.016
X10B00-12M	-	-	-	5662	7209	1.273	6037	1.066
X15C33-10	9800	9724	0.992	18872	17725	0.939	16522	0.875
X15C33-12	9200	9338	1.015	18710	17725	0.947	16522	0.883
X15C66-10	18667	20244	1.084	31030	28762	0.927	27559	0.888
X15C00-10	-	-	-	6600	8292	1.256	7089	1.074
X15C00-10M	-	-	-	6642	8292	1.248	7089	1.067
T15B59	8850	8781	0.992	15602	17092	1.096	15658	1.004
T15B77	11700	11905	1.018	20618	21030	1.020	19596	0.950
T15B00	-	-	-	6259	7659	1.224	6225	0.996

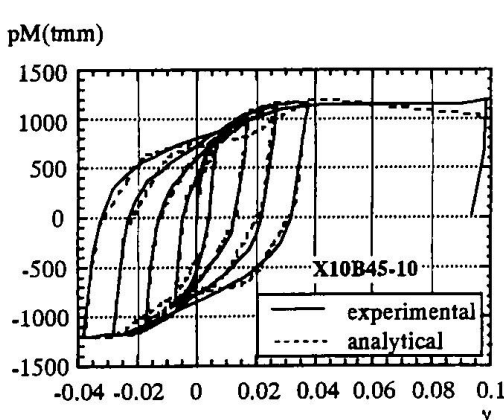


Fig. 1  $pM$ - $\gamma$  relation of panel

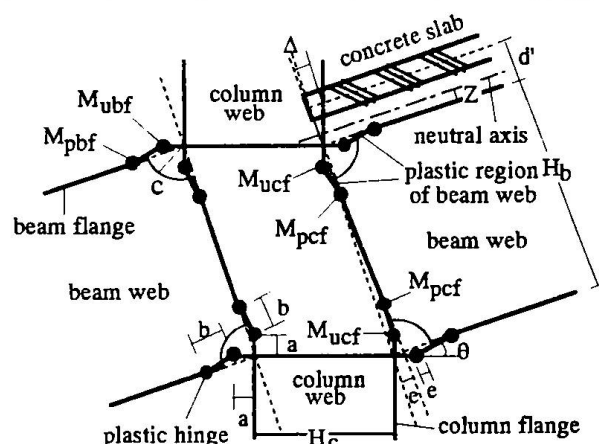


Fig.2 Plastic deformation of the connection

## Composite Rahmen Railway Viaduct of PPC Beam and Steel Box Beam

**Harumi TABATA**

Assistant Manager  
East Japan Railway Co.  
Tokyo, Japan

**Tadayoshi ISHIBASHI**

Dr. Engineer  
East Japan Railway Co.  
Tokyo, Japan

**Norio KAMATA**

Deputy Manager  
East Japan Railway Co.  
Tokyo, Japan

**Yasuaki HOSOKAWA**

Assistant Manager  
East Japan Railway Co.  
Tokyo, Japan

### Summary

The railway viaduct required aesthetic improvements, as the space under the bridge was to be used as a footpath, so it was required to reduce both the number of pillars on this viaduct and, further, to reduce the diameter of the pillars. Consequently, the beams were basically constructed in the form of a PPC box-type, and at places where the bridge is long, the structure fashioned as a steel box beam. The piers were made of steel pipe wound RC pillars. In order to increase the bridge's anti-earthquake properties, the structure was converted to a complex Rahmen viaduct which is unified between these 2 types of beams and piers. This report describes the materials and design of these connectors.

### 1. Circumstances

At the time of Nagano Winter Olympic Games in 1998, the Hokuriku Super Express will be extended to Tokyo Station. To accommodate this extension, a railway viaduct on the Chuo-Line (about 970 m in length) is to be constructed. This viaduct was constructed taking into considerations the scenery surrounding the Tokyo Station which is noteworthy as the gateway of Japan (Figure-1).

### 2. Whole structure

The pillars of this viaduct were made of reinforced concrete (RC) on the railway side and steel pipe wound RC on the road side, making the shape on each side very different (Figure-2). If a pier is made into a single gate-type structure, when a large sideways horizontal force is applied such as in the case of an earthquake, because of the difference in displacement in the upper end of the pier, a large distortion occurs in the pier. For this reason, the entire viaduct was made into a Rahmen structure of multiple lengths, and the rigidity of the entire body (against plane distortion) was increased.

### 3. Connection of beam and pier

As for the structural form of the upper area, the general parts were made of PPC beam, but the parts of the crossing over the road were made of steel box beam because the length of bridge was relatively long (39 m.) The viaduct was in the form of a complex Rahmen structure which unified 2 types of beams as well as the crossbeams of the piers. The connecting part of the beam and the pier is shown in Figure-3. The design of the connecting part was made so as to secure an adequate

safety ratio ( $F=1.0$ ) against the destruction of the cross section material, and to prevent stretching stress at the time of active load effects, considering the influence of temperature. As an example of PC cable arranged to this connecting part, there is a 12E15.2×6 set at the upper position of original point.



Figure-1 Viaduct completion forecast picture

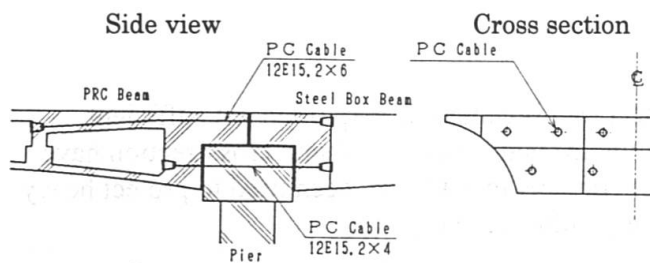


Figure-3 Connecting parts between beam and pier

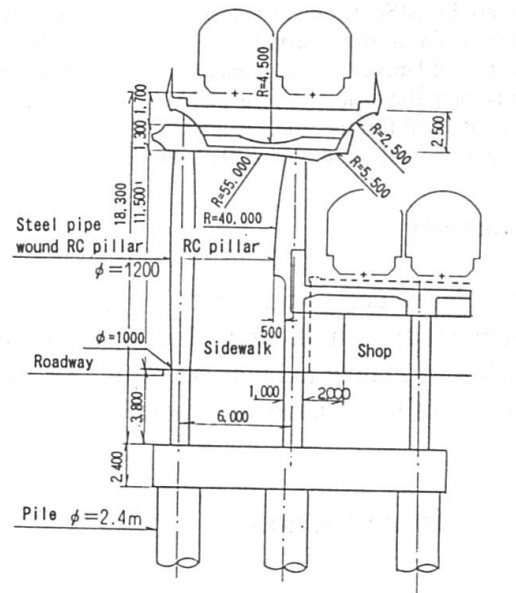


Figure-2 Cross section of viaduct (unit:mm)

#### 4. Connections between steel pipe wound RC pillars and footings

As shown in Figure 1, the pillars of the viaduct on the left side were planned between the road and the footpath. Therefore, the pillar was to be made as thin as possible in order not to obstruct the passage of pedestrians. To cope with these demands, and considering the scenery, the pillars were made to a diameter of 1.0 meter on both ends and 1.2 meters in the center in the shape of an entasis (shaped like a cigar.) As for the constitution of the cross-sections of the pillars, steel pipes were used as Stirrup, and steel pipe wound RC pillar were constructed so as to allot the stretching forces to the iron bars in the concrete. In order to decide the arrangement of the iron bars at the connecting part of the upper crossway beam and steel pipe wound RC, experiments in horizontal load changing, using a 1/3-size model; results were applied to the actual design.

#### 5. Postscript

Investigations were made in accordance with the above descriptions; the particular nature of each structure was determined, and the structure was erected. This viaduct was completed in November, 1996, and the train is currently in operation. The Hokuriku Super Express will begin operation starting in Autumn, 1997.

## Punching Failure Mechanism of Composite Slab-Column Joints

### Andrzej B. AJDUKIEWICZ

Professor in Struct. Eng.  
Silesian University  
Gliwice, Poland

He got his MSc degree (1961) and PhD (1968) at the Silesian Technical University. At present he is there the head of Department of Structural Engineering. Author of several books and over 130 papers.

### Alina T. KLISZCZEWICZ

Assistant Professor, PhD, CE  
Silesian University  
Gliwice, Poland

She was graduated in 1972 and got her PhD in 1984 from STU. The author of over 60 papers and the leader of research projects.

### Jacek S. HULIMKA

Assistant, MSc, CE  
Silesian University  
Gliwice, Poland

He got his MSc degree in 1987 from STU. Involved in experimental research on concrete structures.

### Summary

The idea of composite joints in slab-column skeletal structures deals with introduction of precast members from high-strength concrete as combined head-and-column elements. As behaviour of such joints under axial or eccentric loads has not been clarified, therefore the series of full-scale models of joints have been tested up to failure to obtain basic data about the failure mechanism.

### 1. Introduction

The carrying capacity of flat-plates without shear reinforcement is very often not sufficient, particularly at interior column supports. Recently, in such cases the column cross-section have been enlarged or the special shear reinforcement or steel inserts have been used to protect heavy stressed support zones against the rapid punching failure (see [1]).

On the other side, the tests of monolithic slab-column joints indicated the significant role of compressive strength and deformability of concrete in slab around the column face, where biaxial compression was stated [2]. Therefore, application of high-strength concrete should be considered as the simplest method of the zone strengthening [3],[4]. The idea of composite structure with precast head-and-column elements from HSC (e.g. C70 or C80) and the remaining parts of slab from ordinary concrete was proposed in the first row for simple multi-storey buildings, like car-parks [5]. At least two benefits in such buildings are expected: the support zones strong enough without additional shear reinforcement and reduction of column sections.

To introduce the idea into the practice some designers' doubts should be clarified. The behaviour of such joints up to failure as well as carrying capacity of joints must be tested on full-scale models (to omit the size effects). Synthesis of observations from the tests of first series of six models are presented in this paper.

### 2. Test Observations

In monolithic joints (Fig.1a) axisymmetrically loaded up to punching failure the shape of failure surfaces are always observed as truncated cones. The inclination  $\alpha$  of basic crack depends mainly on the flexural reinforcement ratio and oscillate from  $25^0$  to  $35^0$ .

In composite joints, in which the difference in concrete strength in members was not significant and both concretes were from the range of normal-strength concrete (e.g. C30 in head and C15 in slab) the behaviour at failure was very similar to that in monolithic joints (Fig.1b). The difference in failure crack was small: angle  $\alpha \approx \beta$  from  $32^\circ$  to  $36^\circ$ .

Quite different situation was recorded in tests of models with relatively strong heads - precast parts from concrete about C70 and monolithic slab from ordinary concrete C15. The failure was observed in two phases. The main top crack in slab occurred earlier at about 60% of ultimate load as a first phase of punching. The second phase was observed as sudden, noisy crack at the maximum recorded load. After cutting reinforcement the failure surface in the shape of double truncated cone was uncovered (Fig.1c). The angle  $\alpha$  was from  $40^\circ$  to  $48^\circ$ , while the angle  $\beta$  was from  $19^\circ$  to  $21^\circ$ . The value of ultimate punching load in this case was about 10% greater than that in case presented in Fig.1b, at the same ratio of flexural reinforcement in both cases.

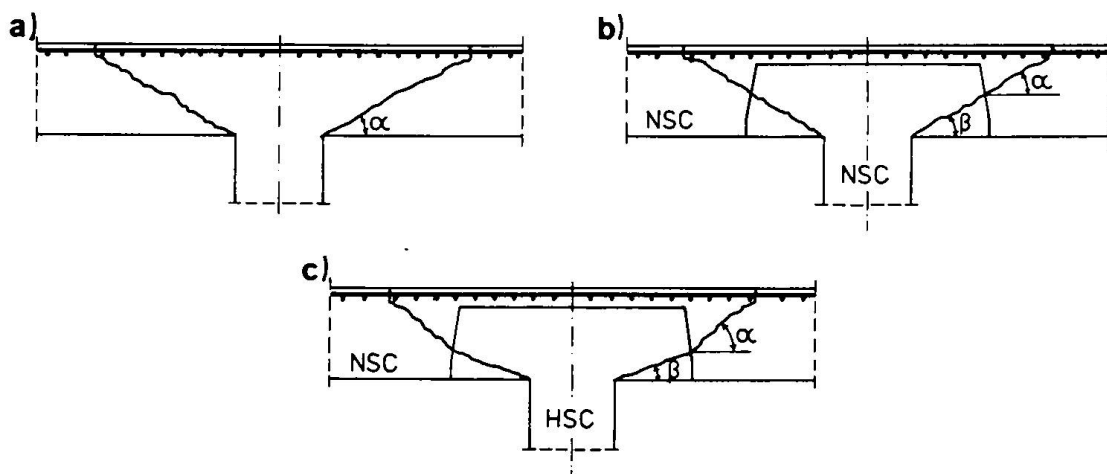


Fig.1. Recorded shapes of failure surface in axisymmetrical punching shear of models

### 3. Conclusions

The behaviour of composite slab-column joints with HSC head-and-column members was observed significantly different from that known from monolithic joints. The two-phase failure of such composite joints was recognized as more advantageous due to the warning signal than the increment in the final punching resistance.

### References

- [1] Ajudkiewicz A., Starosolski W.: *Reinforced-Concrete Slab-Column Structures*. Elsevier, Amsterdam-Oxford-New York-Tokyo, 1990, p.XXIV+372.
- [2] Broms C.E.: *Punching of Flat Plates - A Question of Concrete Properties in Biaxial Compression and Size Effect*. ACI Structural Journal, V.87, No 3, 1990, pp.292-304.
- [3] Ajudkiewicz A., Kliszczewicz A.: *Application of High-Strength Concrete in Composite Skeletal Structures*. Third Int. Symposium on Utilization of High Strength Concrete, Lillehammer, 20-24 June 1993, pp.449-456.
- [4] Hallgren M.: *Punching Shear Capacity of Reinforced High Strength Concrete Slabs*. Doct.Thesis. The Royal Institute of Technology, Stockholm, 1996, p.206.
- [5] Ajudkiewicz A., Kliszczewicz A.: *Simple Construction of Composite Slab-Column Structures*. Proc. of 15th IABSE Congress, 16-20 June 1996, Copenhagen, pp.589-584.

The Antrenas bridge is located in the department of Ardèche, in the south of France. It is a single-span bridge with a total length of 86 m and a width of 11 m. The bridge is a composite structure, consisting of a tubular steel arch and a ribbed concrete slab. The arch is supported by two concrete piers, each with a height of 15 m and a width of 8 m. The bridge is located in a valley, with a river flowing underneath it. The surrounding landscape is hilly and forested.

## The Antrenas Tubular Arch Bridge

### J. BERTHELLEMY

Senior Engineer

S.E.T.R.A.

Bagneux, France

Born 1957, TPE civil

engineering degree 1979.

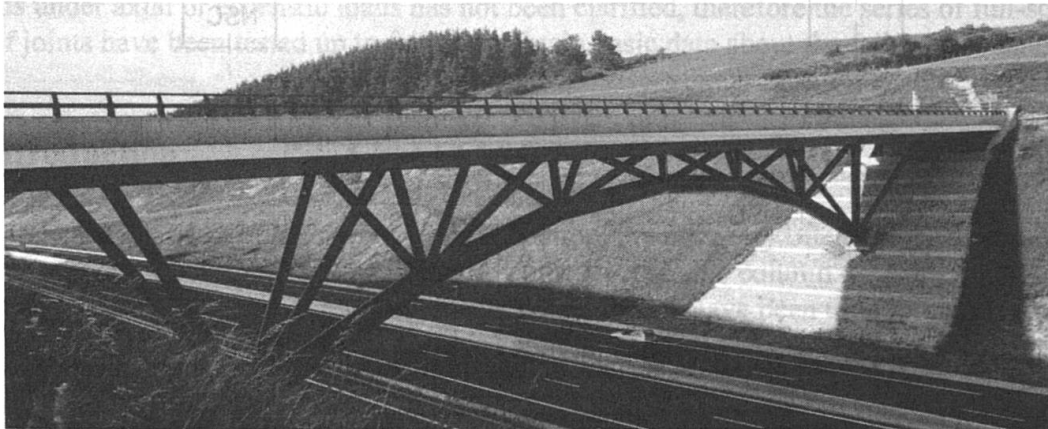
He joined SETRA in 1980.

Experience in steel bridges and their pathology. He has been involved in the design of innovative composite bridges.

### 1. Presentation

Antrenas bridge is original and innovative. The tubular steel skeleton is an arch connected to a prestressed concrete slab to achieve a composite structure which is also a truss. Steel arch principal tube is filled with reinforced concrete, which again creates local composite elements.

The bridge is set in a remarkable landscape where the A75 motorway crosses the Gévaudan. The A75 cuts a dissymmetrical gap through the granite ridge to a depth of about 15 metres for a width of 85 metres at the top. The western slope of A75 is one metre higher than the eastern slope.



The bridge carries a 11 metres wide roadway. Its total length is 86 metres between the end support axes. It is designed to give the passage to exceptionally heavy 110-ton trucks.

The bridge alignment is straight; it is perpendicular to the motorway axis. The tube keeps a 4.85 metres height clearance for traffic over the entire width of the motorway as well as over the access road. Its longitudinal profile has a one per cent slope.

### 2. General design

The bridge consists of a single tubular steel arch with a 56 metres long span, whose overall shape is parabolic, with a mean radius of approximately 60 metres. The deck is a ribbed concrete slab. Two longitudinal concrete ribs are supported by steel struts joining arch and deck.

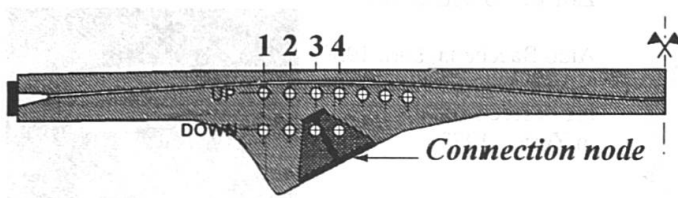
The steel tube of the arch has a circular section with a 1.2-metre diameter. Its sheet is 32 millimetres thick. This tube is located in the transversal symmetry plan of the structure, and rests on foundation blocks embedded in the slopes.

A steel propping system was developed to support the formwork for concreting the deck. Transferring the load from the temporary steel scaffolding props to the steel arch was a delicate operation requiring various jacking sequences.

To compensate the shortening effects of the arch under permanent loads, it was decided to jack it 25 millimetres at each of its springs. This reduced horizontal slipping thrusts in the punctual connection nodes.

The deck has a total width of 11 metres. The slab has a mean thickness of approximately 35 centimetres. At the ribs the maximum thickness is 95 centimetres.

The deck is longitudinally prestressed by seven pairs of 12\_T15\_S tendons running from end to end. This slab is also prestressed in the transverse direction by 4\_T15\_S tendons. Two tendons are positioned over each local steel node connecting concrete ribs and tubular skeleton's struts. As shown below, those punctual nodes are sunken in the concrete ribs.



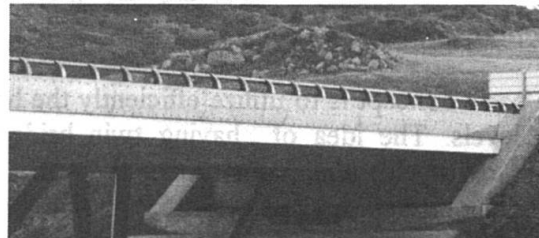
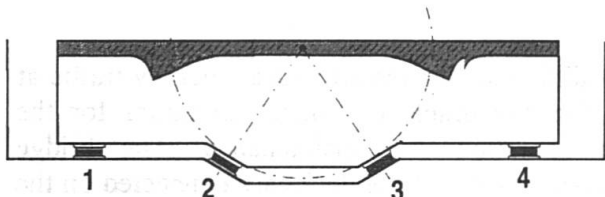
**Longitudinal 7 tendons disposition :**

**4 of them are undulating tendons:**

**UP : position at connection nodes**

**DOWN : position between punctual connection nodes supporting deck.**

The bearing system at the abutments provides sideways locking as well as taking up the vertical forces. Each cross-beam at the abutments is a counterweight on four neoprene bearings. Shear forces are very low in those neoprene bearings, even in the inclined ones.



**Roles of bearings :**

**1 - 2 - 3 - 4 : vertical load blocking**

**1 and 4 : torsion blocking**

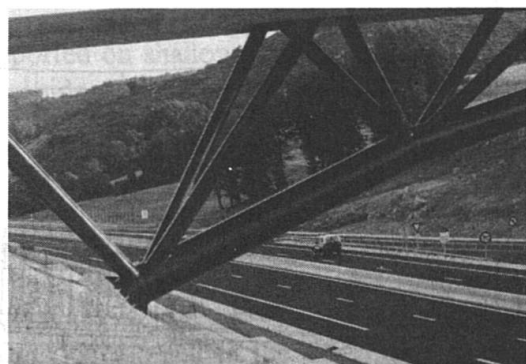
**- 2 and 3 : lateral load blocking.**

### 3. Design of the tubular steel framework

Because most of the bridge mass is in the slab, and not in the arch, it is preferable to give the arch a polygonal profile, almost perfectly funicular in transmitting permanent loads. Furthermore, from the economic standpoint, a non-developable toric shape could not be achieved under acceptable conditions with a 32 millimetres thick steel sheet.

Straight tube sections were therefore positioned between two successive butt welded joints at nodes.

It was decided to fill the bottom parts of the arch with concrete to improve the structure's resistance to collisions with outsize vehicles.



### 4. Conclusion

The contract, for a value of 11.3 million francs and an overall execution time of 16 months, was signed with the contractors **GTM** and **Richard-Ducros**. At a slightly higher cost than for an ordinary bridge, the Project Manager achieved an exceptional structure, well-suited to the landscape topology. In 1995, the Antrenas Bridge, designed by **SETRA** received the Silver Ribbon Award from the French Ministry of Public Works. Michel Virlogeux and the consulting architects Dezeuze and Zirk were also commended by the French association of steel-building companies called "Syndicat de la Construction Métallique de France" for an Architecture Prize awarded in the road bridges category.

## The Dreirosen Bridge over the Rhine at Basel

**Dialma Jakob BÄNZIGER**  
Civil Engineer  
Bänziger+Bacchetta+Partner  
Zürich, Switzerland

D.J. Bänziger, born 1927,  
received his civil engineer-  
ing degree from the ETH  
in Zürich 1951.



**Aldo BACCHETTA**  
Civil Engineer  
Bänziger+Bacchetta+Partner  
Zürich, Switzerland

Aldo Bacchetta, born 1950,  
received his civil engineer-  
ing degree from the ETH  
in Zürich 1973.



### Summary

The basic concept is to utilize efficiently the height difference for the structure given by traffic at two levels. The idea of having twin bridges offers favourable economic conditions for the structure itself, the constructional work, the operation and maintenance. The bridge superstructure consists of two-storey composite constructions, whose decks are connected on the outside by continuous steel trusses of transparent form.

### 1. Basic Concept

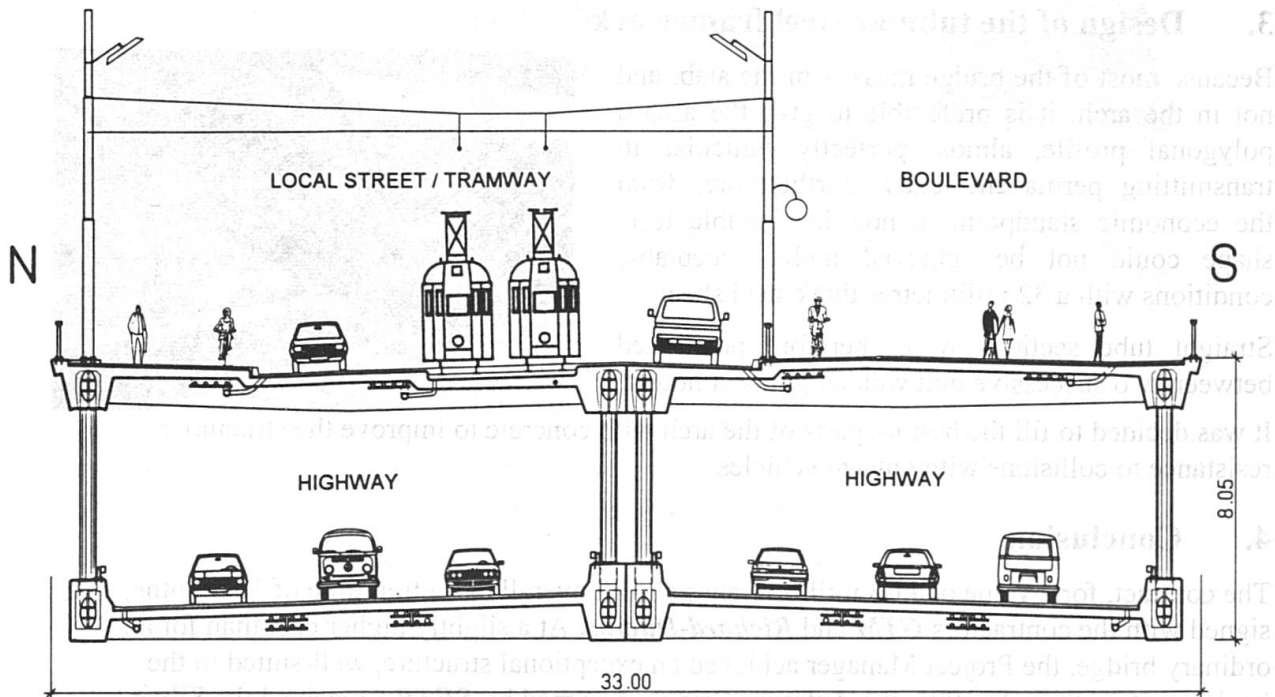


Fig. 1 Cross-section of bridge with the traffic areas

From the point of view of urban construction the rather simple three span structure is impressive visually on account of its delicate truss work providing sufficient transparency to allow viewing both into and through the structure. Two parallel concrete chords, which carry the steel trusses,

emphasize the spanning of the River Rhine. The main elements of the bridge are continued harmoniously into the shore area of Kleinbasel.

The choice of an equal width of the upper and lower levels for constructional and noise protection reasons and a shift of the traffic lanes on the upper level to the northern side leaves on the southern side some considerable space for an attractive boulevard.

## 2. Structure

### 2.1 Bridge Superstructure

By keeping the existing pier axes the spans amount to 77, 105 and 84 m. The total height of 8.05 m and the constructional height between the axes of the upper and lower chords of 6.50 m can thus be kept to a minimum. The slenderness ratio ( $h_k : 1$ ) is 1:16. In order to ensure transparency and throughviewing the truss diagonals were selected to consist of slender concrete-filled steel tubes, which together with the concrete chords form the bridge truss. The dimensions of the concrete chords were chosen such that the joints of the steel truss are perfectly and permanently encased in concrete. The bridge decks comprise longitudinally and transversely prestressed ribbed slabs with a rib spacing of 7.0 m and a span of 14.95 m. The total width of the superstructure is 33.0 m.

### 2.2 Piers and Abutments

The massive piers for the new bridge (40 x 4 m) were constructed at the same place as those for the existing bridge. Only the upper parts of the old piers will be removed. The pier shafts and the caissons will be integrated in the new pier foundations (constructed using bored piles) and the new piers. Both abutments are built up of three parts. They consist of two external and one massive internal pier.

### 2.3 Approach Structures

The approach structures consist of frame structures supported on shallow foundations, of 126 m length on the Grossbasel side and 132 m on the Kleinbasel side.

### 2.4 Constructional Work

The constructional work is based on a division into two independent parts. In a first phase the existing Dreirosen bridge, moved a distance of 15 m upstream, takes the whole of the traffic. In this way one can proceed with the construction of the one half of the bridge at its permanent place. Afterwards the traffic will pass over the new half of the bridge and the second upstream half of the bridge will be constructed in a slightly shifted position after the demolition of the existing bridge. Finally, the new upstream half of the bridge will be manoeuvred hydraulically into an adjacent position next to the new downstream half of the bridge.

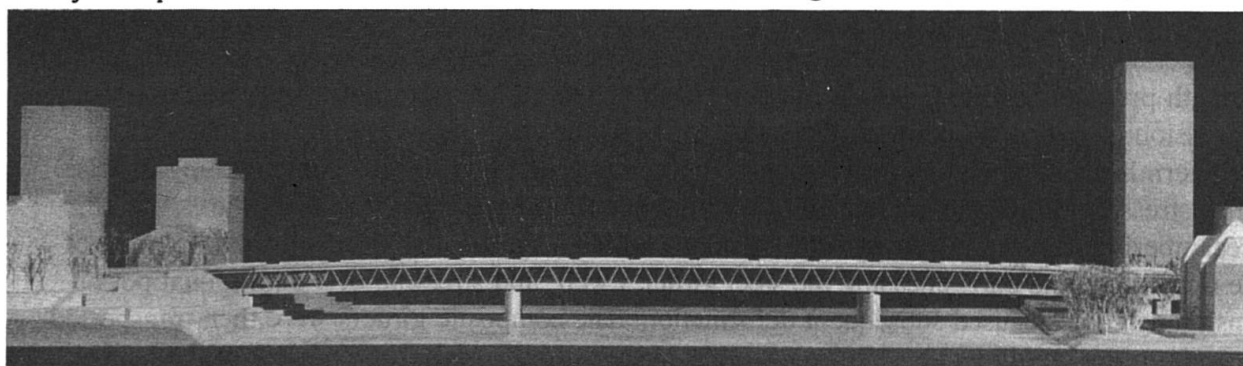


Fig. 2 Photo of Model

## Deformation-Compatibility of Steel Truss and High-Strength Concrete Girders

**Philippe VAN BOGAERT**  
Head of bridge design office  
TUC Rail  
Brussels, Belgium



Philippe Van Bogaert, born 1951, received his civil engineering degree from Ghent University in 1974 and PhD in 1988. He is currently head of bridge design office with TUC Rail Cy - Brussels and professor of Bridge Engineering at Ghent Univ.

### Summary

The railway fly-over at Lot, was built for the crossing of the high-speed railway line from Brussels to Paris over domestic tracks. Its superstructure consisting of lateral composite girders with steel truss elements bolted to the upper flanges, required geometric compatibility of the composite girders and the truss elements. The influence of a set of parameters was examined. From the recordings of all deformation steps, it was found that the composite girders with high-strength concrete showed little time-dependent deformations.

### 1. Structural concept

The railway fly-over at Lot (see fig 1) is located some 7 km to the south of Brussels. It was built for the crossing of the high-speed railway line from Brussels to Paris over domestic tracks. It consists of 16 spans of 42.60 m, the total length of the fly-over becoming 682 m. The fly-over had to be prefabricated entirely, since it was designed to be built over tracks remaining in service. The design of the superstructure is remarkable in this sense that a complete composite structure was built (see the superstructure cross section fig 2). The piers have alternatively a triangular or straight shape. The triangular piers comply with the truss shape of the superstructure and are composite members, resisting the braking and acceleration forces of trains. Two lateral composite girders are equipped with an intermediate reinforced concrete deck plate and transverse stiffening ribs. Steel truss elements are then bolted to the upper flanges of the composite girders.

The lateral girders consist of welded steel I-beams of 2.2 m depth. These are encased in high-strength precast concrete C 80/95. While producing the girders, they were subjected to a succession of stress and deformation states. At first, the steel beams were fabricated with a predetermined initial rise and precambered by concentrated forces, thus compensating the rise. After stressing of bonded tendons, a lower concrete flange was cast. Releasing the precambering forces and cutting of the tendons initiated again a rise of the girders. Casting of the upper concrete part, encasing the steel girder's web, and stressing of 4 additional post-tensioning cables caused subsequent deformation. The composite girders were then transported by train to the building site. After concreting of the stiffened slab the geometry of the bridge decks had to similar to the truss geometry, which were already fabricated.

## 2. Deformation-compatibility and effect of high-strength concrete

The most difficult part was to predict the deformation state of the composite girders at the construction stage where the truss elements were presented. From laboratory tests a secant deformation modulus of the concrete was determined. However, all parameters, governing creep and deformation were not kept under control. As the girders were placed on the piers,

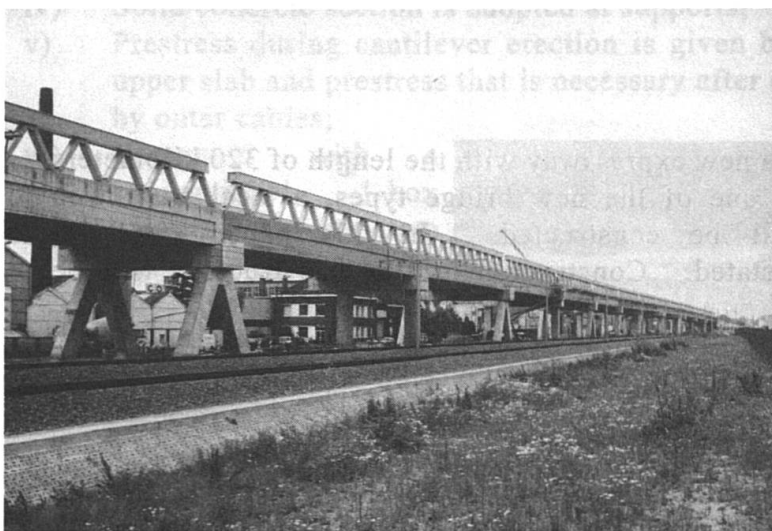


Fig. 1 Overall-view of fly-over

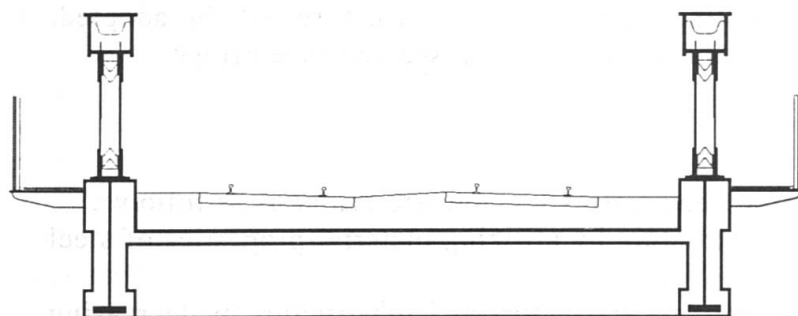


Fig. 2 Superstructure cross section

the concrete age varied from 43 to 210 days. The values of concrete resistance varied from 93 to 119 MPa. In addition, the relative concrete strength at which the precambering was loosened, the strands where cut, or the post-tensioning was applied varied considerably too. From the recordings of all deformation steps, the influence of these parameters was examined (see fig 3 for charts of deformations as a function of  $f_{c28}$  and concrete age). Due to the use of high-strength concrete the time factor and other creep factors were almost insignificant. Eventually the fabrication tolerances of the steel beams were found to be the most significant parameter for determining the deformations of the girders. Thanks to this the deformation steps were predicted accurately, thus achieving the required geometric compatibility.

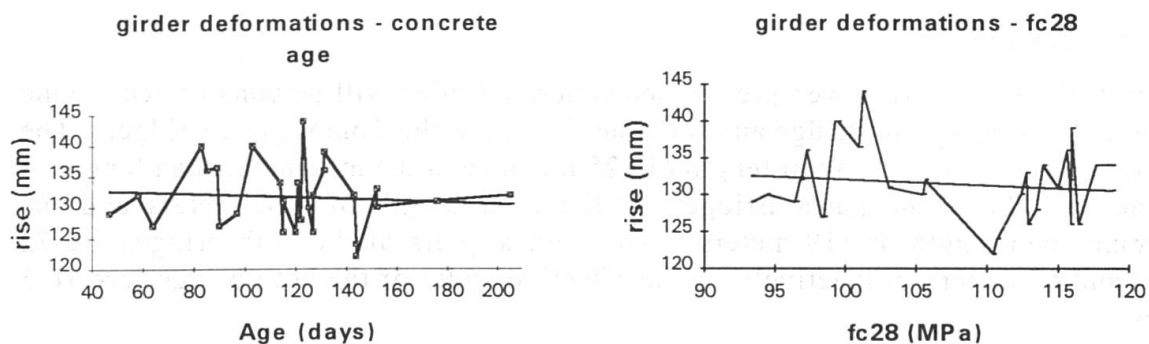


Fig 3 : Composite girder deformations versus factors

## Planning of Steel Truss Web Prestressed Concrete Bridge

**Yasuo INOKUMA**

Chief Engineer

Japan Highway Public Corporation

Shizuoka, JAPAN

### Summary

The Second Tomei Expressway is a new expressway with the length of 320 kilometers linking Tokyo and Nagoya. As one of the new bridge types, a steel truss web prestressed concrete bridge will be constructed. In this paper structural characteristics of this bridge is stated. Construction of the substructure will be starting from 1997.

### 1. Introduction

The Second Tomei Expressway is a new expressway with the length of 320 kilometers linking Tokyo and Nagoya. A section of the expressway in Shizuoka Prefecture, located about the center between Tokyo and Nagoya, runs through mountainous area. The section has the mainline length of 134 kilometers. About 33 % of the total section length, namely 44.3 kilometers, will be bridges and viaducts. As many bridges and viaducts should be constructed, various new structure will be adopted. One of new type of structures is a steel truss web prestressed concrete bridge.

### 2. Purpose

The purposes of adopting steel truss web prestressed concrete bridge is as follows:

- i) To have a rational composite structure by utilizing material properties of steel and concrete;
- ii) To have a rational combination of superstructure and substructure by decreasing weight of superstructure and width of bottom slab;
- iii) To have a structure type, even with noise barriers, that gives less impression of massiveness.

### 3. Structure

Two unit of the steel truss web prestressed concrete bridge will be constructed. One is named the Sarutagawa Bridge and the other is named the Tomoegawa Bridge. The Sarutagawa Bridge has the total length of 625 meters and the maximum span length of 110 meters. The Tomoegawa Bridge has the total length of 478 meters and the maximum span length of 119 meters. The highest piers of the both bridges are 72 meters and 69 meters, respectively. The effective width of the both bridges are 16.5 meters.

Main characteristics of this structure are as follows:

- i) The upper and bottom slabs are cast-situ concrete constructed by cantilever erection method;
- ii) Section of truss members and span of upper slab are decreased by adopting 4-plane main truss structure;
- iii) Fabrication cost of truss members is decreased by using box shape steels;
- iv) Solid concrete section is adopted at supports;
- v) Prestress during cantilever erection is given by prestressing steel arranged in upper slab and prestress that is necessary after completion of the girder is given by outer cables;
- vi) Compared with a conventional 1-box prestressed concrete girder, weight of the girder and the total dead load become about 86% and 88% respectively.



Structural details of connecting panels are one of the important points of this structure. It is required that panels can be connected easily between concrete blocks. It is also required that the panels can absorb errors during cantilever erection. Various types of connecting panels were compared and the type with cast iron cones is proposed.

The upper slab is supported discretely by top ends of the truss members. This support mechanism is different from the ordinary slab that is supported continuously by solid webs. Finite element analyses were done using a finite element model and design bending moments and shear force

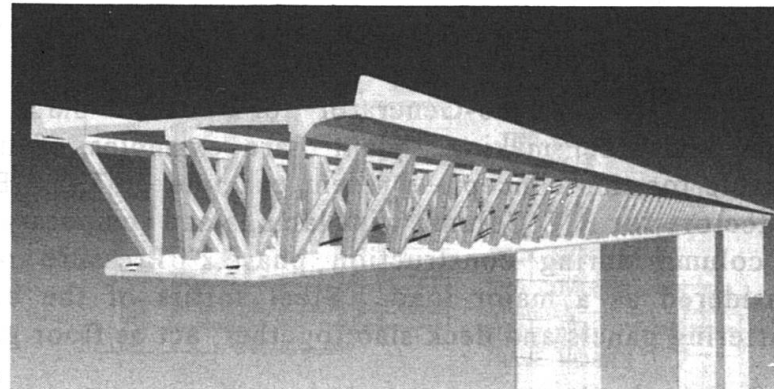


Fig. 1 Cross Section

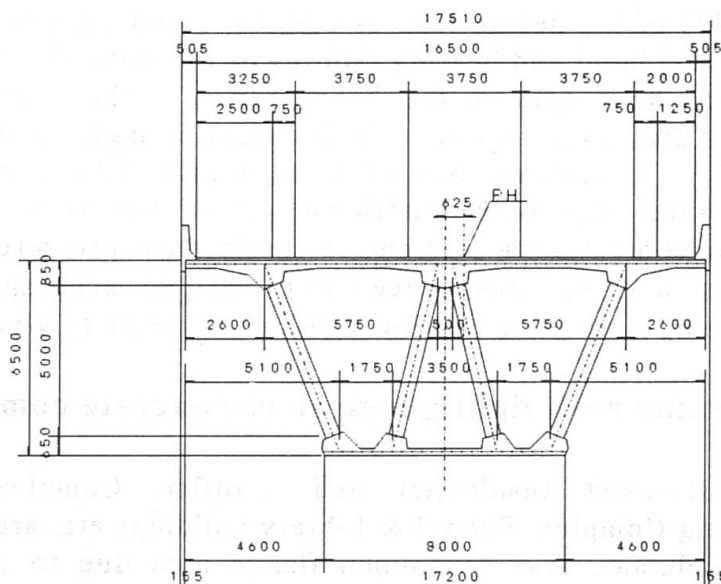


Fig. 2 Cross Section at the Pier

#### 4. Conclusion

In this paper design concept of the steel truss web prestressed concrete bridge is introduced. Construction of the substructure will be starting from 1997 and construction of the superstructure will be starting from 1999.

## Connections for Ease of Fabrication and Erection with Cold-Formed Steel Permanent Formwork

**V.V.V.S. MURTHY**  
Senior Manager  
NSL Ltd  
Patancheru, India

**M.N.CHANDRASEKARAN**  
General Manager  
Contracts, NSL Ltd  
Patancheru, India

**George JACOB**  
Senior Manager  
Execution, NSL Ltd  
Patancheru, India

### 1. Steel - RCC Hybrid composite frame. (Figs. 1 & 2)

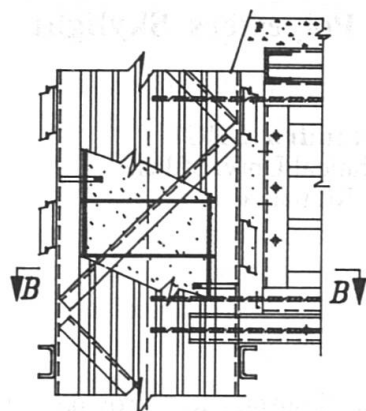
Buildings for Turbo-Generator of power plant, raw material crushing plant, and steel making plant are examples of heavy industrial structures suitable for this concept. Present example of T.G. Building has Corner angle protectors for R C Column with lacings and temporary shuttering panels, to act as column during construction phase. Pressure of wet concrete is also considered as a major load. Steel soffits of the beams with temporary side shuttering panels and deck slab together, act as floor grid system.

The channel cleat on the column carries the shear from beam( $V_d$ ) and the weld connections between the cleat and column carry force ( $T_s$ ) from beam soffit based on 50% of the design load of column, assuming mobilisation or weld forces after frictional bond and bearing failures of the embedded soffit.  $T_s = V_d L_c/a$  (Where  $L_c$  is the shear span of the beam and 'a' is the lever arm). The force in the weld ( $P_w$ ) =  $2d_{pw} t F_{xx}$ , where  $t$  is thickness of angle cleat.  $F_{xx}$  is weld strength. Force ( $T_s - P_w$ ), is resisted by soffit anchorage into column. Anchorage frictional resistance ( $R_f$ ) with coefficient of friction ( $\mu = 0.57$ ), and for normal forces on the contact area ( $A_c$ ) due to confinement pressure  $P_c$  of 0.722 N/Sqm, is given by  $R_f = \mu P_c A_c$ . Resistance due to vertical anchorage( $R_b$ ) by bearing,  $R_b = \sigma_b A_b$ , where  $\sigma_b$  is ultimate bearing stress of concrete (1N/Sqmm).  $A_b$  is bearing area.

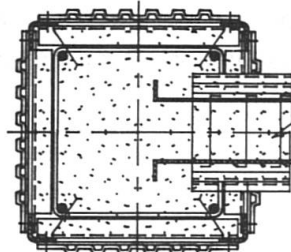
### 2. Frame with light guage steel-concrete composite(Figs. 2 to 5)

Multistoreyed residential and office Complex, Commercial and High-rise Parking Complex, School & Library buildings etc. are examples of this concept. For columns, loss of column flange area due to notch (for continuity of RCC between beam & column) is compensated by extra bar reinforcement, to prevent buckling of this zone. Transverse stirrup is replaced by diaphragm which also acts as stiffener to column envelop steel. Welding between the cleat and column is found to be critical, as one of the specimens failed in this area.

Contribution of stiffness of column element to joint-stiffness is a vital parameter for Euro-Code 3 based classification of beam-column joints. Continuity aspects like improved rotation capacity and ductility make these connections amenable to semi-rigid and rigid beam-column joints. Substitution reinforcement to permanent shuttering sectional area, provides continuity in beam-to-beam connections. Ease of handling, 30% increase in strength-to-weight ratio, simple connections and speedier construction are the merits of above two systems.

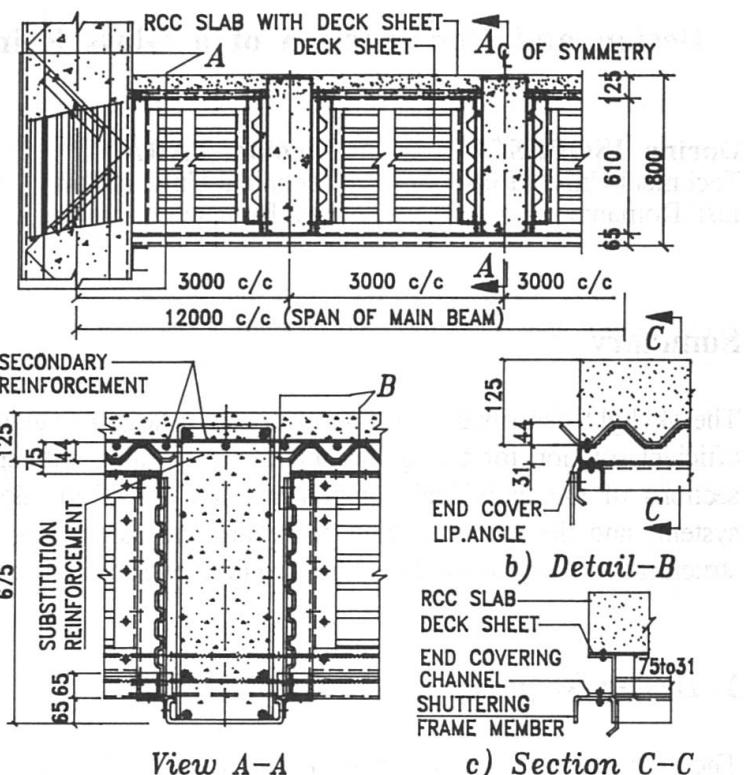


Detail-A



Section B-B

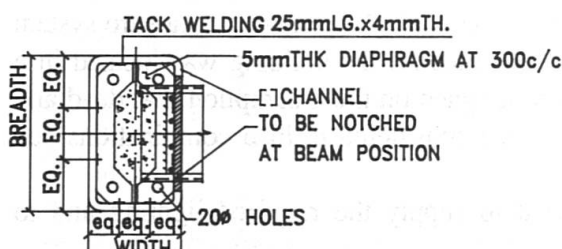
Fig.1 Beam-Column Joint



View A-A

c) Section C-C

Fig.2 Composite Slab-Beam-Column system



a) Typ. Col. Section E-E

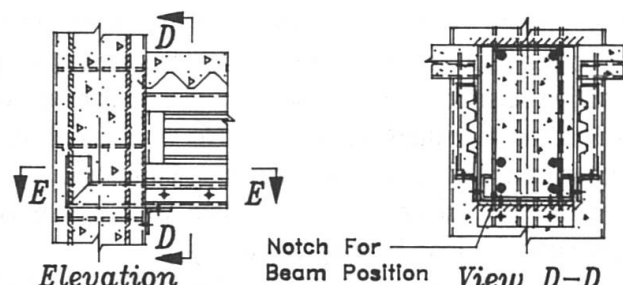


Fig.3 Beam-Column Connection With Concrete Filled Tubular Column

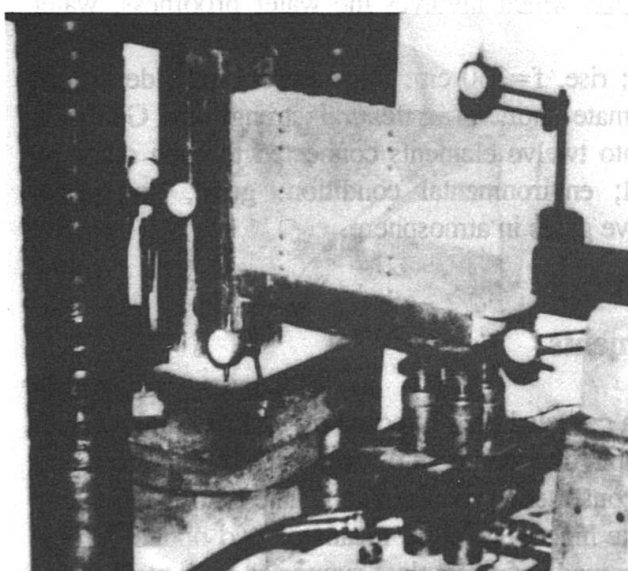


Fig.4 Test Set UP For Beam-Column Joint Connection

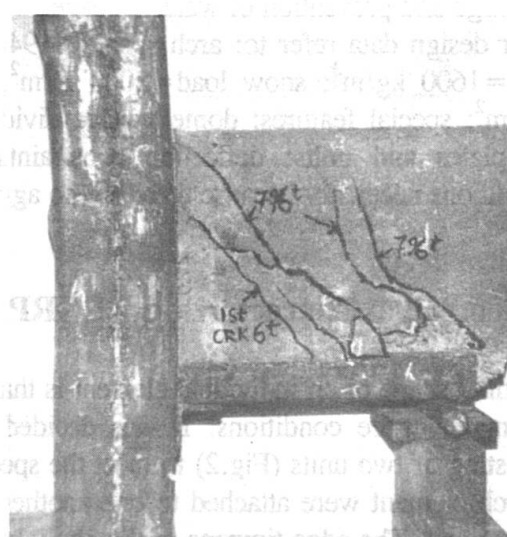


Fig.5 Beam Column Joint Specimen After Test To Failure

## Design and Construction of a Glass Reinforced Polyesters Skylight

**Dorina ISOPESCU**  
Technical Univ. of Iasi  
Iasi, Romania

**Nicolae TARANU**  
Technical Univ. of Iasi  
Iasi, Romania

**Alexandru SECU**  
Technical Univ. of Iasi  
Iasi, Romania

### Summary

The skylight described in the paper covers a large rectangular horizontal surface and provides an efficient solution for a large administrative building with special lighting requirements. The cross sections of the individual components, the use of the double curvature, the proposed jointing system, and the manufacturing procedure and assembling satisfy the most important functional, structural and architectural qualities required by such an enclosure system.

### 1. Design Requirements and Constraints

The architectural constraints and the structural build up of the edifice have led to a rectangular in-plane surface (9.40 m x 10.50 m) to be covered by the lighting aperture.

The skylight has been contrived as a cylindrical dome made of glass reinforced polyesters (GRP), (Fig.1), chosen to perform as structural as well as enclosure material. A light weight closure system was also required in order to minimize the earthquake load, because the building was located in a very active seismic area. The skylight elements have been designed on the assumption that dead and snow load act simultaneously on it. No wind loads have been considered in load combinations due to sheltering effects of the neighbouring buildings.

An appropriate thickness of the dome wall was selected to supply the required lighting and to preserve enough load bearing capability.

The particular cross section (Fig.3) has been chosen in order to fulfill the following structural and functional requirements: strength and stiffness during handling transport and assembling; in service loadbearing capability and rigidity; covering function which involves the water proofness, water discharge and prevention of water seepage.

Other design data refer to: arch span,  $L=940$  cm; rise,  $f=330$  cm; thickness=3 mm; density of GRP=1600 kg/m<sup>3</sup>; snow load=1000 N/m<sup>2</sup>; ultimate short term flexural strength of GRP=25 MN/m<sup>2</sup>; special features: dome surface divided into twelve elements connected to each other by end plates and bolts; deflection constraints: nil; environmental condition: good, no special precautions necessary because there are no aggressive gases in atmosphere.

### 2. Geometric Characteristics of GRP Elements

The final shape of an individual element is that of a corbeled arch imposed by architectural, service and maintenance conditions. It was decided to split the dome into twelve arch type elements consisting of two units (Fig.2) to meet the special construction requirements. The two units making an arch element were attached to one another at the highest level by means of two bolted vertical diaphragms. The edge timpans of the skylight were made of wire glass supported on a steel frame that also provides wind bracing. All dome elements and timpans rest on a reinforced concrete corbel.

### 3. Manufacture and Erection of GRP Elements

An open mould method, namely the hand lay-up technique, was used to take full advantage of the fact that the polyester resin does not need special conditions like heat or pressure for complete polymerisation to occur. The mould was made of timber slats to achieve the double curvature pattern of the element. A release agent was applied to the mould to prevent bonding between GRP element and the timber form.

The reinforcement in the form of woven fabric and strand mat had been pre-cut to the correct size. A gel coat necessary to protect the fibres on the exposed surface of the composite was sprayed on the mould surface. After the gel coat became tacky and firm a first layer of resin was brushed over and the first layer of glass reinforcement was placed in position and consolidated with rollers. The required layers of resin and reinforcement have been applied until the designed thickness of the wall element was obtained. Curing of the GRP elements took place in a construction workshop under a temperature range,  $17^{\circ}\dots20^{\circ}\text{C}$ .

Each arch element, made of two parts, was assembled with bolts then erected and laid up in the final position. A light weight steel scaffolding was used to offer a temporary support to the first GRP element while being set up on the first one and this sequence was used until the skylight was completed.

The final joints between the GRP elements and the concrete corbel were made of mild steel bolts and sealed with a plastic compound. Then, the lateral steel formed timpans filled with coloured wire glass were erected. Eventually the border elements and the timpans were jointed.

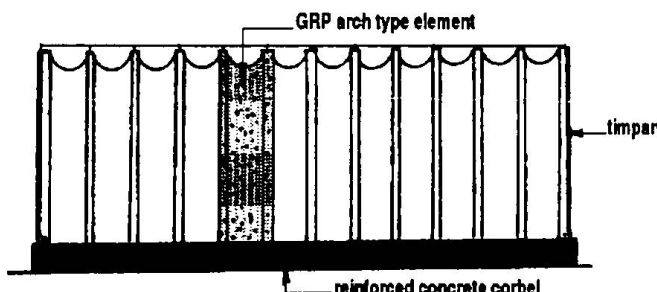


Fig. 1 GRP skylight

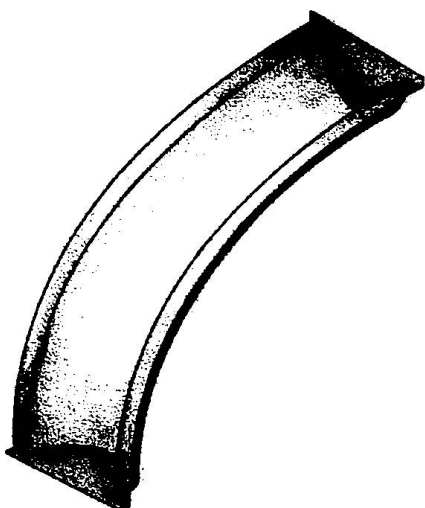


Fig. 2 The unit of arch type element

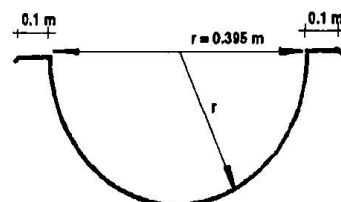


Fig. 3 The cross section of unit

## Large-Span Architecture with Hyperbolic Composite Thin-Shell Structure

**Xianrao ZHAO**

Associate Prof.

Wuhan Urban Constr. Inst.

Wuhan, China

**Hailong ZHANG**

Professor

Wuhan Urban Constr. Inst.

Wuhan, China

**Weilie ZHAO**

Senior Arch. Eng.

Baokun Arch. Design Co.

Hainan, China

**Kui ZHAO**

Arch. Eng.

Baokun Arch. Design Co.

Hainan, China

**Summary** The large-span elemental erecting architecture with composite hyperbolic thin-shell structure is a scientific and technological result of structure, architecture, construction and material. The application, calculation principle and construction craft of this architecture form are introduced in this paper.

**Key words:** hyperbolic thin-shell, composite structure, binder

### 1. Introduction

The large-span architecture has been widely applied in the fields such as large scale gymnasium, airport, ware house, exhibition etc.. Thin-shell structure, cable structure and net-frame structure have been widely used. Of course, the construction of those kind of structure is difficult.

In 70's decade of this century, the structural principle, originated in the Chinese pre-fabricated hyperbolic arch bridge, has been successfully applied in the architecture design in China. The authors of this paper have participated in the design and construction of the assembly hall of the Chinese Petroleum University, which is one of the typical structure of these kinds. By elemental pre-fabricating and erecting method, 40m span hyperbolic thin-shell roof with bearing and maintenance functions are conveniently achieved. The compressive shell of the roof is composed by wire mesh concrete hyperbolic curved shell plate, and its low chord drawing member is composed by welding channel steel.

### 2. Structure Scheme

There are 2 types in this architecture form, one is the shell-plate structure scheme and the other is the rib-plate scheme. In the shell-plate structural scheme, the elemental hyperbolic thin-shell is divided into 5, 7, or 9 blocks along the span direction and assembled one by one on independent support frame. (Fig. 2). In the rib-plate scheme, the elemental hyperbolic thin-shell is divided into arch ribs and cross curved plates. The arch rib is parallel to the span, while the cross curved plate is perpendicular to it. The arch rib is pre-fabricated by reinforced concrete or welded with shaped steel, and divided into 2 or 3 segments for erection. The finished rib should be fixed firstly by tension rod, and then the cross curved plate are assembled between two ribs. The cross curved plate is made of wire mesh concrete, metal or glass fiber reinforced plastic(GFRP). The span of cross curved plate adopts the distance between two adjacent ribs or takes 5m, 6m, 9m, etc..(Fig. 3)

### 3. Key Point

An important characteristic in our study is that it provides a supplementary scheme for the natural lighting of the large-span architecture. Based on the demand for natural lighting, some of the shell part in the hyperbolic thin-shell elements are replaced by GFRP. Of course the by-product is the abundant color style on the structure. GFRP is a kind of widely used new construction material which can be easily shaped and colored, which has high strength, and which is light-penetrated. That is why we use this material.

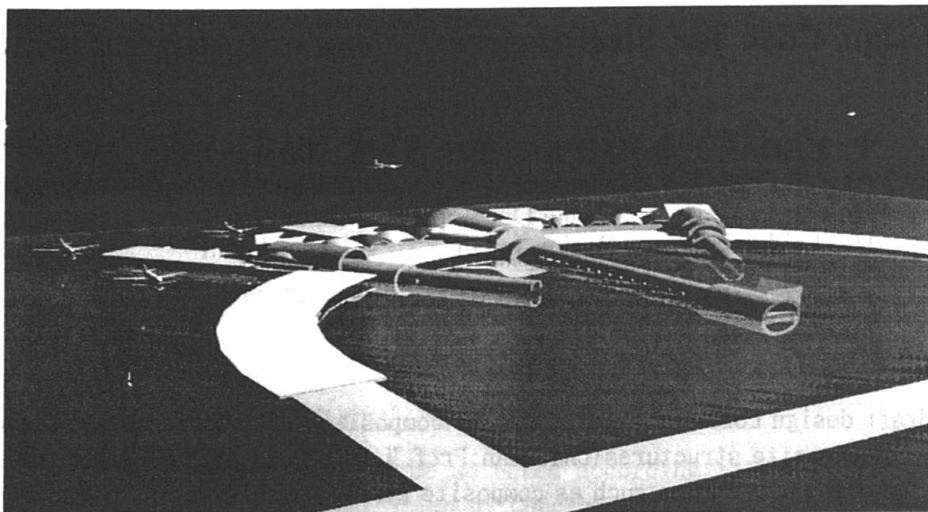


FIG.1 AN AIRPORT DESIGN

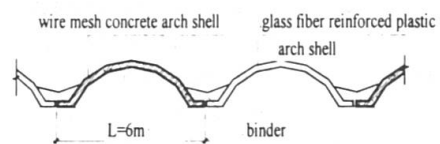
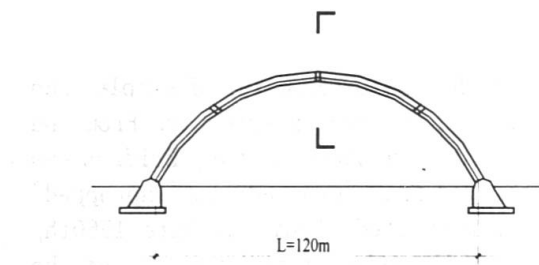


FIG.2 SHELL-PLATE SCHEME

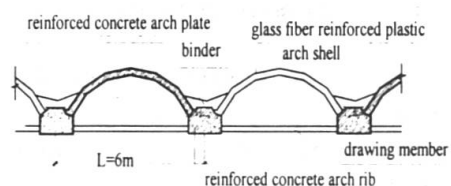
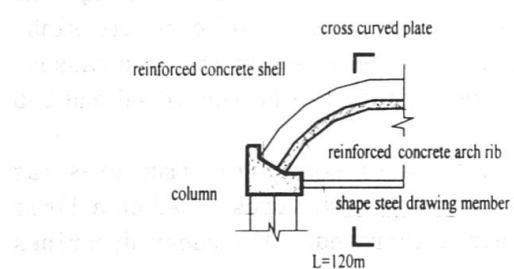


FIG.3 RIB-PLATE SCHEME

What should be pointed out is that, on designing this kind of architecture, careful consideration should be taken on the aspects of architecture scheme, structure scheme, construction scheme as well as material features so as to make ultimate use of its features and ensure its safety and utility. For example, in the construction of rib-plate structural scheme, the arch rib actually acts as the temporary support frame for the erection of cross curved plate. But after the completion of the whole element and the integration construction, the rib and the plate become an integrated bearing element. As we know, the elasticity and the expansion coefficient of GFRP can be changed by adjusting the ratio and type of glass wire, raisin and additives. This feature provides the theoretic basis and practical possibility for the design of composite element which is made by this material and other materials.

## A Draft Design Code for Steel-Concrete Composite Girder in Japan

<b>H. HIRAGI</b> Assoc. Prof. Setsunan Univ. Osaka, Japan	<b>T. UEDA</b> Assoc. Prof. Hokkaido Univ. Hokkaido, Japan	<b>M. KAMEI</b> Manager Osaka Develop. Osaka, Japan	<b>Y. IWAI</b> Manager Mitsui Zosen Osaka, Japan	<b>M. SATO</b> Manager Sho-Bond Ibaragi, Japan
--	---	--	---	---

### Summary

In Japan, a new draft design code for steel-concrete composite girder bridges was elaborated by the committee on composite structures (Chairman: Prof. H. Nakai) in JSCE. The code is mainly for the civil engineering structures such as composite girders in highway bridges and it was written by the format based on a limit state design method.

### 1. Introduction

The first composite girder bridge (CGB) in Japan was Kanzaki Bridge (Osaka city) of simple span length of 12m. The design was based on German experience and our own experiments. From the practice, The Codes for Design and Construction of Composite Girders on Highway Bridges was published in 1957. Then, the construction method was changed from "propped" to "unpropped" to build more easily. Also, many continuous CGB were constructed. From the late 1960th, non-prestressed continuous CGB had taken the place from difficulties in prestressing at the intermediate support and this type of continuous composite girders was specified in the Japanese Specifications for Design of Highway Bridges (JSHB), 1973. New Kanzaki Bridge is the longest non-prestressed continuous CGB of the span length of 88m. Since 1980th, the construction fever of CGB has decreased remarkably due to deterioration of concrete slabs in composite bridges. Shrinkage of concrete and running of heavy vehicles are the main causes. Recently, by using precast prestressed concrete slabs, the defects can be recovered and CGB are coming to life again.

Under these circumstances, the committee on ultimate strength of composite structures was organized in JSCE in order to prepare a design code for composite structures based on a limit state design method and a draft design code for CGB was elaborated. The paper describes the outline of the code.

### 2. Application Range and Fundamentals

The draft codes are available to simple composite girders, prestressed or non-prestressed continuous composite girders and composite girders with in-site RC slabs, precast RC slabs and composite decks.

### 3. Classification of Composite Girders

The composite girders are classified into compact ones and non-compact (slender) ones in relation to the rotation capacity of the cross section. In the compact girder, the composite cross sections can form a full plastic hinge and the ultimate strength of the section can be calculated by the plastic analysis. In the non-compact sections, the ultimate should be limited up to the own when the extreme tension-side fiber stress of steel girder reaches its yielding strength.

The compact section can be determined whether the following equation Eq. (1) is satisfied as well as Eurocode 4 and BS5400,

$$b/t \leq 9\epsilon \quad (1)$$

$$d/w \leq 33\epsilon/\alpha \quad (2)$$

where,  $\alpha$  : ratio of compression zone of web to the web height,

$$\epsilon = \sqrt{(235/f_y)}$$

The composite action between slab and girder can be expected with ordinary stud arrangement designated in JSHB.

#### 4. Strengths for Materials and Members

Structural steel and concrete should be selected according to the Draft Codes for Steel Structures and the Standard Specification of Concrete of JSCE, respectively.

Headed studs are common for shear connectors. Alternative connectors can be used on pertinent approvals of experiments or research data.

#### 5. Verification for Limit States

Safety for each limit state should be verified with the following fundamental equation Eq. (2) :

$$S_d/R_d \leq 1.0 \quad (2)$$

where,  $R_d = \phi \cdot R(f_d)$ ,  $S_d = S (\gamma \cdot F_d)$ .

Here, the loading effects  $F_d$  and safety factors  $\gamma$  for loads may be adopted of ones designated in the Draft Code for Steel Structures.

The bending moments at internal supports in continuous composite girder may be redistributed by only their 15% from internal supports towards the midspan.

#### 6. Verification for fatigue of studs

The safety for fatigue of studs should be verified with Eq. (3) and (4) [1].

$$\Delta \tau_d / \Delta \tau_R \leq 1.0 \quad (3)$$

where,  $\Delta \tau_d$  : the maximum design shearing stress range (Mp),

$\Delta \tau_R$  : shearing stress range (Mp),

$$\log \Delta \tau_R = 2.74 - 0.117 \log N \quad (4)$$

#### 7. Structural details

When the slabs are constructed by in-situ concrete, haunch should be provided at the girder place. The effective breadth of concrete flanges should be determined in accordance with JSHB. When precast slabs are used, a careful attention is necessary for stud arrangement. In the case, group arrangement of plural studs in a position is required and their strength.

#### Reference

[1] Maeda, Y., Matsui, S. and Hiragi, H. : Effect of Concrete-Placing Direction on Static and Fatigue Strength of Stud Shear Connectors, Tech. Rept. of the Osaka Univ., Vol. 33, No. 1733, pp. 397-406, 1983

## A Draft Design Code for Concrete Filled Steel Tubular Columns in Japan

<b>S. ISHIZAKI</b> Manager Sakai Iron Works Osaka, Japan	<b>A. KURITA</b> Professor Osaka Inst. Tech. Osaka, Japan	<b>E. MIZUNO</b> Assoc. Prof. Nagoya Univ. Nagoya, Japan	<b>A. NAKAJIMA</b> Assoc. Prof. Utsunomiya Univ. Utsunomiya, Japan	<b>N. KAWAGUCHI</b> Professor Kokushikan Univ. Tokyo, Japan
---	--	---	---	--

### Summary

In Japan, a new draft design code for concrete filled steel tubular columns was elaborated by the committee on composite structures (Chairman : Prof. H. Nakai) in JSCE. The code is mainly for the civil engineering structures such as piers of highway bridges, compression members of truss and arch bridges, etc. and it was written by the format based on a limit state design method.

### 1. Introduction

In early 1960th, steel reinforced concrete columns were developed for buildings and concrete filled steel tubular(CFST) columns were applied to electric power transmission towers, in Japan. In the latter half of 1970th, applicability and advantages of CFST columns to the highway bridge piers were investigated through many experimental works. Thereafter, a design recommendation was specified by Hanshin Expressway Public Corporation. In late 1980th, the application was realized for large scale highway bridge piers. Recently, the CFST columns have been attracted special attention as a seismic advantageous type.

Under these circumstances, the committee on ultimate strength of composite structures was organized in JSCE in order to prepare a design code for composite structures based on a limit state design method and a draft design code for CFST columns was elaborated. The paper describes the outline of the code.

### 2 Application Range and Fundamentals

The types of composite columns are limited to CFST columns as shown in *Fig. 1*, because the columns of bridge piers are remarkably larger than those of buildings. Besides, rigid diaphragms for restraining the filled concrete should be provided at both ends of the column to ensure enough composite action between the filled concrete and steel tube without any shear connectors. The code can be also applicable for steel contribution factor  $\delta$  between the following limits, as same as BS5400 and DIN18806.

$$0.2 \leq \delta \leq 0.9 \quad (1)$$

where,  $\delta$  is the steel contribution factor for compressive strength of composite section.

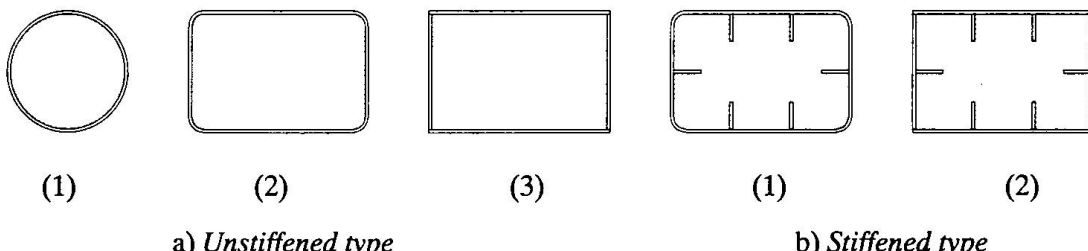


*Fig. 1 Typical cross sections of concrete filled steel tubular columns.*

### 3. Basic design strength of composite cross section

#### 3.1 Design strength for axial compression

Ultimate strength of composite column under axial compression  $P_u$  can be calculated by using the local buckling strength  $f_{cuo}$  based on ECCS buckling curve and design strength of concrete  $f'_{cd}$ .

$$P_u = \phi \kappa (f_{cuo} A_s + 0.85 f'_{cd} A_c) \quad (2)$$

where,  $\phi$  is the resistance factor and  $\kappa$  is the reduction factor for general buckling given by cross section of steel member and slenderness ratio of column referred to ECCS buckling curve.  $A_s$  and  $A_c$  are the cross section areas of steel and concrete, respectively.

#### 3.2 Design strength for flexure

Flexural strength of composite column  $M_u$  can be calculated by using the plastic section modulus  $Z$  obtained by assuming linear strain distribution at the cross section and neglecting the tension side concrete, because the slip is restrained by rigid end diaphragms. It is experimentally certified that the ultimate bending strength decreases to about 90% of the full plastic moment by local buckling. Therefore, the stress  $f_{cuo}$  is used for the maximum strength of plate under compression.

$$M_u = \phi f_{cuo} Z \quad (3)$$

#### 3.3 Local buckling strength of steel tube

For the composite column with rectangular cross section, local buckling strengths of steel tube after hardening of filled-concrete are given for both unstiffened and stiffened type by considering that the plates can deform only outside of the column. For the column with circular cross section, the strengths as steel members may be used.

## 4. Verification for Ultimate Limit State

The safety of composite columns at ultimate limit state can be verified by using basic design strength given by Eqs.(2) and (3) and the design resultant force for ultimate limit state.

The equations for verifying the composite columns subjected to combined axial compression and flexure are given for uniaxial and biaxial bending using the factor based on  $M-N$  interaction curves corresponding to  $\delta$  obtained by many experimental studies. Moreover, the effect of shearing stress due to shearing force and torsional moment to the ultimate strength of composite column is considered by reducing the maximum strength of steel tube based on yielding criterion by Von Mises' hypothesis.

## 5. Verification for Serviceability Limit State

The permanent deformation due to yielding of surface steel plate must be prevented in order to keep the serviceability and durability of composite columns. Therefore, a verification for working stress is specified in addition to the verification for deformation.

## 6. Design Details

#### 6.1 Connection of beam-column

When concrete is casted in beam over a half of the flange width from the corner of beam-column joint, shear lag phenomenon hardly occurs in the flange plate of beam. Therefore, the concrete filling range in beams is specified, and the check for shear lag phenomenon is omitted at beam-column joint after hardening concrete.

#### 6.2 Diaphragms

Three-types of diaphragm are specified such as end diaphragms to restrain the slip between filled concrete and steel tube, diaphragms at the beam-column joint to transmit the bending moment of the beam to the column, and intermediate diaphragms to prevent the local buckling of the tube.

## Dynamic Response of Curved Composite Cellular Bridges

**Khaled M. SENNAH**  
Teaching and Research Assistant  
University of Windsor  
Windsor, Ontario, Canada

Khaled M. Sennah, born 1962, received his civil engineering degree at Alexandria University, Egypt. Presently carrying out research on static and dynamic responses of curved composite bridges.

**John B. KENNEDY**  
University Distinguished Professor  
University of Windsor  
Windsor, Ontario, Canada

John B. Kennedy, born 1932, received his engineering degree at University of Wales, U. K. His field of research has been on skew and curved composite bridges as well as soil-metal structures.

### Summary

This paper is a summary of an extensive parametric study, using the finite-element method, in which 120 simply-supported curved composite bridge prototypes are analyzed to evaluate their natural frequencies and mode shapes. The parameters considered in the study are: end-diaphragm thickness, cross-bracing system, degree of curvature, and number of cells. Results from tests on four 1/12 linear-scale simply-supported composite three-cell bridge models of different curvatures are used to substantiate the analytical modelling.

### 1-Results and conclusion

Dynamic analysis of simply-supported curved multi-cell composite bridges was conducted using the finite-element modelling. This modelling was verified by results from free-vibration testing of four simply-supported composite three-cell bridge models. Figure 1 shows the cross-sectional details of the models. Two diaphragms, 5 mm thick, were placed radially at the extreme end sections. No inner bracings were used in the second model while in the other models, five cross-bracings of rectangular cross-section 13×5 mm were installed in the radial direction, at equal intervals. The span-to-radius ratios were 1.0 in both the first and second models, 0.375 in the third model, and 0.0 in the fourth model. Table 1 summarizes the natural frequencies and mode shapes of the bridge models. Good agreement between the experimental and theoretical findings can be observed. It is observed that the dominant mode of vibration of a curved bridge is a combined flexural and torsional mode, with the bridge frequency decreasing with an increase in the degree of curvature. Also, the presence of cross-bracings enhances the first two natural frequencies in the first model when compared to those in the second model. Figure 2 present the effect of end-diaphragm thickness on the dominant frequency. It is observed that the presence of end-diaphragms enhances the dominant frequency and its mode shapes. Figure 3 shows that for curved bridges, a minimum of three cross-bracings are adequate to enhance the dominant frequency due to increased torsional resistance. Figure 4 shows that the dominant frequency decreases with increase in the curved span as well as in the degree of curvature. In the case of one- and two-lane bridges, when the number of cells is  $\leq 3$ , increasing the number of cells increases the dominant frequency as shown in Figure 5. In the case of bridges with any number of lanes and with number of cells  $\geq 3$ , the change in the number of cells has no significant effect on the dominant frequency. Expressions for the first flexural frequency and hence the dynamic load allowance for this type of bridges has also been deduced and reported elsewhere\*.

\* Sennah, K. M. 1997. Static and dynamic responses of curved composite concrete deck-steel multi-cell bridges. Ph.D dissertation, University of Windsor, Windsor, Ontario, Canada.

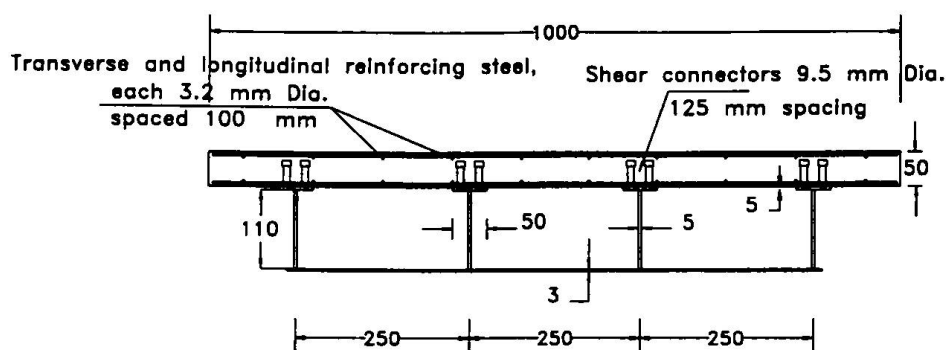


Fig. 1. Cross-sectional details of models

Model No.	L (m)	$\frac{L}{R}$	First natural frequency (Hz)			Second natural frequency (Hz)		
			Experimental	Finite-element	Mode shape	Experimental	Finite-element	Mode shape
1	2.6	1	38	39	LF-TS	125	133	TS
2	2.6	1	36	38	LF-TS	81	91	TS
3	2.6	0.375	44	46	LF-TS	—	138	TS
4	2.6	$\infty$	45	47	LF	—	136	TS

Note: LF: Longitudinal flexure; TS: Symmetric Torsion

Table 1. Natural frequencies and mode shapes of tested bridge models

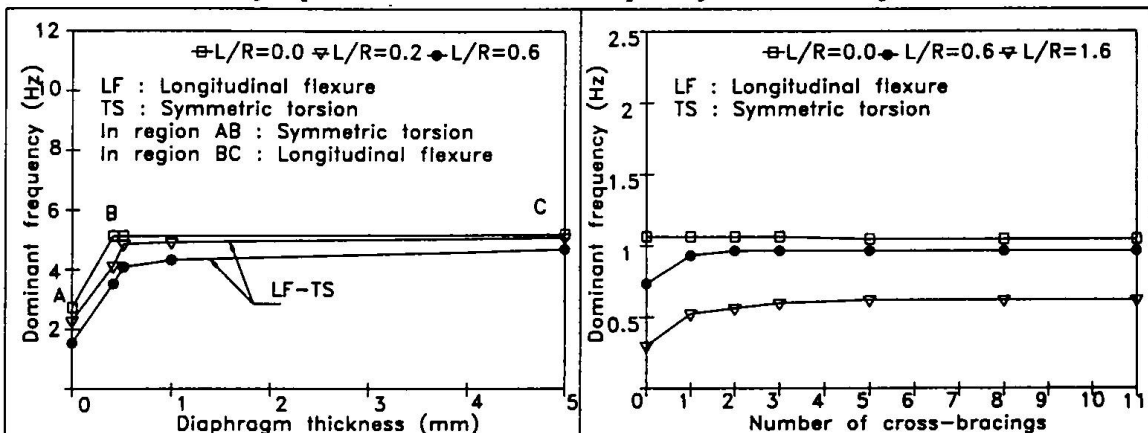


Fig. 2. Effect of end-diaphragm thickness on the dominant frequency of three-lane five-cell bridges

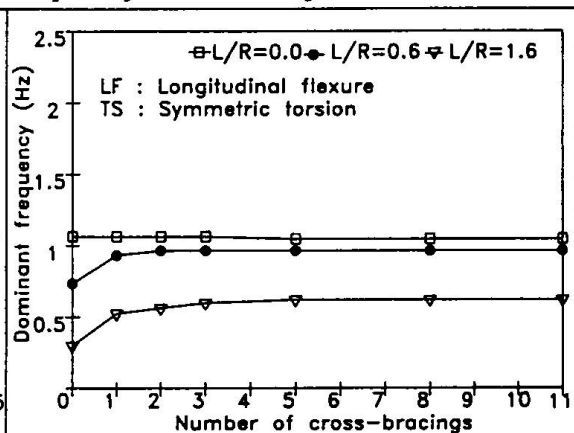


Fig. 3. Effect of cross-bracings on the dominant frequency of two-lane three-cell bridges of span = 100 m

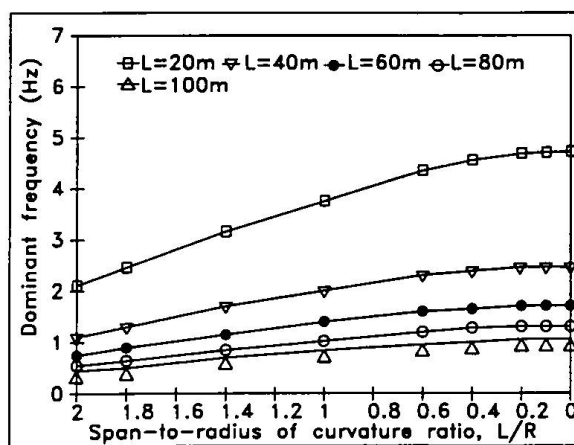
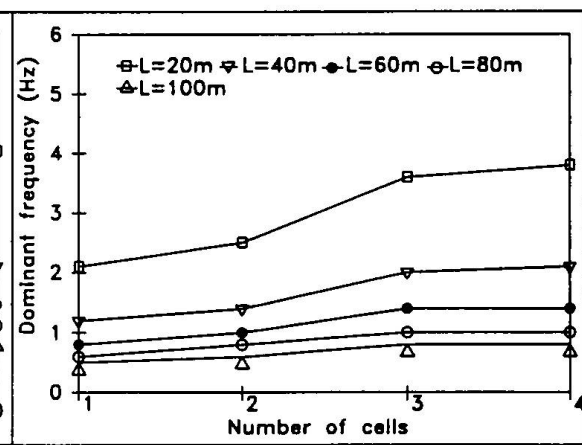


Fig. 4. Effect of curvature on the dominant frequency of two-lane three-cell bridges

Fig. 5. Effect of number of cells on the dominant frequency of two-lane three-cell bridges with  $L/R=1.0$

## Study on Ultimate Strength and Ductility of Composite Column

**Katsuyoshi NAKANISHI**

Research Associate  
Osaka City University  
Osaka, Japan

**Toshiyuki KITADA**

Associate Professor  
Osaka City University  
Osaka, Japan

**Koji TAKENO**

Design Engineer  
Yokogawa Bridge Co., Ltd.  
Tokyo, Japan

**Hirosi NAKAI**

Professor  
Osaka City University  
Osaka, Japan

### Summary

In response to the disaster of many steel bridge piers by the Hyogo-Ken Nanbu Earthquake which occurred in the Hanshin Districts(Osaka and Kobe), Japan in 1995, an experimental study was performed in order to investigate the ductility as well as ultimate strength of concrete filled steel box columns with hollow cross section subjected to such strong earthquakes as the Hyogo-Ken Nanbu Earthquake and to propose a method for improving the seismic performances of steel bridge piers. It is concluded that these composite columns have superior seismic performances.

### 1. Introduction

Since many steel bridge piers were locally buckled and damaged due to the Hyogo-Ken Nanbu Earthquake, a new seismic design method is required for the steel bridge piers not to suffer serious damages due to a strong earthquake. As one of them, a method for inserting the additional steel tube into the inside of steel bridge pier can be considered. In this method, the ductility of the bridge piers is significantly enhanced, if their cross section is designed in such a way that the axial compressive load caused by the dead load of the superstructure is mainly carried by the inner steel tube, and then the local buckling of the steel pier is prevented by filling the concrete between outer steel column and inside steel tube<sup>1)</sup>. Hereafter, this kind of column is referred to as a composite column with hollow cross section.

### 2. Experimental Tests

Ten cantilever column specimens, listed in *Table.1*, are adopted for the experimental tests. Eight of them are the composite column specimens and the other two are the steel column specimens. Eight composite column specimens consist of (1)two specimens with hollow cross section each having an additional inside steel tube, (2)two specimens with hollow cross section having an inside plastic tube, (3)two specimens with hollow cross section having an inside steel tube except for the lower part of them, and (4)the remaining two specimens of solid cross section filled with concrete.

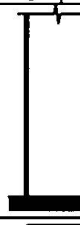
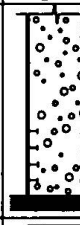
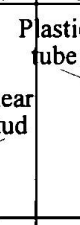
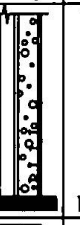
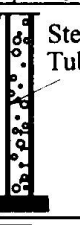
Firstly, five virgin specimens with the different types of cross section were tested under the condition of the horizontal cyclic load at the top of the specimens with the constant axial compressive force. Secondly, a large seismic load was applied to the remaining five specimens through a hybrid(pseudo-

dynamic) testing equipment under the same axial compressive force by using one of the acceleration records of the Hyogo-Ken Nanbu Earthquake. Thereafter, the same cyclic test, as was conducted to the virgin specimens, was executed for these five specimens to investigate the ultimate strength and ductility of the specimens before and after applying the large seismic load.

### 3. Experimental Results

The Seismic hysteretic response curve and their cyclic curves of the composite column specimens with inside steel tubes are depicted in *Fig.1(a)-(c)*. It can be seen from these figures that these composite column specimens still remain the ultimate strength more than the fully plastic strength and less deterioration of strength due to the cyclic loading in the cases even after applying the strong seismic load.

*Table.1 Characteristics of Specimens*

Specimen No.	1	2	3	4	5	6	7	8	9	10
Side Elevation										
Cross Section										
Loading Method	C	C&S	C	C&S	C	C&S	C	C&S	C	C&S

C : Only cyclic loading      C&S : both of cyclic loading and seismic loading

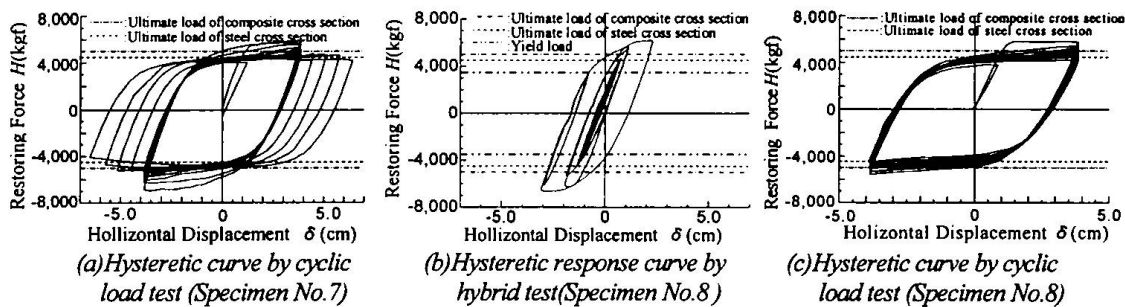


*Fig.2 Experimental Results of composite column specimens with inside steel tube*

### 4. Conclusion

- (1) The composite column specimens with hollow cross section having inside steel tubes and solid cross section are of high ductility in comparison with the steel column specimens and the composite column specimens with hollow cross section having inside plastic tubes.
- (2) The seismic performance of four types of the composite column specimens subjected to the large seismic load have almost similar tendency.

**Acknowledgments :** This study was supported in a part by grants from the Japanese Ministry of Education, Science and Culture (K. Nakanishi, Principal investigator)

**Reference :** 1)K. Nakanishi, T. Kitada and H. Nakai : Experimental Study on Deterioration of Ultimate Strength and Ductility of Damaged Concrete Filled Steel Box Columns, Proceedings of Association for International Cooperation and Research in Steel-Concrete Structures, pp.127-130, Kosice, SLOVAKIA, June 20-22, 1994.

## Ultimate Strength and Ductility in Concrete-Filled Double Steel Tubular Columns

**Akimitsu KURITA**

Professor, Dr. Eng.

Osaka Institute of Technology

Osaka, Japan

**Yasutaka TAKEHARA**

consulting Engineer

Chuo Fukken Consultants Co., Ltd.

Osaka, Japan

**Takashi UEDA**

Consulting Engineer

Chuo Fukken Consultants Co., Ltd.

Osaka, Japan,

**Hironobu HAMAMOTO**

Graduate Student

Osaka Institute of Technology

Osaka, Japan

### Summary

This paper deals with the ultimate strength and ductility in concrete-filled double steel tubular columns. Two types of rectangular and circular cross-section were treated herein. First, the interaction curves concerning the ultimate strength of the cross section between axial force and bending moment are presented in comparison with normal composite columns. To evaluate the earthquake resistance of the column, the ductility is an important factor. Therefore, the ductility of these columns are, next, reported and compared with the reinforced concrete columns.

### 1. Assumptions for analysis

The following assumptions are used for the analysis of the column. a) The plane cross section of the column remains plane. b) The concrete strength in tensile area is ignored. c) Steel and concrete parts show full composite action. d) The state of full plastic stress is assumed for the analysis of  $M-N$  interaction.

### 2. $M-N$ interaction curve

As one of the numerical examples for the circular section, Fig.1 shows  $M-N$  interaction curves of the cross section for concrete-filled double steel tubular column in comparison with the steel and the concrete-filled single steel tubular columns. The numerical data for the calculation is shown in Table 1. From the curves, it is found that the maximum load carrying capacity ratio ( $M_{max}/M_{pl}$ ) is 1.90 for concrete-filled single steel tubular columns. In the case of concrete-filled double steel tubular column, however, its value is 1.35. The reason of this decreasing can be explained clearly that the cross sectional area of concrete in concrete-filled double steel tubular column is less than the concrete-filled single one. Therefore, it is recognized that the effect of cross sectional area of concrete for the maximum load carrying capacity of the composite column is one of the important factors for the design. The  $M-N$  interaction curves for the rectangular section have same properties with circular section.

Table.1 Numerical Condition

Yield strength of outside steel tube $\sigma_{y1}$	235 N/mm <sup>2</sup>
Diameter of outside steel tube $d_1$	2000 mm
Thickness of outside steel tube $t_1$	9 mm
Yield strength of inside steel tube $\sigma_{y2}$	235 N/mm <sup>2</sup>
Diameter of inside steel tube $d_2$	1200 mm
Thickness of inside steel tube $t_2$	9 mm
Specified concrete strength $\sigma_{ct}$	23.5 N/mm <sup>2</sup>

### 3. Ductility

To evaluate the ductility of the column, an actual bridge pier shown in Fig.2 was selected. The calculations were executed for three types of column, namely, reinforced concrete, concrete-filled single and double steel tubular column in which the column has same external dimensions. The yield and ultimate horizontal displacement at the top of column,  $\delta_y$  and  $\delta_u$ , are defined as the values when the strains of steel and concrete reach the yield and ultimate strains at most outer side of steel and concrete, respectively. Using these values the rate of ductility for column,  $\mu$ , is calculated as follows:

$$\mu = \delta_u / \delta_y$$

Fig.3 shows the relationships between horizontal force and displacement of three columns. Concrete-filled steel tubular columns have large load carrying capacity and ductility compared with reinforced concrete column. Furthermore, the ultimate displacement in double steel tubular column is smaller than concrete-filled single one. However it is identified that the both composite column has almost same load carrying capacity.

### 4. Conclusion

A burden against the foundation can be reduced by employing the double steel tubular structure for column since the dead weight of bridge pier reduces. Furthermore, it can be mentioned that the concrete-filled double steel tubular column has almost same mechanical characteristics compared with the concrete-filled single one.

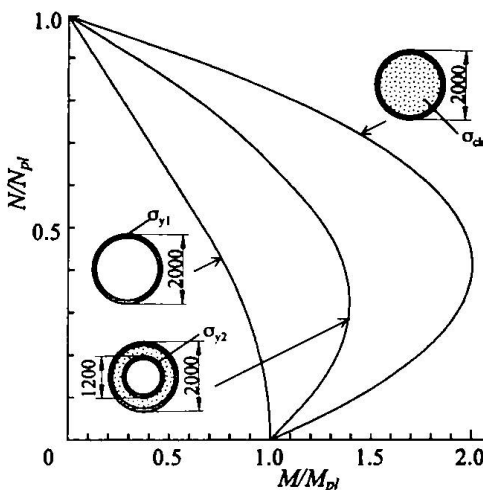


Fig.1 M-N interaction curves of three types of column section

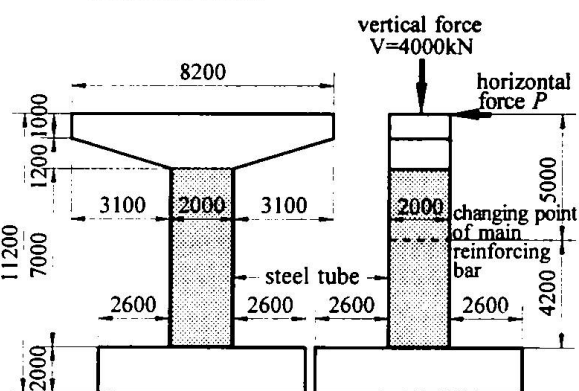


Fig.2 Analytical model

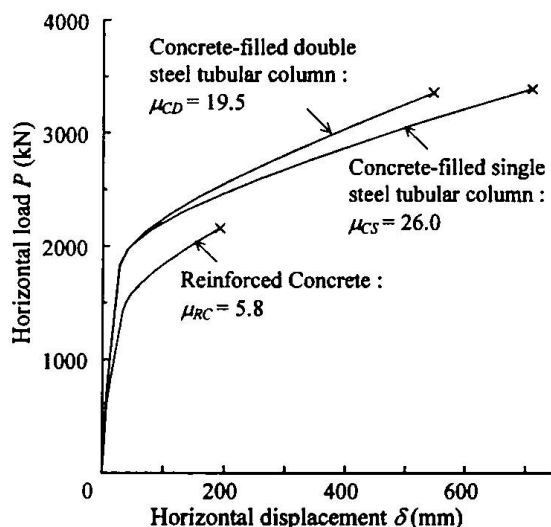


Fig.3 P-d Relationship

## Stable Ultimate Deformation of Confined Columns Subjected to Seismic Loads

**Yuping SUN**  
Research Associate  
Kyushu University  
Fukuoka, Japan

Yuping Sun, born 1961, received his PhD from Kyushu University in 1992. His research interests include seismic behaviour of reinforced concrete columns, confinement of high-strength concrete, and non-linear analysis of concrete members.

**Kenji SAKINO**  
Professor  
Kyushu University  
Fukuoka, Japan

Kenji Sakino, born 1946, received his PhD from Kyushu University in 1982. His research interests include earthquake resistance of reinforced concrete columns and shear walls, confinement of high-strength concrete, and inelastic behaviour of concrete-filled steel tubular columns.

**Teruhisa OBA**  
Graduate Student  
Kyushu University  
Fukuoka, Japan

Teruhisa Oba, born 1973, completed his bachelor of engineering at Kyushu University in 1995. He is currently a graduate student in graduate school of engineering at Kyushu University.

### Summary

A method to evaluate the stable ultimate deformation of the confined concrete columns under seismic loading was proposed. In this method, stable ultimate deformation of a column was defined as the deformation reached when the axial strain at the center of the critical section was equal to half of the peak strain of the confined concrete. The validity of the proposed method was verified by comparing the theoretical ultimate deformation obtained using this method with the measured results of confined concrete columns under cyclic reversed bending moment.

### 1. Introduction

The ultimate deformation plays a fundamental role in evaluating seismic performance of the reinforced concrete columns. For easiness, the deformation in which the load is dropped to 80% of the maximum value has been conventionally defined as the ultimate deformation of the column under seismic load. However, the value of 80% in the conventional definition hasn't any physical meaning relating to the damage degree that can be tolerated by the column; besides, conventional definition might overestimate the deformability of the column under high axial load [1]. Therefore, it is necessary to develop a new criterion to define the ultimate deformation of the concrete column. The purpose of this paper is to propose a criterion for defining the ultimate curvature of the concrete column confined by transverse reinforcement.

### 2. Stable Ultimate Deformation

Fig. 1 shows idealization of the strain distribution of confined section under cyclic moment. As shown in Fig. 1, under high axial load, a compression zone exists in the section, this zone always subjects to compressive deformation while the moment is a reversed cyclic type. It is apparent that in order for the concrete section to provide stable resistance, the maximum compression strain (the strain in the center) at this zone should be limited below the peak strain  $\varepsilon_{co}$  ( $\varepsilon_{co}/2$ ) of the concrete (see Fig. 2), beyond which the strength deterioration in the concrete will become significant.

From the above theoretical consideration, the stable ultimate curvature of the confined column can be defined as the curvature in which the compressive strain  $\varepsilon_{cc}$  in the center of the section reached half of the peak strain  $\varepsilon_{co}$  of the concrete. Authors' experimental work [1] has indicated that the envelop curve of cyclic response coincided with monotonic curve until the ultimate curvature

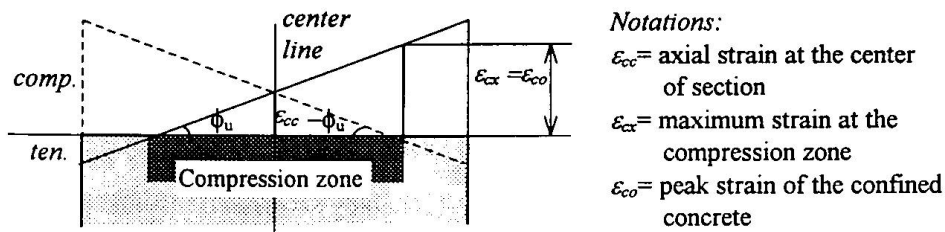


Fig. 1 Idealization of the strain distribution of column section under cyclic moment

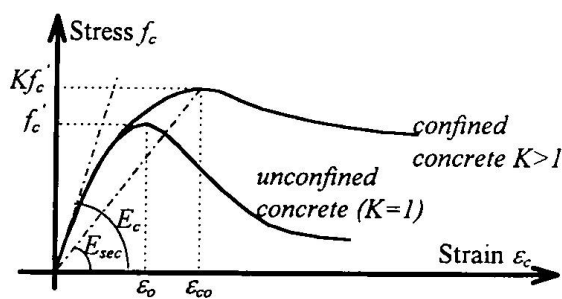


Fig. 2 Stress-strain curve for concrete

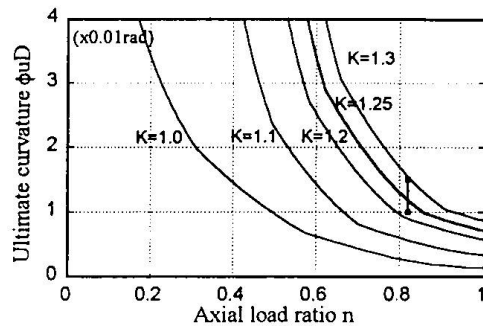


Fig. 3 Stable ultimate curvatures

defined by the above-described criterion. Therefore the ultimate curvatures for the confined column can be obtained by only calculating the monotonic M- $\phi$  curves of the critical section of the column corresponding to various levels of axial load and confinement from transverse steels.

Fig.3 shows theoretical ultimate curvature ( $\phi_u D$ )-axial load ratio (n) curves for the test columns described in Ref.1. The parameter K shown in Fig.3 is the ratio of the confined concrete strength to the concrete cylinder strength, an index denoting the confinement degree, and D is depth of the section. For calculating the M- $\phi$  curves, a stress-strain curve for the confined concrete proposed by the first two authors [2] has been used. The solid squares in Fig.3 denote the lower and upper limit (0.01-0.015rad) of the test results of specimens. It can be seen that the theoretical solid line with K=1.25, which represents the confinement degree of the specimen presented in Ref.1 and is obtained using authors' confinement model [1], predicted the experimental results very well. On the other hand, following the conventional definition, the ultimate curvature would be 0.02-0.025rad, and clearly overestimated the ultimate deformation capacity of the test column.

### 3. Conclusion

A new criterion was proposed to relate the ultimate curvature to the axial deformation of the confined columns. Theoretical predictions obtained based on this criterion and authors' stress-strain model for the confined concrete exhibited good agreement with the measured result.

### References

- [1] Sakino,K., et al., "Factors influencing the flexural behavior of confined concrete columns," The AIJ Annual Convention, Sept. 1996, Vol. C, pp.47-52. (in Japanese)
- [2] Sun, Y., et al., "Flexural Behavior of High-Strength RC Columns Confined by Rectilinear Reinforcement," Journal of Struct. Constr. Eng. AIJ, No. 486, pp.95-106, Aug. 1996.

## Evaluation of Seismic Resistivity of CFT Steel Pillar

**Kiyomitsu MURATA**

Chief Engineer

Railway Technology Research Institute

Tokyo, Japan

**Manabu IKEDA**

Engineer

Railway Technology Research Institute

Tokyo, Japan

**Masato YASUHARA**

Engineer

Railway Technology Research Institute

Tokyo, Japan

**Masanori KINOSHITA**

Senior Researcher

Nippon Steel Corporation

Chiba, Japan

### Summary

Aiming at establishment of a new seismic design method in which ductility is taken well into account, a series of alternating bending tests under constant axial compressive force with Concrete Filled Tubular, called CFT, steel pillar models were carried out. The study based on experimental results enabled the quantitative evaluation of seismic resistivity of CFT pillars. The fruits obtained through this study will be reflected in Model Code for Railway Hybrid Structure Design to be made public by Japan Ministry of Transport in 1997.

### 1. Introduction

Newmark's energy preservation rule is well known as a concept of the seismic design, where the ductility of pillars is taken into consideration. This idea is to check the bending yield point capacity to horizontal seismic load as corrected according to the ductility of pillars. In order to apply such a seismic design method to CFT pillars, it is necessary to establish the method of quantitatively evaluating the yield point load, yield point displacement and also relationship between the limit plastic displacement and the pillar components. Therefore, the study was done according to the following steps.

- Step1 Alternating bending test with CFT pillar models
- Step2 Analytical study on yield point load and yield point displacement
- Step3 Statistical study on quantitative evaluation of ductility

## 2. Alternating bending test on CFT pillar models

The alternating bending test under axial compressive force with 1/3 models of CFT pillars was executed. The experimental parameters are diameter-thickness ratio, axial compressive force, concrete strength, and steel pipe strength.

## 3. Analytical study on yield point load and yield point displacement

The yield point load and yield point displacement were calculated with a fiber element model dominated by elasto-plastic stress-strain relationship of steel and concrete materials. *Figure 1* shows the comparison between the experimental values and the calculated ones.

## 4. Statistical study on quantitative evaluation of ductility

The expression of quantitatively evaluated ductility was induced from the recurrence analysis based on experimental results as well as on analytical ones. *Figure 2* shows the comparison between the calculated ductility and experimental one.

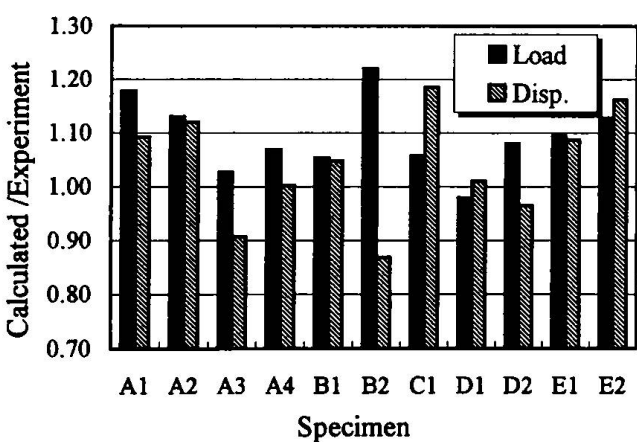


Fig 1 Yield Point Load & Displacement

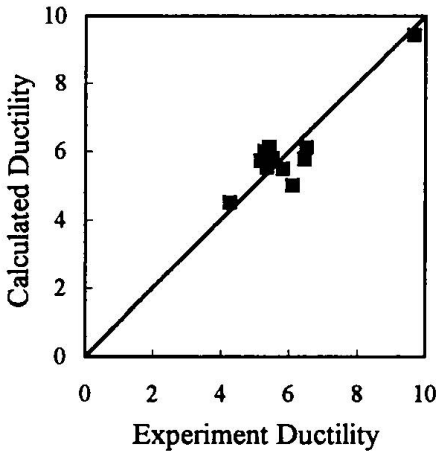


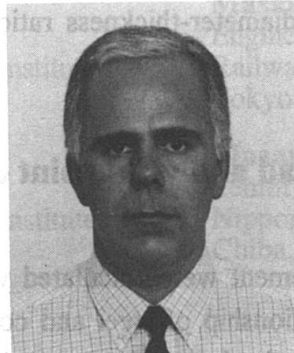
Fig 2 Ductility

## 5. Conclusions

The quantitative evaluation expression for seismic resistivity of CFT pillars was induced. As a result, a more rational and accurate evaluation of yield point load, yield point displacement, and ductility necessary for the seismic design of CFT pillars has been made possible.

## Collapse and Rehabilitation of Composite Trussed Structures

**F. GASTAL**  
Prof. of Civil Engineering  
Federal University of Brazil  
Porto Alegre, RS Brazil



F. Gastal, born 1951  
received his Ph.D. from  
North Carolina State  
University - USA in 1986.  
He's interest is in numerical  
and experimental structural  
analysis

### Summary

A failure case of a 2.400 m<sup>2</sup> area of an industrial roofing structure is presented. The investigation leading to the cause of the disaster, the numerical and experimental study using reduced models and the rehabilitation procedures for the remaining part of the structure are described. Conclusions are also drawn concerning the application of external tension reinforcements to restore the original load capacity of the structure.

### 1. Introduction

Composite steel-concrete trussed members are widely used in Brazil as supporting structures for roofing large industrial facility areas, and the complete lack of maintenance in such structures is for certain the main cause of serious problems of deterioration and corrosion.

The case in study concerns one of such structures, used to shelter an industrial area enclosing an environment with strong emissions of chemically active dust and vapours.

The whole building structure of 12000 m<sup>2</sup> is divided into four sections, constructed from 1960 up to 1987, and containing different structural models for the trusses.

Trusses of type I consist of a two span indeterminate structure of 51 m long. Trusses of type II are simply supported, 30 m long structures, covering the collapsed area. Both are constructed in reinforced concrete but have unprotected steel bars as the tensioned diagonals. The type II truss, however, has no diagonals in the central frame.

Trusses of type III and IV, more recently constructed, were in good conditions.

### 2. Investigation of the Collapsed Area

The collapsed structure was composed by seven type II trusses. Many nodes were ruptured and showed they were not properly reinforced as plane frame nodes.

Corrosion in the exposed bars was more evident near the lower nodes, where the bars were immersed in a thick layer of chemically active dust, accumulated over the years. One of the ruptured tendons had its cross sectional area reduced by almost seventy percent.

Four other trusses of the same type, however, were still standing. A weak connection was observed to link those two areas. Rupture at this point certainly occurred before any sufficient overload could be transferred to the neighbour trusses, and the collapsing wave was stopped.

The inspection was extended to the rest of the building and showed that trusses type I, covering the main building area, were also very deteriorated. It was further observed that some of the steel bar diagonals were completely loose, subjected to no tension.

### 3. Numerical Analysis

Considering the pre-cracking stiffness of the nodes, a plane frame finite element model was used for the analysis of the trussed structures.

A first analysis was made for trusses type I and II, considering the original design properties. It confirmed that two of the steel diagonals in trusses of type I had no tension whatsoever.

Further investigative analyses showed that if the continuous trusses type I were considered as two separate, simply supported spans, all member would have been well dimensioned and those diagonals properly tensioned.

All evidences pointed to the conclusion that the trusses were originally intended to be separated and, for some reason, constructed as continuous over the internal support.

A second analysis was performed for trusses type II considering the measured properties of the materials and the reduced sections of the steel diagonal bars. The result showed that the tensile force in the ruptured and deeply corroded diagonal was beyond its reduced area capacity. The remaining members were not overstressed.

Rupture was expected to have begun in that diagonal and caused failure of the whole structure.

A third analysis was made withdrawing that particular bar from the structure. The moments at the nodes of that frame raised up to extremely high values, far beyond its capacity. That would certainly create a mechanism and destroy the structural symmetry, leading to an unavoidable failure mechanism of the whole structure.

### 4. Design of the Reinforcement

The continuous trusses type I and the remaining trusses type II, not affected by the collapse, were completely rehabilitated and strengthened for restoring their original load capacity.

An external reinforcement was devised using epoxy glued steel plates around the nodes, also fixed with bolts, in which steel bars were welded. The reinforcement was placed parallel to the tensioned diagonals and as new crossed diagonals at the central frame of trusses type II.

Reinforcement was also positioned at the bottom cord of trusses type II and the top central cord of the continuous trusses type I, to help supporting its constructively created continuity.

### 5. Experimental Analysis

Reduced models have been very didactic for the learning process of engineering students.

The case in study would perfectly fit its purpose and two reduced models made of microconcrete and galvanised wire were built. One to reproduce failure of trusses type II and another, exactly alike, to test the effectiveness of the reinforcement.

Both 400 by 38 cm models were positioned in a testing frame and instrumented for the measuring of nodal displacements and strains at the bars, nodes and reinforcement.

The first model was loaded, at each nodal point, and behaved very linearly. To reproduce the corrosion rupture of the steel diagonal a thin saw was used to slowly reduce its cross section.

After cutting over half section, the bar suddenly ruptured and the moments at the nodes of the same frame increased abruptly. The very same, numerically predicted, failure mechanism was formed and the structure suffered an immediate collapse.

The second model was subjected to service load, as the first one, and behaved alike. Maintaining the load, the reinforcement was placed, as it would be done in the prototype structure.

The external loading was eventually increased by fifty percent. The model responded stiffer and tension was properly transferred to the reinforcement, as expected.

Like in the first model the diagonal bar was also cut, and now its force was adequately transferred to the reinforcement. The external load was again increased by fifty percent and the reinforced model was able to sustain it very adequately.

### 6. Conclusions

The strengthening procedure was considered adequate and built in the real structures. The most convenient feature of this technique consists on its economy and simplicity. The structure may be strengthened while supporting the service load and there is a minimal disruption on the production process in operation.

## Use of Aluminium Alloys in Retrofitting Ancient Suspension Bridges

**Federico MAZZOLANI**

Professor

University of Naples

Napoli, Italy

**E. MELE**

Dept. of Struct. Analysis and Design

University of Naples

Napoli, Italy

### Summary

The retrofitting of suspension bridges can take profit of the specific aluminium alloy characteristics for obtaining the maximum structural effectiveness, particularly if compared to classical solutions based on the use of steel. This paper also emphasizes how different structural materials can optimally co-operate in the suspension bridge scheme, thus characterizing the rehabilitated structure as a particular composite construction. The above aspects are discussed with reference to some case studies.

### 1. Introduction

During the seventies a rehabilitation program of ancient suspension bridges, constructed between the end of the 19th century and the beginning of the 20th century, has been developed in France. The old structures were made of wooden deck, masonry piers, steel girders and steel suspension chains. The adoption of aluminium alloy floor girders in the retrofit project of three bridges (the Montmerle and the Trevoux bridges on the Saone river; the Groslée bridge on the Rone river), allowed for conserving as much as possible some of the old structural elements, and brought to very effective solutions, both from the cost and the structural performance points of view.

In the Montmerle bridge (two 80 m bays), the use of aluminium both for the two truss beams with bolted connections, and for the deck slab, led to the possibility of increasing the weight of the road vehicles, while preserving both the existing cables and piers without significant strengthening. In the retrofit of the Groslée bridge (a single 174 m long bay) the floor structure is made of three longitudinal aluminium truss girders, connected to a light reinforced concrete slab. In this scheme a remarkable example of co-operation among different structural materials, each of them utilised in an optimum working condition, can be observed: the old masonry piers, the harmonic steel suspension cables, the stainless steel suspension ties, the aluminium alloy reticular girders with high strength steel bolted joints and the light reinforced concrete slab floor.

### 2. Pre-requisites of aluminium structures

The aluminium alloys can be considered as a family of materials which exhibit a wide range of mechanical properties depending on the type of alloy and the technological treatments [1]. Therefore it is possible to identify alloys which have strength comparable to the common structural steel, and, at the same time, a weight which is one third of the steel one. Due to this specific combined characteristics a high structural effectiveness can be obtained through the use of

aluminium alloys. In addition, in the special case of retrofitting suspension bridges, the lightness of the material adopted for the girders allows for reducing the stress both in the steel cables and in the old masonry piers, thus allowing for the maintenance of these existing structural elements. As a further consequence of the reduced structural weight, i.e. of the dead loads, an increase of the live loads, i.e. of the maximum weight of vehicles which the bridge can sustain, can be obtained. Finally the corrosion resistance of the aluminium leads to avoid any surface protections, even in the case of bridges crossing rivers, thus reducing both the initial and the maintenance costs.

### 3. Advantages of aluminium versus steel

For the Montmerle and the Grosléé bridges, extensive structural analyses of the actual retrofit aluminium solution and of an alternative steel solution, both subjected to several load conditions, have been carried out in [2], in order to examine the structural behaviour in the two cases and to point out the reasons which suggested the choice of the aluminium solutions instead of the steel ones. The comparison between the results obtained for the steel and aluminium solutions in both cases substantially showed that: bending stresses in the girders are less in the aluminium solution than in the steel one, axial stresses in the suspension cables are approximately equal in the two solutions and deformations in the floor girders are lightly larger in the aluminium solution, as expected due to the lower Young modulus of the material, but the values of the absolute displacement are still in an allowable range.

In addition to the numerical analyses of these particular case studies, a wide parametric analysis has been carried out in [3] on a simplified structural model of suspension bridge, accounting for second order effects. The main geometrical and mechanical parameters have been varied in a wide range, in order to point out their influence on the distribution of stresses and deformations among the different structural components, and therefore to show under which conditions the maximum benefits can be obtained through the use of aluminium structural elements. It has been observed in [3] that the detrimental effect of the larger deformability of aluminium is significantly reduced by accounting for second order effects in the structural analysis model.

### 4. A new proposal

A structural retrofit project of the oldest Italian suspension bridge, the "Real Ferdinando" bridge on the Garigliano river, based on the use of aluminium alloy girders, has been recently proposed in the context of a wider rehabilitation program of the zone [4]. The original bridge had a single 85 m bay scheme and the suspension system consisted of two pairs of steel chains, connected to steel ties which sustain the two steel longitudinal truss girders and the wooden transverse beams and floor slab. The proposed project, designed in order to satisfy the requirements of: (a) historic preservation, (b) stiffening of the floor structures, and (c) adoption of innovative technologies and materials, is based on the use of aluminium alloy girders, allowing for the conservation of the original geometrical configuration and appearance. The comparison between the results of structural analyses showed the following advantages of the aluminium with respect to an alternative steel solution: significant reduction of the dead loads; reduction of the required section area of the suspension cables; elimination of the costs necessary for corrosion protection treatments; reduction of repair and strengthening measures required for the masonry piers; easier and less expensive transporting and erection operations due to the lightness of the structural elements.

### References

1. F.M. Mazzolani: Aluminium Alloy Structures. E&F SPON, Chapman & Hall, 2<sup>nd</sup> ed., 1995.
2. R. Landolfo, F.M. Mazzolani, E. Mele: Riesame dei ponti sospesi di Montmerle e di Grosléé: confronto fra acciaio e alluminio. Atti del XII Congresso C.T.A., Isola di Capri, ottobre 1989.
3. F.M. Mazzolani, E. Mele: I ponti sospesi in acciaio e in lega d'alluminio: analisi parametrica. L'edilizia - anno 4° - N° 7-8 - Luglio - Agosto 1990.
4. F.M. Mazzolani: Il restauro strutturale del ponte "Real Ferdinando" sul Garigliano. Costruzioni Metalliche, n.2, 1990.

## Shear Strengthening of Existing Reinforced Concrete Slabs : an Experimental Investigation

**Philippe MENETREY**  
Structural Engineer,  
Emch+Berger AG  
Bern, Switzerland

Philippe Menétrey, born 1963, received his civil engineering and doctoral degrees from the Swiss Fed. Inst. of Tech. in Lausanne and his Master of Science degree from the Univ. of Colorado at Boulder (USA). He has been involved in experimental and numerical research on punching failure in reinforced concrete.

**Eugen BRÜHWILER**  
Professor  
Swiss Federal Inst. of Techn.  
Lausanne, Switzerland

Eugen Brühwiler, born 1958, received his civil engineering and doctoral degrees from the Swiss Fed. Inst. of Tech. (ETH) in Zurich and Lausanne. Post-doctoral stay at the Univ. of Colorado, Boulder (USA). Four years with the Swiss Federal Railways. Since 1995, he is Professor at ETH Lausanne.

### Summary

The strengthening of existing reinforced concrete slabs with vertical posttensioned steel bolts is investigated by testing six slabs. Shear strengthening increases the failure load and leads to a more ductile behavior. By prestressing or injecting the bolts, the peak-load is only slightly increased, but the slip of the bolt inside the slab is avoided and therefore, the serviceability is improved. The prediction of the peak load for slabs with both injected and non-injected bolts is discussed.

### 1. Description of the experiments

The punching tests (Menétrey and Brühwiler [1]) are performed on octagonal slabs of 1.2 m in diameter and 120 mm thick, supported at its extremity by RHS steel pieces (arranged around a diameter of 1.1 m) and loaded at the center through a circular steel column (diameter 120 mm) with an hydraulic jack by controlling the vertical displacement. The concrete compressive strength on cylinder after 21 days is  $f_c = 33.4$  MPa. All slabs are reinforced with horizontal orthogonal bars (steel quality S500) at the bottom and at the top. The percentage of the bottom reinforcement is  $\rho = 0.94\%$ . Slab 1 is not strengthened and slabs 2 to 6 are perforated and strengthened with eight high strength steel bolts placed around a radius of 140 mm equipped with force measuring device. The strengthening system is composed of a bolt type M 10 with an ultimate tensile strength:  $f_u = 851$  MPa, yield strength at 0.2% strain:  $f_y = 736$  MPa. The bolts of slabs 3, 5 and 6 are post-tensioned with the nut on top of the slab. The injection around the bolts are set for slabs 4, 5 and 6 with an epoxy-resin.

### 2. Tests results

The test results are presented with the load-displacement curve (Fig. 1a) and the mean force in the bolts versus the vertical displacement of the slab (Fig. 1b). It follows that the punching load is increased from 280 kN up to 380 kN or 37% due to the strengthening. The vertical displacement at maximum load is significantly increased by the strengthening as it has more than doubled. It is observed that slab 1 is characterized by a punching cone inclined at an angle of approximately  $30^\circ$ . For all strengthened slabs, the punching cone is formed between the column diameter and the perimeter defined by the bolts. The inclination of the punching cone is approximately  $70^\circ$  (Fig. 2). This means that all the strengthened slabs exhibit a punching failure which is characterized by a punching crack that did not cross the strengthening bolts.

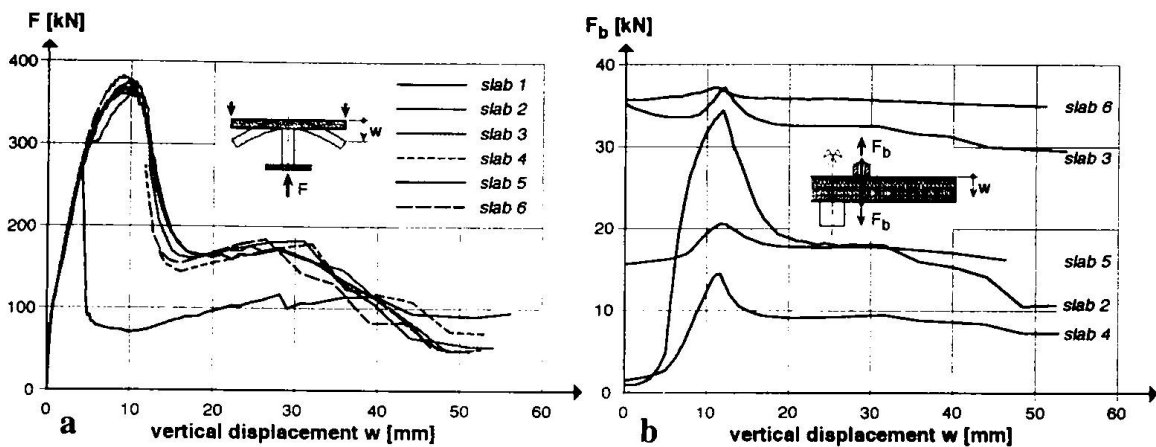


Fig. 1: Load-displacement curves and mean force in the bolts versus vertical displacement

The post-peak descending branch of the load-displacement curve is characterized by a strong reduction of the load carrying capacity with increasing displacement characterizing punching failure (Fig. 1a). After peak, the first drop of the load carrying capacity is about 200 kN for all the slabs (strengthened or not) which indicates that this decrease is due to a similar failure mechanism, that is, the concrete failure.

The present experimental results are similar to the well known characteristic of bolted joints in steel construction for which the failure load for both with and without prestressing force is the same. In addition, prestressing the bolts improves the serviceability of structures.

Injection modifies the slab mode of resistance so that it resists globally resulting in reduction of the stress level in the bolts (compare slab 2 and 4 in Fig. 1b). The injection also improves the serviceability of the slab and provides a protection against corrosion of the bolts.

### 3. Prediction of the punching load

The punching load for the slab without strengthening bolts is predicted with the analytical model developed by Menétrey [2] which leads to  $V_{\text{pun}}=250$  kN. The punching load of the strengthened slabs with a punching crack inclination of  $70^{\circ}$  is influenced by the punching and the flexural strength (as proposed by Menétrey [3]) resulting in  $V_{\text{fail}}=364$  kN.

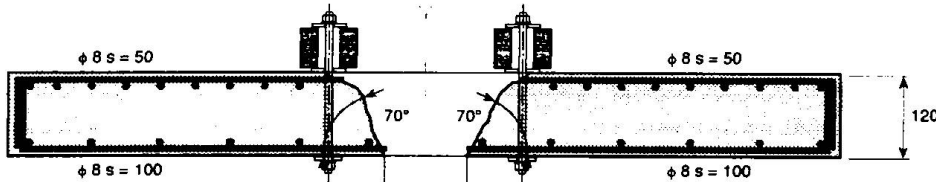


Fig. 2 : Sketch of the punching crack in the strengthened slab

The punching load of slabs strengthened with non-injected bolts is obtained by adding the dowel and the bolt strength. The punching load of slabs strengthened with injected bolts is recovered by adding the concrete, the dowel and the bolt strength.

#### References:

- [1] Ph. Menétrey and E. Brühwiler. Shear strengthening of existing reinforced concrete slabs under concentrated loads, Report MCS-EPFL, CH-1015 Lausanne, 1996.
- [2] Ph. Menétrey. Analytical computation of the punching strength of reinforced concrete. ACI Structural Journal, 93(5), 1996.
- [3] Ph. Menétrey. Relationships between flexural and punching failure. Submitted to ACI Structural Journal.

## Major Repairs to Frank Lloyd Wright's Largest House: Wingspread, Racine, WI, USA

Robert SILMAN  
President, Robert Silman  
Associates  
New York, NY, USA

Robert Silman, born in 1935,  
received degrees from  
Cornell University and New  
York University. He has been  
President of his firm for 31 yrs.

### Summary

Frank Lloyd Wright's design for Wingspread was a brilliant conception but contained several inherent structural deficiencies. These did not manifest themselves significantly for the first 56 years of the house's life, but in 1994 large displacements occurred due to heavy snows. Repairs were made using a carbon fiber-epoxy thin shell laminated directly to the timber roof to form a composite structure. This shell was built up *in situ* from 13 layers of quad-axial carbon fiber.

### Project Description

Wingspread, built in 1938 in Racine, Wisconsin, USA, the largest house ever designed by Frank Lloyd Wright (over 4,000 m<sup>2</sup> floor area). The roofs and walls are framed almost entirely of small dimension lumber (50 x 100 mm to 50 x 250 mm nominal), spaced closely (generally 40 cm on center). At the center of the house is the octagonal Great Hall (15 x 18 m) supported in the center by a very large brick chimney and on four of the sides by seven brick piers on each. The sloping wood roof of the Great Hall is interrupted by three concentric rings of glass skylights each stepped slightly lower than the one above. Radiating out from the Great Hall in orthogonal directions are wings containing bedrooms, kitchen, garage, etc. -- thus the name: Wingspread.

Over the years small cracks had appeared in the plaster and wood ceiling of the Great Hall as well as the East Wing. The heavy snows during the winter of 1993-94 however caused a major displacement near the skylight rings in the Great Hall with cracks larger than 40 mm opening. In addition the exterior walls of the East Wing were noticed to be considerably out of plumb due to thrust at the top of the wood stud wall caused by load from the gable roof rafters. Clearly immediate action was necessary to stabilize and repair this structure, now used as a conference center for the Johnson Foundation.

Temporary shoring was installed and the roof tiles were removed (they were not original in any case, having been replaced in 1993). The permanent repair for the great Hall sought to achieve several objectives. First it should never be visible in the completed work. Second it should minimize disturbances to the existing interior finishes. And third it should be as economical as possible while still conforming to the rules of historic preservation.

After extensive computer modeling using Finite Element Analysis, it was decided to create a shell structure out of the lower roof by coating the bare wood sheathing with 13 layers (12 mm total thickness) of quad-axial carbon fiber fabric set in a 50%-50% matrix of epoxy resin which was bonded to the wood. Prior to the first layer of carbon fiber installation the wood was thoroughly cleaned and large diameter screws were installed through the sheathing into the rafters at 15 cm on centers in oversized holes flooded with epoxy. Thus the carbon fiber was bonded to the wood sheathing which was in turn acting compositely with the rafters. Each layer of carbon was offset approximately 7-8 cm from the layer below to provide a scarf joint at every lap of fabric. Vacuum bagging was not practical for this on site installation so air bubbles were forced out using toothed rollers. The entire operation was conducted inside an environmentally controlled temporary timber framed structure built over the top of the roof. Upon completion, the composite membrane was post cured at 60° C for 24 hours.

Extensive testing was conducted prior to installation, particularly to determine the modulus of elasticity of the composite membrane. Stiffness, not strength was the chief characteristic sought after in the design. Test specimens showed a compressive modulus of  $E = 34$  mPa.



Fig. 1 Installation of Carbon Fiber Fabric



Fig. 2 Impregnating Fabric with Epoxy

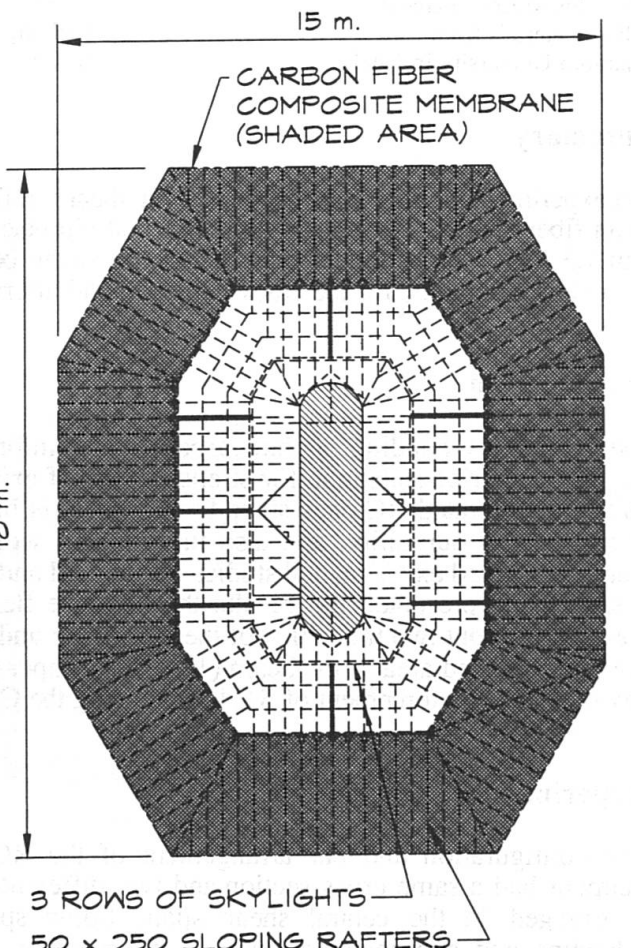


Fig. 3 Roof Framing Plan

## Shear Reinforcement of RC Beams Using Carbon Fiber Sheets

**Yoshiyuki MITSUI**  
Professor  
Kumamoto University  
Kumamoto, Japan

Yoshiyuki Mitsui, born in 1940,  
received his D.Eng. degree in  
structural engineering from Osaka  
University in 1974.

**Kiyoshi MURAKAMI**  
Associate Professor  
Kumamoto University  
Kumamoto, Japan

Kiyoshi Murakami, born in 1957,  
received his D.Eng. degree in  
building materials from the  
University of Tokyo in 1986.

**Koji TAKEDA**  
Graduate Student  
Kumamoto University  
Kumamoto, Japan

Koji Takeda, born in 1967,  
received his M.Eng degree in  
building materials from  
Kumamoto University in 1994.

**Hiromichi SAKAI**  
Manager  
Mitsubishi chemical Corp.  
Kitakyushu, Japan

Hiromichi Sakai, born in 1952,  
received his D.Eng. degree in  
building materials from Kumamoto  
University in 1994.

### Summary

An experimental study was conducted on shear reinforcement of reinforced concrete beam using carbon fiber sheets. The results indicated that ultimate shear strength of the strengthened beam is about 1.3 to 1.8 times higher than that of the virgin beam and similar shear-reinforcing effects of the sheets are obtained for the crack-damaged and afterwards repaired beam.

### Introduction

External epoxy-bonding of thin carbon fiber reinforced plastics sheets (hereafter called the CF sheet) is a superior technique for strengthening of existing reinforced concrete (RC) structures or repair of deteriorated RC ones since the CF sheet is light in weight, high in stiffness and strength and superior in durability, and also the bonding work is easy and not skilled. Authors have already performed experimental studies on flexural and shear reinforcement of RC beams using the CF sheets and presented the results that ultimate flexural strength of the strengthened beam is increased by about two times that of the virgin one and any shear cracks can not be observed in the shear-strengthened area of the beam (1,2). This paper presents the results of a further experimental study on shear reinforcement of RC beams using the CF sheets.

### Experimental

The configuration and bar arrangement of the RC beam specimen is shown in Fig.1. The specimens had a same cross section and two different lengths and shear spans. The stirrups were not arranged in the central shear span. Some specimens were initially crack-damaged by pre-loading and subsequently repaired by injecting epoxy resin into the cracked parts. The arrangement of the CF sheet is shown in Fig.2. Double sheets were bonded crosswise each other over both sides of the beam by epoxy resin adhesive. One more sheet was intentionally arranged on the soffit of the beam to reinforce the tension side of the beam. The bonding work was performed according to the same procedures as presented in Ref.1 and 2. The test was conducted under antisymmetric loading system as shown in Fig.2.

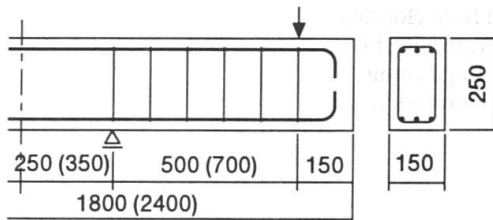
### Results, Discussion and Conclusions

Photos 1 shows failure mode of the strengthened beam after the test. The bonded sheets were

peeled off by force. All of the specimens failed due to diagonal tension cracking in the central shear area. Table 1 shows the measured values of cracking load  $P_{cr}$  and ultimate load  $P_u$  of the beam with the central shear span  $L=250\text{mm}$ . The cracking load  $P_{cr}$  was estimated from shear deformation behaviors measured in the central shear span. Specimen A was initially crack-damaged nearby ultimate stage by pre-loading, and subsequently repaired and strengthened. Specimen B was lightly crack-damaged, and strengthened. The results obtained are as follows. The reinforcing effect of the sheet was small for crack initiation. The ultimate shear strength of the strengthened beam increased by about 1.4 times that of the virgin one. The increasing rate of strength was about 1.3 to 1.8 for the beam with  $L=350\text{mm}$ . Similar reinforcing effects of the sheet were obtained for the crack-damaged beam and the crack-damaged and afterwards repaired beam.

## References

1. K.Takeda et al.: Composites Part A 27A(1996) 981-987.
2. Y.Mitsui et al.: Textile Composites in Building Construction 96, 91-98.

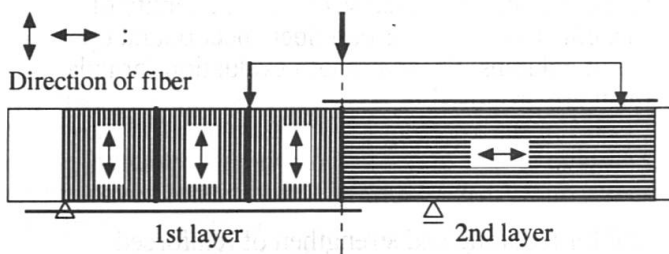


Main reinforcement : upper ; 3-D10 (SD345)  
lower ; 3-D10 (SD345)

Stirrup :  $\phi 5$ , @100mm

Concrete : nominal strength = 21MPa

Fig.1 Configuration and bar arrangement of specimen



Carbon fiber sheet (CF sheet) :  
T. S. = 3400 MPa, T. M. =  $2.3 \times 10^5$  MPa  
Section area of CF =  $167 \text{ mm}^2/\text{m}$   
Adhesive agent : epoxy resin  
Crack repairing material : epoxy resin

Fig.2 Arrangement of CF sheets and loading method (antisymmetric load)

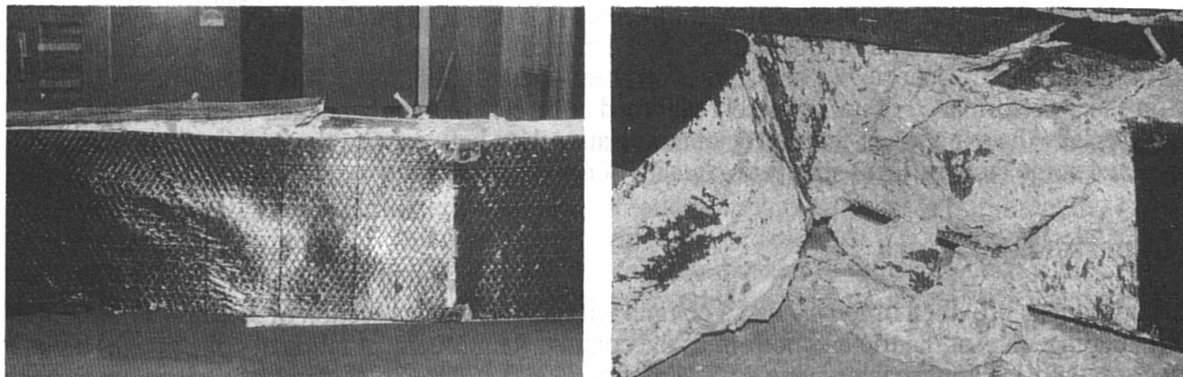


Photo 1 Failure mode of the strengthened beam after the test

Table 1 Test results (central shear span  $L = 250\text{mm}$ )

Specimen No.	State of Specimen	$P_{cr}$ (kN)	$P_u$ (kN)
A	virgin	125.5	188.3
	repaired and strengthened	58.8	268.7
B	virgin	103.0	-
	strengthened	73.5	274.6
C	strengthened	132.4	256.9

$P_{cr}$  : cracking load  
 $P_u$  : ultimate load

## Shear Strengthening of RC Columns by Carbon Fiber Sheet

**Osamu JOH**

Professor

Hokkaido University

Sapporo, Japan

Osamu Joh, born 1943, graduated from Hokkaido University, received Dr. degree of Engineering from the University.

**Atsunori KITANO**

Lecturer

Hokkaido University

Sapporo, Japan

Atsunori Kitano, born 1966, graduated from Hokkaido University, received M.S. degree of Engineering from the University.

### Summary

This paper describes an experimental study on the use of carbon fiber sheet for seismic retrofit of non-ductile reinforced concrete columns. Fifteen column specimens designed originally to be failed in shear were tested under some variables which are shear span ratio, axial stress level, quantity of sheet reinforcement and etc. The test results show the effectiveness of carbon fiber sheet bound up column faces for improving the strength and ductility of columns. Shear strength evaluation formula using of an effective coefficient for sheet reinforcement are proposed.

### 1. Introduction

A carbon fiber sheet was developed as a new material for repairing and strengthen of reinforced concrete members. The sheet is arranged with long carbon fibers in one way. Consequently, it has high strength in one way, and has good workability because of light weight, flexibility and no use of concrete. The sheet is used in real structures for increase of flexural strength of beams, stiffening of slabs with bending cracks, repairing of columns failed in shear and so on. There are many studies of effects on flexural performance, but few studies on shear strength. The paper was an experimental study on shear performance of normal steel reinforced concrete columns bandaged with carbon fiber sheet. Especially the experiment focused to obtain relationships between the shear strength of such columns and some factors: shear span ratio, quality of carbon fiber sheet, axial stress ratio and so on.

### 2. Experimental Work

Twelve specimens provided originally had a column with a square cross section of 300 mm x 300 mm and two loading stabs at the top and bottom of the column. Reinforcement ratios of column axial bars and of hoop with 150 mm spacing were 2.65 % in gross and 0.124 %, respectively, for all columns. The specimens consisted of four variables: shear span ratio, reinforcement quality of carbon fiber (hereafter CF) sheet, column axial stress and repaired/strengthened. This variable of 'repaired' means a reloading test of the specimens which were repaired with CF sheet after failing in shear as original RC columns (CS2, CM2 and CL2, see Table). Then total number of test units was fifteen.

The arrangement of sheet reinforcement was the way which CF bandages cut out with 30 mm width from the sheet were bound up the column faces in every 50 mm pitch with one or three layers. This striping was to observe easily development of cracking on the columns. Each bandage had a lap joint of about 100 mm length at the ends, and was glued concrete with epoxy adhesive. The properties of CF sheet were thickness of 0.111 mm, tensile strength of 3.55 GPa, Young's modulus of 235 GPa, elongation of 1.5 %. The specimens were subjected to constant axial load in stress ratio of 0, 0.2 or 0.4 and lateral load reversals in drifts angles of 1/500, 1/200, 1/100x2, 1/50x2, 1/33x2, 1/25x2 and 1/20x2. Moment diagram of column was a point symmetry about the column midheight.

Table Summary of test results and analyses

note: S=Shear, B=Bond unit: V (kN), R (10<sup>-3</sup>rad.)

Name of Specimen	Shear span ratio	Axial stress ratio	CF reinf. ratio%	Conc. f <sub>c</sub> (MPa)	Experimental results			Calculated results			
					Stiffness reduct. expV <sub>r</sub>	expR <sub>r</sub>	Max. load expV <sub>u</sub> expR <sub>u</sub>	Fail. mode	Shear calV <sub>s</sub>	Bond calV <sub>b</sub>	exV <sub>u</sub> calV
CS2	1.11	0.2	0.0	28.7	287	2.00	293 2.00	S	303 (245)	(245)	0.99
CS2-ARe	1.11	0.2	0.0444	27.2	-	-	297 20.8	S	335 (269)	(269)	0.87
CS2-A	1.11	0.2	0.0444	27.2	297	2.90	305 10.4	S	326 (261)	(261)	0.92
CS2-3A	1.11	0.2	0.1332	30.7	323	3.50	340 8.92	S	376 (290)	(290)	0.87
CS0-3A	1.11	0.0	0.1332	32.9	242	4.20	350 30.0	S	342 (263)	(263)	0.98
CS4-3A	1.11	0.4	0.1332	24.0	304	2.87	320 5.29	S	371 (283)	(283)	0.83
CM2	1.68	0.2	0.0	29.9	264	6.20	264 6.20	B	(234) 213	(234)	1.24
CM2-ARc	1.68	0.2	0.0444	29.9	-	-	170 20.	B	(267) 235	(267)	0.83
CM2-A	1.68	0.2	0.0444	29.4	271	5.08	271 5.08	B	(265) 233	(265)	1.16
CM2-3A	1.68	0.2	0.1332	26.5	283	6.23	302 20.1	S+B	291 (265)	(265)	1.04
CM0-3A	1.68	0.0	0.1332	27.9	208	6.27	292 20.3	S+B	258 (243)	(243)	1.13
CM3-3A	1.68	0.3	0.1332	28.3	323	6.80	336 20.1	S+B	320 (288)	(288)	1.05
CL2	2.24	0.2	0.0	30.0	239	10.1	239 10.1	B	(199) 194	(199)	1.24
CL2-ARo	2.24	0.2	0.0444	30.0	-	-	156 20.1	B	(231) 215	(231)	0.73
CL2-A	2.24	0.2	0.0444	23.0	215	9.12	215 9.12	B	(204) 186	(204)	1.15

$$\text{calV}_s = [0.115 \text{ kp ku} (180 + \sigma_B) / (M / Vd + 0.12) + 2.7 \sqrt{(p_w \cdot \sigma_y + \alpha \cdot f_p \cdot f \sigma_u) + 0.1 \cdot \sigma_u}] b \cdot j \quad (\text{Eq.1})$$

$$\text{calV}_b = \tau_b [0.95 + 0.0018 \sigma_u - 0.066 M / VD] n \cdot \phi \cdot d \quad (\text{Eq.2})$$

$$\text{where } \tau_b = [0.3 + 0.8C / \phi + 13 \phi M / V] \sqrt{\sigma_B + (a_w \cdot \sigma_y + \alpha \cdot f_a \cdot f \sigma_u / f \chi) / (11 n \phi)}$$

### 3. Test Results and Discussion

Response performances of all test units is shown in the table. All columns of S-series (small shear span) were failed in diagonal compressive shear. Shear strength of column CS2-A with one-layer binding increased slightly comparing to that of column CS2 with no sheet, but ductility of the former was improved remarkably. Column CS2-3A with three-layer binding exhibited enhancements of shear strength and ductility. Columns of M-series (middle shear span) with no or one-layer binding were failed in bond split along column axial bars, and those with three-layer binding were failed in the mode mixed with shear and bond split. Columns CM2 and CM2-A failed in bond split had similar maximum strength and deformation at ultimate stage. High reinforcement with CF sheet can improve bond split strength more effectively than shear strength, judging from the fact as the failure mode was changed from the bond split failure to the mixed one. Columns CL2 and CL2-A of L-series (large shear span) showed similar characteristics to CM2 and CM2-A in the strength, ductility and failure mode.

To evaluate the shear strength of columns, Ohno-Arakawa Modified Equation (Eq.1) proposed for RC columns was used. In order to apply this equation to evaluate the shear strength of RC columns bound with CF sheet, the value of fiber reinforcement ratio/p multiplied by its tensile strength  $f \sigma_u$  was added in the second term of steel reinforcing effect in the equation. At this time, the use of a reduction factor  $\alpha$  of about 2/3 needed to close the calculated values to the experiment values because CF fiber did not reach its tensile strength at the maximum strength of columns. The ratio of  $\text{expV}_u / \text{calV}_s$  was 0.99 for column CS2 with no sheet and 0.95 in average for columns failed in shear or mixed mode. This means it might be better to use a less value for the reduction factor. As for evaluating the bond split strength of columns, the same manner mentioned above was applied to Shibata-Sakurai Equation (Eq.2). The ratio of  $\text{expV}_u / \text{calV}_b$  was 1.24 and 1.25 for CM2 and CL2 with no sheet, respectively, and was 1.19 in average for columns failed in bond split or mixed mode. This means the reduction factor of 2/3 is almost an adequate value for evaluation of bond split strength.

### 4. Conclusion

Lateral load reversal tests of non-ductile R/C columns exhibited the following performances:

- 1) reinforcement by binding of one-layer carbon fiber sheet around column faces can improve the ductility only,
- 2) three-layer binding is required to increase not only the ductility but also the diagonal shear and bond split strengths,
- 3) effectiveness of carbon fiber sheet binding on shear strength decreases according to column axial stress level,
- 4) the use of reduction factor for carbon fiber reinforcement is needed to evaluate the shear and bond split strengths.

## Seismic Retrofit of Concrete Columns Using Advanced Composite Materials

**Yan XIAO**

Asst. Professor of Civil Eng.  
Univ. of Southern California  
Los Angeles, CA, USA



Yan Xiao received his BS degree from Tianjin Univ., China, in 1982, and his MS and PhD degrees from Kyushu Univ., Japan, in 1986 and 1989, respectively. He has been on the faculty of the Univ. of Southern California since 1994.

### Summary

In order to develop design guidelines for seismic retrofit of existing bridge columns using prefabricated composite jackets, six large scale bridge columns (Dia.=610mm) have been tested. Three columns with lap-spliced longitudinal bars were subjected to cyclic lateral forces in a single bending mode, while the other three columns were tested to simulate shear dominated bridge columns under cyclic loading with double bending. Test results demonstrated the superior retrofit effectiveness of the composite jackets.

### Test of Shear Dominated Columns

The reinforcement details of shear test model columns are shown in Fig.1, and the test setup is shown in Fig.2. One column was tested in the "as built" condition and the other two models were tested after retrofit for the full column height using prefabricated composite jackets. Fig.3 shows the installation of the individual cylindrical prefabricated composite jacket. The "as built" column suffered a sudden shear failure during the loading cycle corresponding to a limited ductility factor of 3.0. The retrofitted columns developed significantly improved seismic performance characterized by large energy absorption capacities and stable hysteretic responses up to displacement ductility factors of 12 to 14, as shown in Fig.4.

### Flexural Column Testing Program

Three circular columns with lap-spliced longitudinal reinforcement were tested under constant axial load and cyclic lateral forces in a single-curvature mode. One column was tested in the "as built" condition and others were tested after retrofit for the potential hinge region using prefabricated composite jackets. The "as built" model column failed without developing its predicted flexural capacity due to severe deterioration in the lap-spliced longitudinal bars. The two retrofitted columns, one retrofitted with 5-layer individual prefabricated composite jackets and the other with 5-layer continuous jackets developed significantly improved seismic

performance demonstrating the excellent effectiveness of prefabricated composite jackets for flexural retrofit. The retrofitted columns exhibited stable behaviors until a displacement ductility factor of 8.0. Although a gradual degradation of load carrying capacity was observed during loading cycles corresponding to large deformation, the two retrofitted columns were able to develop an ultimate displacement ductility factor of 10.0.

## Concluding Remarks

Current study provides methods for seismic retrofit and repair of reinforced concrete columns. Prefabricated composite jacketing can also be considered for repair and protection of column supported structures from environmental damage and exposure. Studies will be initiated in near future to address the applications of prefabricated composite jacketing in: columns subjected to freeze/thaw and deicing salt corrosion in snow belt states and countries; structures deteriorated due to water absorption of porous concrete; harbor wharf and pilings; power/telephone poles; structures damaged by fires, etc.

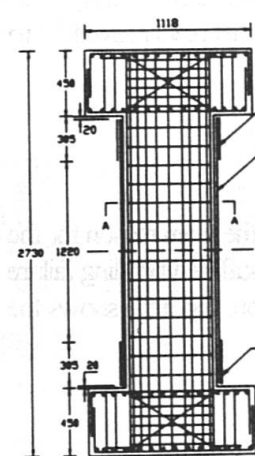


Fig.1. Shear Test Column Details

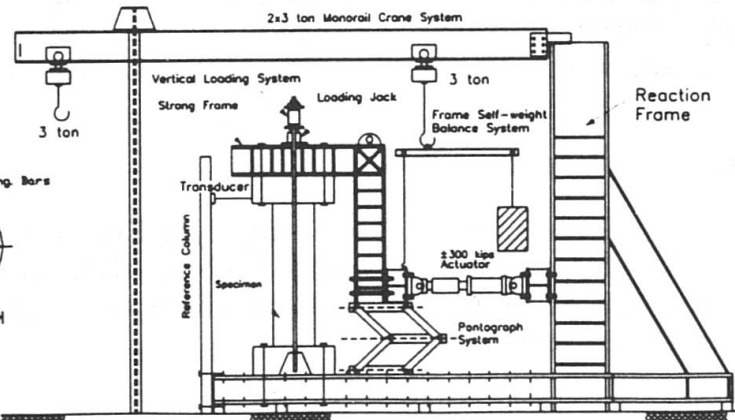


Fig.2. Shear Test Setup

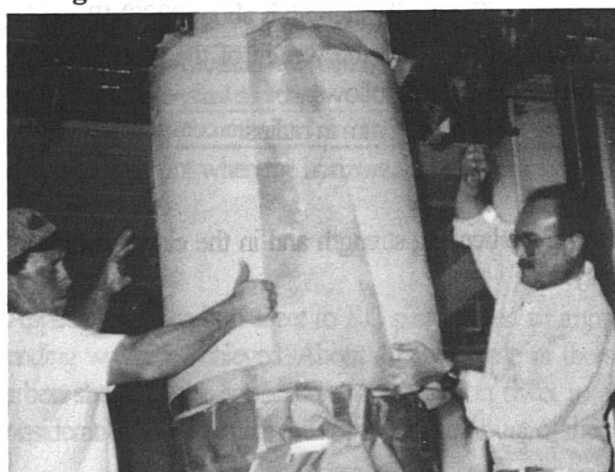


Fig.3. Installation of Prefabricated Composite Jackets

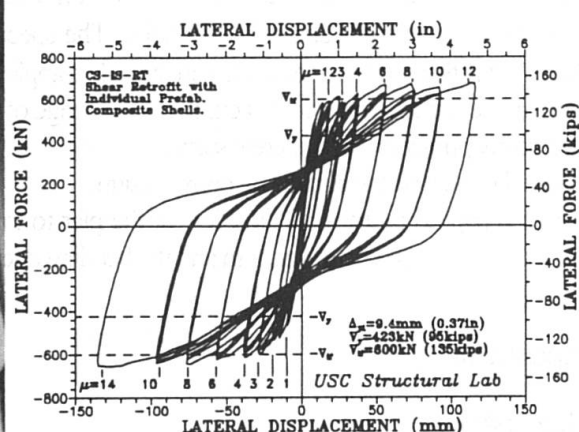


Fig.4. Hysteretic Response of Shear Column with Individual Shell Retrofit

## Strengthening of Reinforced Concrete Bridge Piers by Carbon Fiber Sheet

**Koichi ONO**

Professor of Civil Eng. Dept.

Kyoto University

Kyoto, Japan

Koichi Ono, born 1941,  
received his PhD in Civil  
Engineering from University  
of Toronto.

**Makoto MATSUMURA**

Manager of Civil Eng. Dept.

Konoike Construction Co., Ltd.

Osaka, Japan

Makoto Matsumura, born 1954,  
received his Master of Civil  
Engineering from University  
of Tokusima.

### Summary

The 1995 Great Hanshin Earthquake destroyed many concrete bridge piers as well as the other structures. Lack of shear capacity is considered to be the main reason for the collapse. The piers with a proper capacity in bending ductility were escaped from collapse although they were severely damaged by bending. Strength improvement of the existing concrete bridge piers using carbon fiber sheet is proposed. This method is relatively easy to apply since it is only necessary to glue the sheet on the surface of a pier. The load bearing test of the model piers proved 20 to 40% improvement in the shear strength and 2 times improvement in the bending ductility.

### 1. Damage to RC piers

A lot of RC single piers suffered very severe damage by the Earthquake. Shear failure was the main reason for the collapse. Figure 1 shows the typical shear failure. On the other hand, relatively higher piers suffered bending failure but escaped from collapse although the damage was severe with a large plastic deformation. Figure 2 shows the example of bending failure.

### 2. Strength improvement by carbon sheet

According to the failure pattern of RC single piers, it is important to increase the shear strength and the bending ductility of the existing bridge piers to avoid their collapse by future earthquakes. Figure 3 shows the application of carbon sheet to RC piers. The thickness of the carbon sheet is 0.1mm. The tensile strength is about 2800MPa and the modulus of elasticity is about  $2.5 \times 10^5$  MPa. The specific gravity is 1.8, then the weight of the sheet is only 0.18kg/m<sup>2</sup>. It is therefore very easy for handling. The application procedure is as follows;

1. Clean up the concrete surface and cut the corner edge of piers by more than 30mm in radius.
2. Paint epoxy primer on the concrete surface.
3. Adhere the sheet on the surface by epoxy resin.

The sheet is applied in the axial direction of the pier to improve the bending strength and in the circumferential direction to improve the shear strength and the bending ductility.

### 3. Experiment

#### 3.1 Shear test

A pier model with the column of 119cm high and 60cm square was employed for the shear test. Horizontal force was applied at the top of the column in the back and forth direction under the constant axial force of 539kN. The shear span ratio is 2.5. Five specimens were tested, S-1 being without carbon sheet, S-2 with 1 layer, S-3 with 2 layers, S-4 with 5 layers of carbon sheet and S-5 with steel plate of 3.2mm thick. Figure 4 shows the test results.

According to these results, application of 2 layers of carbon sheet improved the shear strength of the test pier by 40%, while steel plate improved the shear strength by 64%.

### 3.2 Bending test

A pier model with the column of 254cm high and 60cm square was employed for the bending test. The shear span ratio is 5.0. Five specimens were tested. Table 1 shows the summary of the test specimens and test results. These results indicate that reinforcement by the carbon fiber sheet improved the ductility satisfactorily.



Fig. 1 Shear failure of a RC pier



Fig. 2 Bending failure of a RC pier

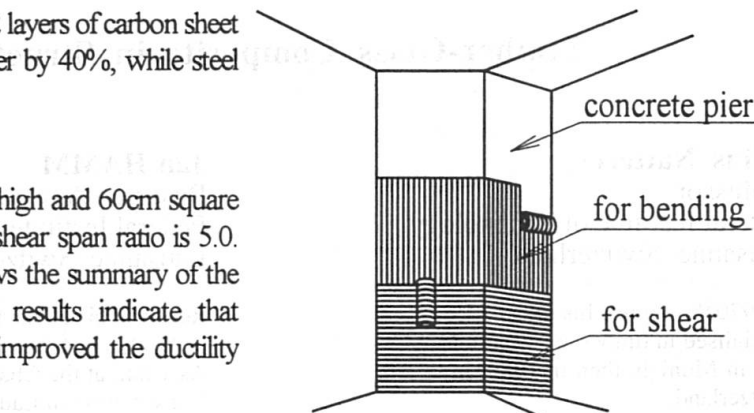


Fig. 3 Application of carbon fiber sheet

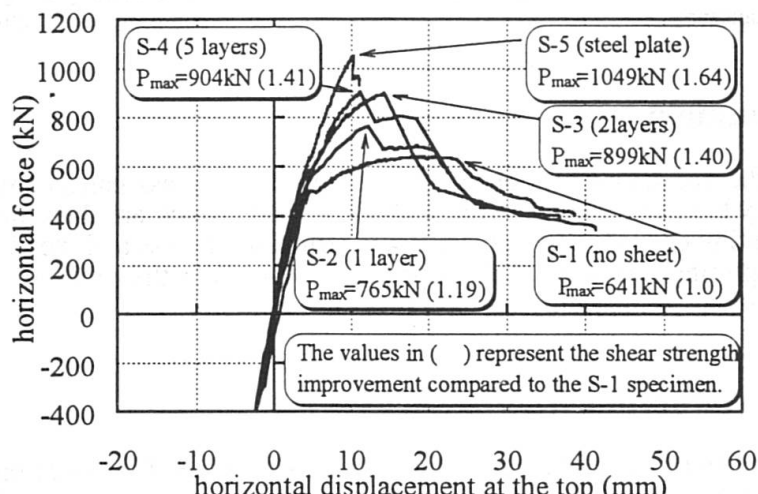


Fig. 4 Load-deflection curve of the shear test model

Table 1 Bending test results

Specimen	Reinforcement	Maximum horizontal force (kN)	Yield displacement $\delta_y$ (mm)	Ultimate displacement* $\delta_u$ (mm)	ductility $\delta_u/\delta_y$
M-1	without carbon sheet	206.8	15.6	87.9	5.6
M-2	2 layers(circumferential direction)	203.8	13.6	98.8	7.3
M-3	4 layers(circumferential direction)	211.7	13.9	107.7	7.7
M-4	4 layers(circumferential direction) +1 layer(axial direction)	228.3	12.2	96.8	7.9
M-5	8 layers(circumferential direction)	225.4	13.1	144.8	11.1

\* displacement when the horizontal force dropped to 80% of the maximum horizontal force

### Conclusion

Application of carbon sheet to RC pier proved to improve the shear strength. Improvement of the ductility in bending was also achieved. About 40% increase of the shear strength was obtained by applying 2 layers of the carbon sheet. In the application of the carbon sheet to an actual pier, the size of the pier should be taken into consideration to determine the appropriate amount of the sheet to obtain the required strength improvement.

### Acknowledgment

The authors wish to acknowledge their indebtedness to Mr. S. Sakanishi of Sunkit Co.,Ltd., Mr. K. Miyata of Nippon Oil Co.,Ltd. and Mr. T. Matsuo of Konisi Co., Ltd. for their cooperation in the experimental work.

## Timber-Glass Composite in Structural Glazing

**Julius Natterer**

Professor

Federal Institute of Technology  
Lausanne, Switzerland

In 1970, he founds his own office specialised in timber construction first in Munich, then in 1983, in Switzerland.  
In 1978, he is named director of the Chair of Timber Construction of the Swiss Federal Institute of Technology in Lausanne

**Jan HAMM**

Research Assistant

Federal Institute of Technology  
Lausanne, Switzerland

Received his civil engineering degree in 1994, since then he is Research Assistant at the Chair of Timber Construction in Lausanne.  
His main research work at the Institute is timber-glass composite in structural glazing. Timber-glass composite in structural glazing

### Summary

In the normal application of glass in buildings, glass panels are mounted in frames and designed to carry their self-weight, wind and snow load, which are then transmitted to the supporting structure. The timber-glass concept is a mixed structure of glass and wood, with both components acting as the supporting structure. This paper aims to present the problems related to such structures, and the solutions proposed by our research.

### Introduction

More and more architects and engineers are looking for an ecological way of construction. Glass is an ecological material in the sense that we can economise energy for heating and for light, if used in construction. In the same way wood is an ecological material because it is the only renewable raw material that stores carbondioxide which is necessary for wood growth. Less energy is needed to fabricate a timber beam compared to metal, aluminium or concrete. Therefore, timber and glass are often used in combination for construction like for greenhouses or facades.

In the traditional (not composite) timber and glass construction, the beam-sections are often so important, that it causes problems with aesthetic and natural lighting. So a timber-glass composite element has been developed, where the wooden frame is directly glued to the glass-plate (fig.I).

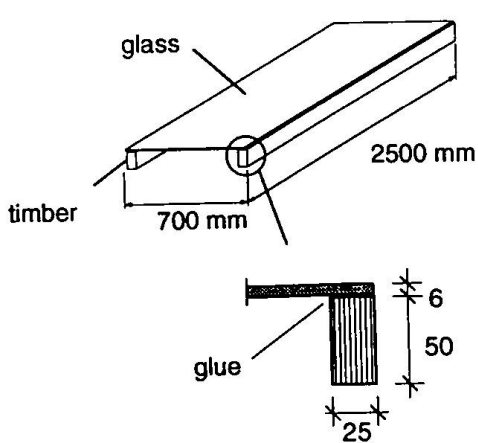
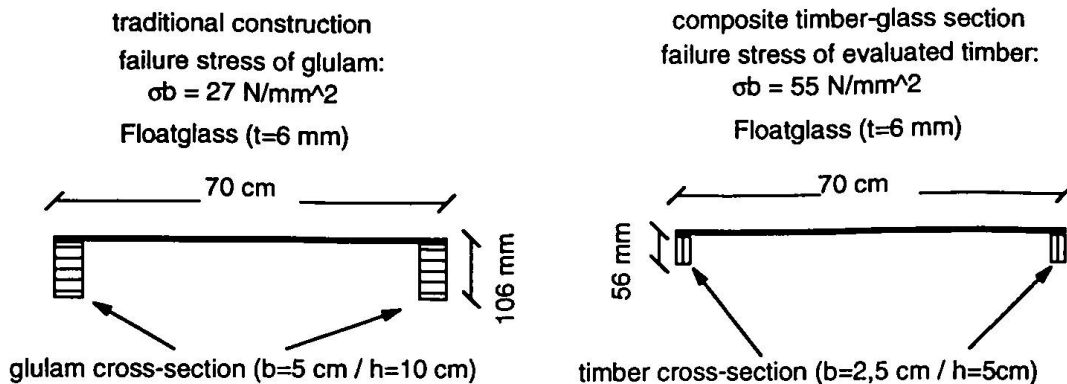


fig.I: composite element timber-glass

A comparison between the traditional and the composite structure shows that the wooden sections are much smaller with timber-glass composite structures (fig.II, next page).

This kind of composite structure has the following advantages:

- prefabricated sections
- minimal cold bridges
- optimised energetic profit
- light structure
- ecological
- economical



*fig.II: comparison between the traditional and the composite structure*

## Tests

To find the right glue for the timber-glass composite structure, several small specimens have been tested under shear compression loading. Because the composite elements are under climatic variations the test specimens were submitted to several cycles. One cycle consisted of 4 hours at -30°C, 4 hours at +70°C, 16 hours at +30°C and 80% humidity. This cycle was repeated up to seven times and specimens were tested after 0-cycle, 2-cycles, 5-cycles and 7-cycles to evaluate the possible degradation. Of the four glues which were tested, only one resisted to the stress-test.

After the right glue was found, 4-point loading tests on timber-glass composite plates were executed. The results of these tests showed that the efficiency of the glueing was nearly 100%. The rupture of these elements was due to the excess of the tensile-bending stress in the wood (in average: 66,24 N/mm<sup>2</sup>).

## Conclusion

The goal of this research is to develop composite timber-glass elements for structural glazing. A glue has been found and tested by shear compression loading after several climatic cycles. It was proven, that composite elements which are loaded perpendicular to its plane has a high rigidity and resistance. The research-team of timber-glass composite for structural glazing is now testing composite elements as shear-walls to stabilise greenhouses and facades. Also composite timber-glass beams will be tested.

## References

Savoy, Eric; *Traité technique du verre*;  
Imprimerie André Demierre SA (1989)

Couvrat, Patrice; *Le collage structural moderne- théorie & pratique*;  
TEC & DOC - LA VOISIER (1992)

Kollmann, F.F.P; *Principles of Wood Science and Technology*;  
Volume I, Springer-Verlag, Berlin (1984)

## Advanced Composite Stay Cables

**Markus WERNLI**

Research Assistant

Univ. of California, San Diego

La Jolla, CA, USA

**Frieder SEIBLE**

Professor and Chair

Univ. of California, San Diego

La Jolla, CA, USA

Markus Wernli, born 1966, received civil engineering from the ETH in Zurich in 1991 and a MS degree in Structural Engineering from UCSD in 1996. His research focus is on the application of advanced composites in civil engineering.

Frieder Seible received his civil engineering degrees from the Universities of Stuttgart, Calgary and Berkeley. He is director of the Powell Structural Research Laboratories. His research focus is on bridge design, seismic design and retrofitting of bridges, large scale experimental testing and the application of advanced composites in civil engineering.

**Summary**

The paper summarizes the ongoing research at the University of California in San Diego about the performance of composite stay cables available on the world market. Research emphasis is placed on investigating the long term behavior of such cable systems, in particular of their anchorages. Five cable systems offered on the world market were selected for the testing; three were composed of unidirectional carbon and two of aramid fiber reinforced polymer. The selected cable systems were subjected to short- and long-term testing.

**Introduction**

The infrastructure industry is in the search for more durable materials for key structural elements. Advanced composite materials like carbon or aramid fiber reinforced plastics stand out for their light weight, excellent performance, durability and chemical resistance and seem to be a good addition to conventional construction materials. Stay cables made of these advanced composites are promising, and an increasing number of products is appearing on the world market. However, a lot of investigation, in particular of the long term behavior, has to be done to gain the necessary confidence into the structural reliability of these new cable systems. In a research program at the University of California in San Diego, available cable systems from the world market were subject to long and short term tests to investigate the behavior of such systems. The results provide short term characteristics and lead to an estimate of their long term behavior. The program is not completed yet. Initial and preliminary results and trends are discussed in the following chapters.

**Cable systems**

Scanning the world market for commercially available cable systems, most of the systems are found in Japan and Europe. Only a few companies offer cables with appropriate anchorage systems which could fulfill the requirements for stay cables.

Two different types of anchorages can be identified. The first one has tendons potted in polymer matrix and the load is introduced by bond forces between the matrix and the composite tendons. The second type is similar to conventional high strength steel tendon anchorages and anchors the

tendons mechanically by wedges and the force is introduced by friction. There are also systems using a combination of mechanical and bonded anchors.

### **Short Term Test**

Three specimen of each of the cable systems were subject to short term load tests. The procedure of the test was similar to those recommended by the Post-Tensioning Institute (PTI) and the Federation Internationale de la Precontrainte (FIP) for steel tendons. However, the recommendations were adjusted for composite cables.

Even though only three specimen per tendon type were tested, the repeatability of the test results was very satisfactory. Cable systems which failed due to slippage in the anchorage had a deviation of 8 % of the average failure load and the other systems only 4 %. The deviation is hereby defined as the difference between the highest and smallest failure load. However, the tested failure load was sometimes significantly higher than the manufacturers specified guaranteed breaking load.

### **Performance of the bond anchorages**

Strain gages at the outer shell of the bond anchors allowed the estimation of the tendon force transfer within the anchorages. The bond stresses between the strand and the matrix were roughly estimated by evaluating the strains at the surface of the sleeve. During cyclic loading, high bond stresses of up to 20 MPa were developed. With each cycle, the peak stress was moving slightly towards the back of the anchorage, and the bond stress concentration at the front of the anchorage was decreasing. During loading to failure, the peak of the bond stress distribution was moving to the back of the anchorage, developing up to 44 MPa of maximum average bond stress before tendon failure. This observation was independent of the failure mode in the cable systems.

### **Long Term Test**

Two specimens of each of the selected cable systems were mounted in separate steel frames for long time monitoring. The tendons were tensioned and then anchored at their specified maximum service load of 65 % and 55 % of their nominal breaking load for carbon and aramid based systems, respectively. This was the same load level as of the upper load during cyclic loading in the previous tests. After about 1000 hours, they were restressed to the service load. The observed initial relaxation is generally high. The bond anchors reveal a similar behavior as during cyclic loading. The peak average bond stresses tend to move more to the back of the anchors.

### **Conclusions**

All cable systems showed a very good performance during the short term tests with a high repeatability. The behavior of the cable systems is different for the two load cases in short term and long term tests. Therefore, the long term behavior cannot be predicted satisfactorily by short term testing. This is true in particular for the bond anchor systems, because of the viscous behavior of the matrix. As a third test for the estimation of the long term behavior of composite cables it is recommended to perform accelerated aging tests of the anchors under sustained load.

## Ultimate Strength of Steel-Concrete Composite Sections under Biaxial Bending

**Jun KAWAGUCHI**  
Research Associate  
Mie University  
Tsu, Mie, Japan

**Shosuke MORINO**  
Professor  
Mie University  
Tsu, Mie, Japan

**Mika UEDA**  
General Building Research  
Corporation  
Suita, Osaka, Japan

### Summary

Effects of loading path on the ultimate strength and the moment-curvature relation of cross sections subjected to axial load and biaxial bending were investigated by analyzing four kinds of cross section: wide flange, square tube, CFT and SRC sections. Three types of loading path were considered. It was found that an identical point on the ultimate strength interaction was reached regardless of the loading paths, and the maximum values of bending moments may be different from those at the ultimate strength point on the interaction.

### 1. Introduction

The ultimate strength interaction curves of reinforced concrete and steel reinforced concrete (SRC) cross sections were extensively investigated, and several mathematical formulas were proposed [1,2]. However, no research was found which mentioned the effect of loading procedure. The purpose of this investigation is to clarify the effect of the loading procedure on the ultimate strength by the numerical analysis of the moment-curvature relation considering the strain reversal and the local buckling of steel elements.

### 2. Moment-Curvature Relations

The moment-curvature relations of four cross sections were analyzed: wide flange, square tube, concrete-filled square tube (CFT) and SRC containing wide flange as shown in Fig. 1. The stress-strain relations of steel, reinforcements and concrete were assumed as shown in Fig. 2. The relation of the steel contains the stress reduction part caused by the local buckling [3]. Materials assumed here were SM490 class ( $\sigma_y = 323.4 \text{ N/mm}^2$ ) for steel, SD40 class ( $\sigma_y = 211.6 \text{ N/mm}^2$ ) for reinforcement, and the  $300 \text{ kgf/cm}^2$  ( $F_c = 29.4 \text{ N/mm}^2$ ) for concrete. Parameters for the stress-strain relations are shown in Table 1.

Figure 3 shows the strain distribution in the cross section subjected to the axial load  $N$  and the biaxial bending moments  $M_x$  and  $M_y$ , which were calculated for given values of the curvature by the numerical integration, dividing the cross section into small elements and assuming the uniform stress distribution in each element. The following three loading procedures were considered:

**A:**  $M_y$  was kept constant, and  $M_x$  was gradually increased.

**B:**  $M_x$  and  $M_y$  were gradually increased so that the deformation angle ( $\theta_f = \tan^{-1}(\phi_y / \phi_x)$ ) was kept equal to the value which was already obtained at the ultimate stage in the procedure **A**.

**C:** Proportional loading with the bending angle ( $\theta_m = \tan^{-1}(M_y / M_x)$ ) kept equal to the value which was obtained at the ultimate stage in the procedure **A**.

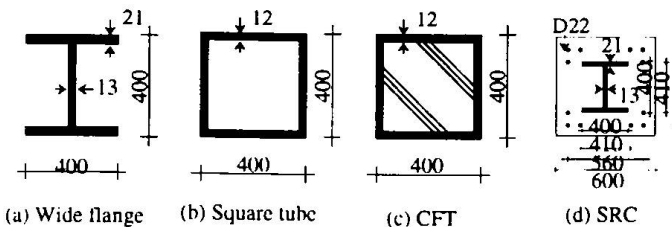


Fig. 1 Cross-sections

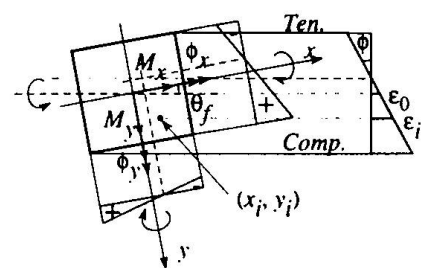


Fig. 3 Strain distribution

Table 1 Parameters

$stE(kN/mm^2)$	205.8
$rbE(kN/mm^2)$	205.8
$st\sigma_{pc}(N/mm^2)$	196
$st\sigma_{pt}(N/mm^2)$	-196
$st\sigma_y(N/mm^2)$	-323.4
$st\sigma_u(N/mm^2)$	288.6
$st\varepsilon_u(\%)$	0.14
$st\varepsilon_{cr}(\%)$	0.67
$con\varepsilon_u(\%)$	0.6(CFT) 0.4(SRC)

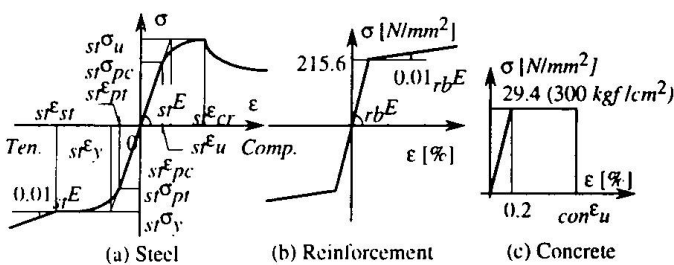


Fig. 2 Stress-strain relations of material

### 3. Ultimate strength

Figure 4 shows the  $M_x$ - $M_y$  paths of four cross sections together with the ultimate strength interaction curve which was calculated at the stage that the compressive strain of any element reached to the strain of the local buckling or the strain of the concrete crash. The procedure **A** in which  $M_y$  was kept constant, and the procedure **C** in which the bending direction was kept constant show the linear relation from the beginning to the ultimate stage on the interaction curve. On the other hand, procedure **B** shows the curved relation. However,  $M_x$ - $M_y$  paths obtained from three analyses met at the exactly same point on the interaction curve for the ultimate strength of the cross section. The maximum values of  $M_x$  and  $M_y$  of the wide flange and the SRC sections are different from the strengths given by the ultimate point on the interaction curves. This is because these cross sections have unequal strengths about two major axes.

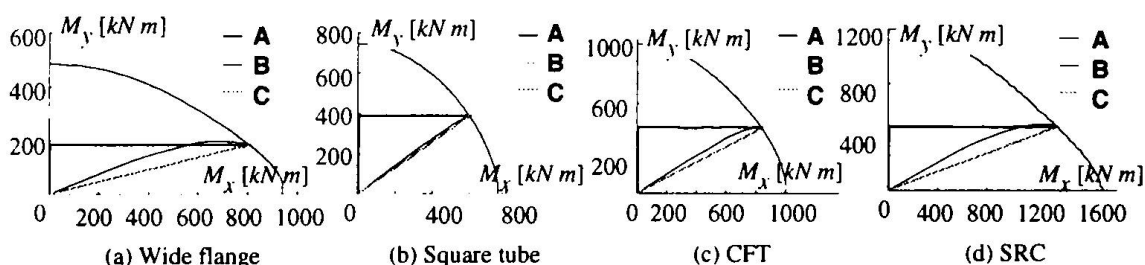


Fig. 4 Biaxial Ultimate Strength

- 1) An identical point on the interaction curve for the ultimate strength of the cross section subjected to the axial load and the biaxial bending moment was reached regardless of the loading procedure.
- 2) The ultimate strength point on the interaction curve was not the same as the maximum point of  $M_x$  and  $M_y$  in the case of the procedure **B** with the constant deformation angle for the section having unequal strength about two major axis.

### References

- [1] B. Bresler (1960), *Design Criteria for Reinforced Concrete Under Axial Load and Biaxial Bending*, ACI Journal, Vol. 57, No. 5, pp. 481-490.
- [2] C. Matsui, S. Morino and Y. Ueda (1984), *Maximum Strength of Steel Reinforced Concrete Section Subjected to Axial Thrust and Biaxial Bending*, Research Papers, Faculty of Engineering, Kyushu University, pp. 95-101.
- [3] J. Kawaguchi, S. Morino, H. Atsumi and S. Yamamoto (1991), *Strength deterioration Behavior of Concrete Steel Tubular Beam-Columns under Repeated Horizontal Loading*, Proc. of 3rd International Conference on Steel-Concrete Composite Structures, pp. 119-124, Fukuoka, Japan.

## Long Term Performance of Timber Concrete Composite Structural Elements

**Ulrich A. MEIERHOFER**

Dipl.-Ing. ETH

EMPA

Dübendorf, Switzerland

### Summary

Little information was available on the long term performance of timber concrete composite structural elements (TCCs) up to now. Recently finished long term shear and bending tests suggest design creep values.

### 1. General remarks

Composite construction originally meant the combination of structural steel and concrete. For many decades the combination of timber and concrete has not been considered as feasible for various reasons, one important being the distinctively different properties of the two materials. Together with a changing attitude of the engineers in combining various materials, the combination of concrete and timber - especially used as floors - also offered various advantages and became more acceptable. A vital point is the development of an efficient connection to transfer the shear forces between timber and concrete. A considerable amount of theoretical and practical research and development in this field resulted in a rapidly increasing knowledge and an implementation in many building rehabilitations and new projects.

Newly acquired knowledge and experience on concrete composite structural elements (TCCs) are not restricted to structural properties such as strength and stiffness, but also encompass fire safety, acoustics, working condition during erection, economics and even aesthetics.

### 2. Long term deformation as governing criterion

The analysis of built up structural elements with semi-rigid connections requires the solution of differential equations and doesn't belong therefore to the everyday's problems of the structural engineer. Solutions have been developed, however, and designs aids are available. For the modelling of the structural behaviour various simplifying assumption must be made including behaviour and properties of materials and connections. To calibrate and verify this assumptions and to establish system behaviour not so far accessible by theoretical means, experimental work is indispensable. This refers particularly to the deformation behaviour of the connectors within the wood.

As had already been shown by early investigations, of all the factors necessary for a satisfactory performance of TCCs, the bending stiffness, particularly the long term bending stiffness or the long term deflection proved to be of special importance. The susceptibility of TCCs to long term deformations is a consequence of creep phenomena as well as relaxation of residual stresses caused mainly by the differential thermal and hygroscopic behaviour of concrete and timber. For a theoretical analysis of this complex phenomena the basics are still lacking and the experimental work - especially on long term deformation - is so far very limited.

### 3. Research and development at EMPA

The Wood Department of the Swiss Federal Laboratories for Materials Testing and Research (EMPA) has undertaken extensive research in this field with a special screw like connector developed by SFS Stadler, Heerbrugg, Switzerland. This connector is characterised by its high slenderness which allows a very efficient installation without predrilling. The lack of bending stiffness of this connector is compensated by a mounting under an angle of  $\pm 45^\circ$  which allows transfer of the shear forces between the concrete and the timber by tension and compression within the connectors (instead of the more common bending and bearing).

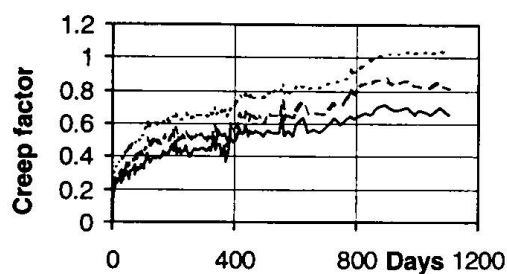
The tests performed encompassed basically withdrawal tests from timber and concrete, shear tests with symmetrical timber/concrete/timber specimens and bending tests with TCCs having spans of nearly 4 m. This work has been performed mainly in the years 1990 to 1993 and was reported in [1,2,3]. Within this period appropriate long term shear and bending tests were started too. Test parameters were the (geometrical) arrangement of the contours, load level and climatic conditions. The maximum load level was fixed in such a way that it superseded to some

extent which was considered a reasonable operational level deducted from the results of the short term tests. The shear creep tests were run under constant climatic conditions (23°/50% r. h.) whereas the bending creep specimens were installed outside under roof, i. e. they were subjected to the natural variation of temperature and humidity. Even though the investigated TCCs had been developed and earmarked for interior use, this severe test configuration was selected to obtain conservative results.

After an extended period of creep (about 5 years for the bending tests and about 3 years for the shear tests) the specimens were unloaded, creep relieve recorded and then tested to failure in a short term test. The results are reported in [4] and some brief information follows.

#### 4. Long term shear tests

*Fig. 1 Development of creep factor of shear tests with different connection stiffnesses*



The main interest was the long time deformations which are shown in *Fig. 1* as the development of the creep factors over a period of about three years. The recovery behaviour after unloading (not shown here) proved to be satisfactory and indicated that the long term high loads did not cause any damage to the structure, resp. connection system. The creep curves may be fitted particularly well by potential curves of the type  $y = a * x^b$  (correlation factors between 0.966 and 0.981), where 'a' varied between 0.10 and 0.16 and the exponent between 0.243 and 0.276. Extrapolated to a period of about 20 years, this implies creep factors between 1 and 1.7.

#### 5. Long term bending tests

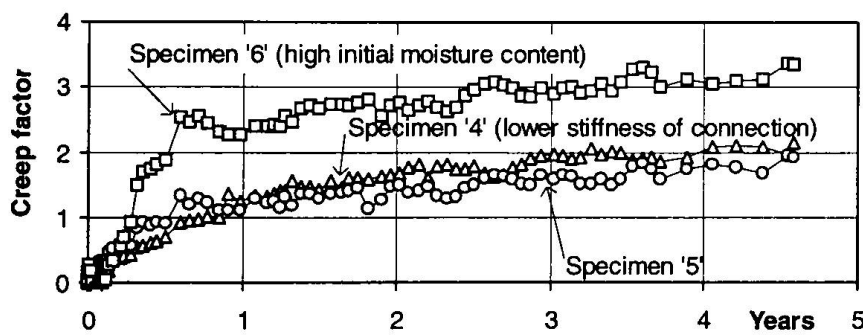


*Fig. 2. Creep of three different TCC-specimens*

The bending specimens, composed of a timber beam 12 cm x 18 cm and a concrete slab 8 cm x 75 cm cross-section were equipped with dial

gauges to measure the sag at mid span and the end slip between timber and concrete. Strain at various points at mid span were recorded also by deformeter. One of the main results is the increase of sag shown in *Fig. 2* as creep factor. Due to the strong influence of climatic residual stresses (changes of humidity and temperature), the sag creep factors are considerably higher than those of the shear tests. Extrapolations of the fitted potential curves suggest a twenty years creep factor between 2.5 for normal and 4.5 for especially unfavourable conditions.

#### 5. Conclusion

Long term deflections of TCCs under higher loads can't be neglected even in indoor climatic conditions. A creep factor of at least 2.5 should be applied until further research results suggest more differentiated values.

#### References

- [1] Timmermann K., Meierhofer U. A. 1993. Timber Concrete Composite Structural Elements; Tests, Research and Development. *Forsch. u. Arb.-Ber. der EMPA Abt. Holz.* Rep. 115/30. English abstract.
- [2] Meierhofer U. A. 1993. A Timber/Concrete Composite System. *Struc. Eng. Int.* 1993(2), p.104...107
- [3] Meierhofer U. A. 1994. Untersuchungen und Entwicklungen zum mechanischen Verbund von Holz und Beton. *Schweiz. Ing. u. Arch.* 1994(37).
- [4] Kenel A., Meierhofer U. A. 1997. Long Term Performance of Timber Concrete Composite Structural Elements. *Forsch. u. Arb.-Ber. der EMPA Abt. Holz.* Rep. 115/35. English abstract. To be published in 1997.

## Vertical Shear Resistance Models for a Deltabeam

**Matti V. LESKELÄ**  
Ph.D. (Civ.Eng.)  
University of Oulu  
Oulu, FINLAND

Matti Leskelä, born 1945, received his Ph.D. in 1986 and has been carrying out research into composite structures from the early 1980's. His latest work has concerned problems of partial interaction and various shear connections in composite structures such as slim floors, composite slabs and concrete filled steel tubes.

### Summary

The Deltabeam is an innovative structural form for beams for use in slim floor construction fabricated by Deltatek in Finland. The principles employed in developing vertical shear resistance in the composite state and in the initial state of steel construction are discussed. Changes in behaviour due to exposure to fire from the underside are introduced, and methods of reinforcing the system are reviewed.

### 1. Introduction

The Deltabeam consists of a boxed steel member in which circular web holes are spaced at constant distances along the span so as to make it possible to fill the box section with concrete and to make the structure behave compositely after solidification of the concrete. In the initial state, as a steel construction, the web holes, extending maximally to 60 % of the web depth, cause an obvious reduction in the vertical shear resistance of the beam, but the resistance is nevertheless adequate for the applications for which the beams are intended. After the solidification of the concrete the vertical shear resistance is enhanced greatly and can cope with all loads introduced in the ultimate limit state.

### 2. Mechanisms for shear resistance

Mechanisms for the evaluation of vertical shear resistance are defined for three states of behaviour: (1) steel construction, (2) composite construction and (3) composite construction when exposed to fire. The principal difference in the effective structure between normal conditions and fire temperatures is that the unprotected bottom flange is normally lost in fire exposure and cannot contribute to the shear resistance.

#### 2.1 Steel construction

The resistance of the steel member to vertical shear forces should be considered with respect to stresses formed due to the combined effects of local and global actions in the sections through the web holes. It is scarcely possible to derive reasonable formulae directly for the maximum stresses around circular holes, however, and therefore an approximation with respect to a beam having square web holes of the same depth is used.

In German research into I-beams with circular and square web holes [1, 2] it has been shown that the ratio of the ultimate resistances in beams with square (resistance  $V_{\square,R}$ ) and circular web holes (resistance  $V_{\phi,R}$ ),  $V_{\square,R}/V_{\phi,R}$ , can satisfactorily be defined as a function of the relative depth of the holes,  $\phi/h$ ,  $\phi$  being the hole depth and  $h$  the depth of the beam. Since it is possible to evaluate the stress state in the case of square holes, the known ratio of the resistances may be applied to convert  $V_{\square,R}$  into  $V_{\phi,R}$ . The principle was verified by means of loading tests and was observed to work well when the resistance was determined based on the first yielding in the edges of the holes. This is also justified, considering the state of construction.

## 2.2 Composite construction

The concrete infill inside the boxed section suggests that a system of compression struts and tension ties will develop in a truss form when the load is increased in steps to failure, i.e. compression struts will be formed between inclined cracks in the concrete contained in the boxed section and the web sections between the holes work as vertical tension ties. The system bears some resemblance to that observed in concrete beams reinforced with vertical stirrups, but it must be noted that the contributions of the concrete and steel to the shear resistance are not additive. This is explained by the considerably higher yield capacity of the web sections as compared to the normal density of stirrups in the reinforced concrete structures.

## 2.3 Composite construction exposed to fire

If no thermal insulation is applied in the bottom flange of the steel section, fire exposure from below will normally make it inefficient, not only for allowing excessive bending of the beam, but also for maintaining shear resistance. To ensure the bending resistance, reinforcing bars are used inside the box section, but these do not contribute to the vertical shear resistance of the structure unless it is ensured that the maximum force in the diagonal compression struts, formed in the same manner as at normal temperatures, is able to anchor to the webs of the steel section. It was observed in loading tests that the diagonal compression struts in beams with no bottom flange were finally pushed out, causing then anchorage failure in the reinforcing bars, which were not able to develop any yield. The majority of the diagonal concrete forces are anchored by the web holes, and the rest of them can be anchored to additional devices such as stirrups and shear plates welded to the inside of the top flange.

## 2.4 Interaction with bending

The vertical shear resistance described in section 2.2 above is such that very thick flanges in the beam are required to prevent the flanges from yielding before reaching maximum resistance. When concentrated loads are used in testing, there are normally high bending moments in the sections where the shear resistance is to be reached, and some interaction with bending is to be expected. The prediction of the vertical shear resistance by the strut and tie models has proved to be satisfactory, however, although the models developed for the shear resistance consider the bending effects only in the case of fire design.

## 3. References

- [1] Petersen, C., Stahlbau, p. 611-612. Friedr. Vieweg & Sohn, Braunschweig/Wiesbaden 1988
- [2] Clauss, H., Tragfähigkeit von Vollwandträgern mit Stegausnehmungen. Diplom-Arbeit am Lehrstuhl für Stahlbau. UniBw München 1986

Leere Seite  
Blank page  
Page vide

## Composite Construction in California Bridge Seismic Retrofitting

**James E. ROBERTS**  
Chief Bridge Engineer  
California Dept of Transp.  
Sacramento, CA, USA



James Roberts, born 1930, received BSCE from University of California, MSCE from University of Southern California. Director of Engineering Services and Chief Structures Eng. Responsible for statewide inventory of 24,000 bridges and structures in California. Focus is on bridge design (major emphasis on seismic design, retrofit strengthening), construction, maintenance and bridge management. Engaged in application of advanced composites in bridge rehabilitation.

### Summary

The California Department of Transportation has funded research at the University of California at San Diego for the past six years to develop field applications of advanced composite materials for both repair of older structures and construction of new bridges. The most highly developed application to date is the use of advanced composites in repair of bridge columns and other supporting elements to improve their ductility for seismic resistance. Epoxy impregnated fiberglass and carbon fiber materials have been tested in the laboratory on half-scale models of bridge columns to determine the ductility that can be achieved in an older, non-ductile concrete column. The tests have confirmed the viability of these materials for strengthening existing structures and field application quality control specifications have been developed.

### 1. Introduction

Following the October, 1989 Loma Prieta earthquake the California Department of Transportation (Caltrans) began a research program, in cooperation with the University of California at San Diego (UCSD), to develop techniques for utilizing epoxy impregnated fiberglass sheets to wrap around older, non-ductile concrete bridge columns as an alternative to the already proven steel jacket technique. The jackets provide sufficient confinement in the concrete to allow them to perform in a ductile manner under seismic loading. It was known that the Japanese had used high strength carbon strands to similarly reinforce industrial stacks and chimneys but the use of glass fiber sheeting had not been used. The major unknown was the durability of the fiberglass materials under cyclic loading and to what level of ductility the columns could be designed. The testing program was conducted under the same conditions that were used in the testing of steel plate jackets. Half scale models of the prototype bridge columns were constructed, wrapped with the desired layers of glass fiber sheets and tested through several cycles of loading at various levels of ductility until the column failed due to degradation of its hysteretic performance. These laboratory tests proved that the epoxy impregnated fiber glass column wraps could develop nearly the same ductile performance as the steel plate jackets.

Material properties are readily available from the manufacturers but there remained the issue of adequate quality control specifications for the field application. These early applications were rather crude, being hand laid in a similar manner as hanging wallpaper. It required some months to fully develop adequate quality control (QC) specifications so the materials tested in the laboratory could be replicated with confidence in the field. The application using epoxy impregnated fiber glass has been approved for two systems and field applications have been in place for over five years.

In 1993, following the end of the cold war and reduction of major aerospace and defense applications, the advanced composites industry began looking for applications of advanced composites in the civil infrastructure. The Caltrans-UCSD testing program was expanded to develop similar applications for the higher strength carbon fibers. This testing program has continued as more manufacturers submit their materials for approval and there are at least five systems approved for field application in California at this time. The carbon fibers are applied by automatic wrapping machines which wrap several 1/4 inch strands simultaneously and can fully wrap a typical four to six foot diameter, 20 foot long bridge column in two hours. Because of the higher strength to weight ratio these materials are very competitive with the steel shell retrofit technique, and they can be applied with much less heavy lifting equipment. The materials are much more resistant to corrosion than the steel jackets and they will require very little maintenance.

Working in cooperation with the University of California at San Diego research team and the ARPA and FHWA technology transfer programs we have been testing other applications of advanced composites in the seismic reinforcing of older bridges and in the construction of major bridge components and ultimately, a complete highway bridge designed for AASHTO loads. The first applications involve resin impregnated fiberglass or carbon sheets on non circular bridge members. These include the use of sheets to wrap and confine the spandrel columns and rib members on several arch bridges where it is difficult to access the locations with heavy equipment. The second application involves the use of small diameter carbon fiber tubes, constructed by the same technology as rocket bodies, for bridge girders. This application has been tested at the laboratory and design details are being developed for a bridge on the state highway system in southern California. The bridge will include deck units which are composed entirely of advanced composite materials and construction is scheduled for late Fall of 1997. The testing program for these bridge components has been underway at UC San Diego for over three years, under the ARPA grant.

## 2. Column Strengthening

The most widely used application of advanced composite materials for bridges in California and other states, to date, is the seismic strengthening of bridge columns to improve their ductile performance in an earthquake. However, there is a larger market for this technology in the simple repair and strengthening of columns which have deteriorated from corrosion. It is relatively easy to clean and repair these columns and encase them with the non-corrosive composite materials. This application will undoubtedly increase the life of the columns or piers. Three manufacturers have developed prefabricated resin impregnated-fiberglass shells which can also be used as the form for concrete in the repair process. Figure 1 illustrates the prefabricated fiberglass column shell which has been approved and can be used also for repair of piling below the water line.

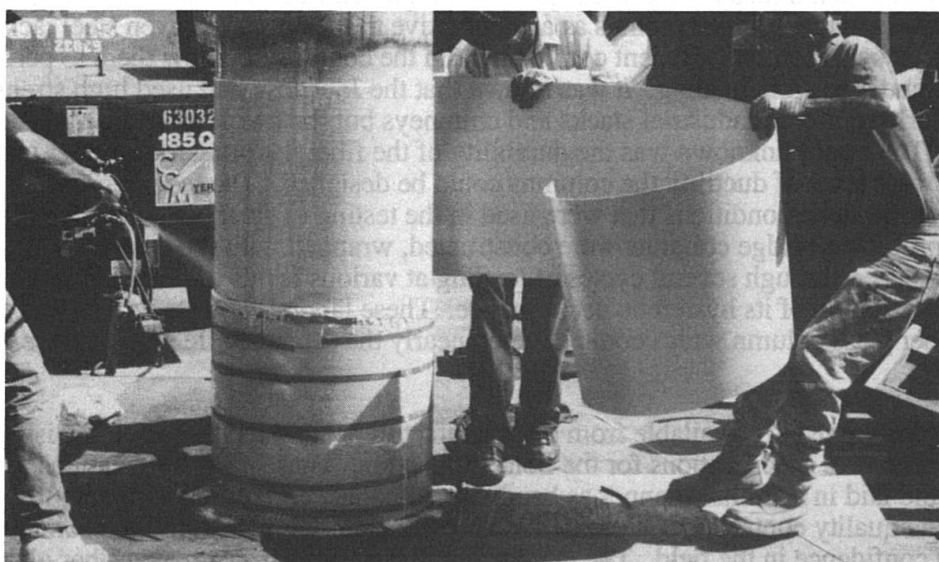


Figure 1 *Installing Prefabricated Fiberglass Shell*

Figure 2a) shows the clamping system utilized to hold the pre-fabricated shell tight until the adhesive cures. This system is the "Clockspring" system, utilizing an Isothalic Polyester resin. Several layers of shells are applied to provide the required ductility. Figure 2b) shows the installation of a full height prefabricated shell. This is the Du-Pont Hardcore system, utilizing a Vinylester resin. These applications were installed in 1996 on the Santa Monica Freeway, Interstate 10, in Los Angeles.

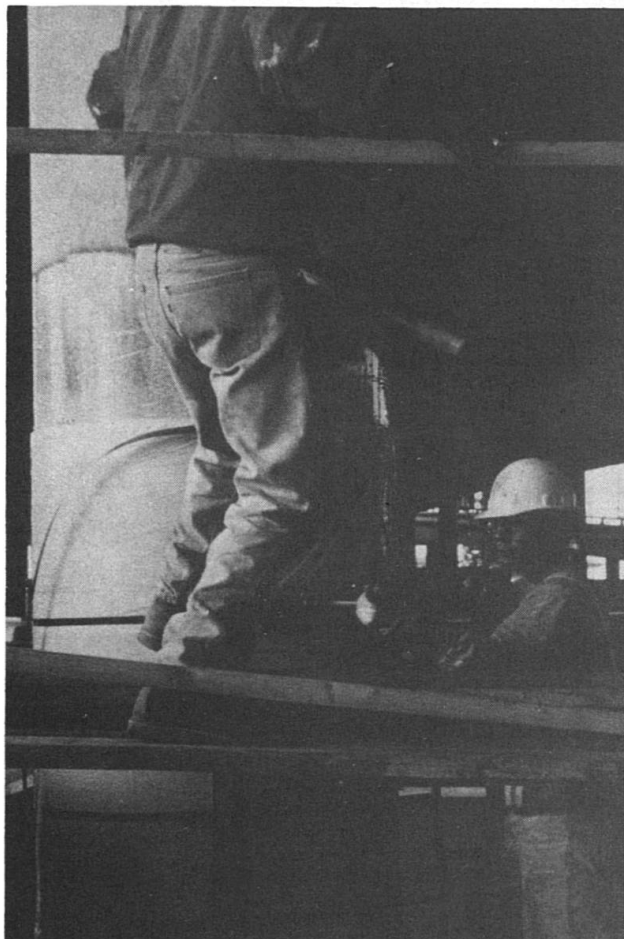


Figure 2 a) Clamping the Pre-Fabricated Shell In Place

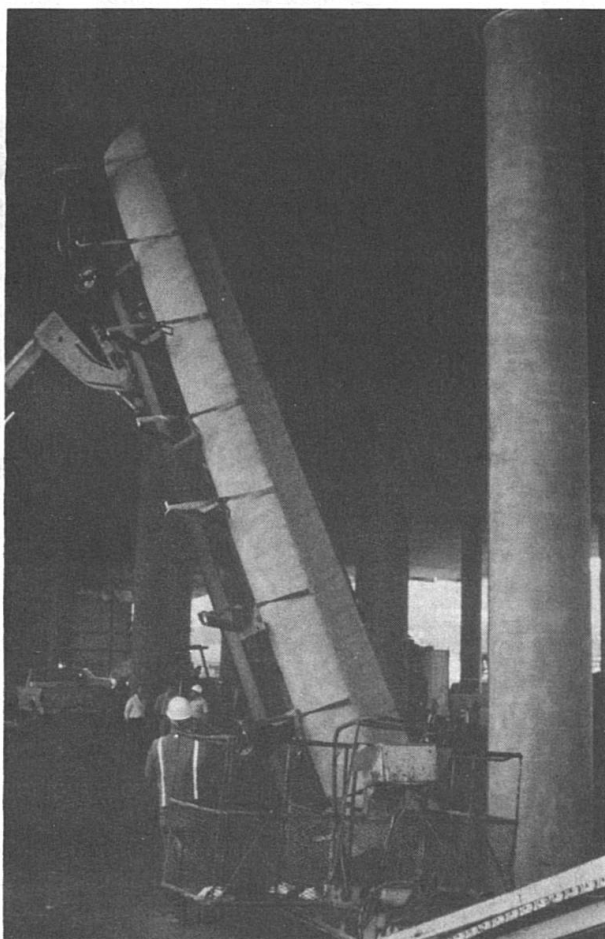


Figure 2b) Installing Full Height Shell

A third prefabricated system has been developed by NCF which utilizes several layers of four foot high single shells. The system, known as "Snaptite" is fabricated and heat cured on a mandrel under controlled curing conditions in the manufacturing plant and shipped to the field much the same as the two systems illustrated in figures 1 and 2. This system appears much less cumbersome to install than the other two prefabricated systems.

Figure 3 shows the use of epoxy-fiberglass as a confinement membrane to increase column ductility and toughness. This was the first application to be tested and approved in California. The material has been used for both circular and rectangular columns. The aspect ratio of the rectangular columns cannot be more than 2:1 or the longer face will buckle under dynamic loading and the needed confinement will not be maintained. This material can be applied as a pre-preg or dry application with the epoxy being applied in the field. One of the initial problems with these materials was uniformity of the final appearance because they are hand laid sheets about three feet wide. Final appearance is dependent on the expertise of the field crew. Attempts have been made to design a machine to improve the application and insure more uniformity, but we have not seen that machine in use in California yet. Careful quality control of the field application and material mixing is necessary to guarantee a quality final product. Figure 4 shows the same material after field

application and painting have been completed. The paint serves two functions; one is protection from ultra-violet light and the second is for aesthetics. The concrete colored paint does an excellent job for both functions. This application was implemented in 1991 on the Glendale Freeway (State Route 134) in Los Angeles. These materials had been tested at the UC San Diego Powell Laboratories in 1990 with excellent results. Both shear and moment ductilities of over eight (8) have been achieved in these tests.

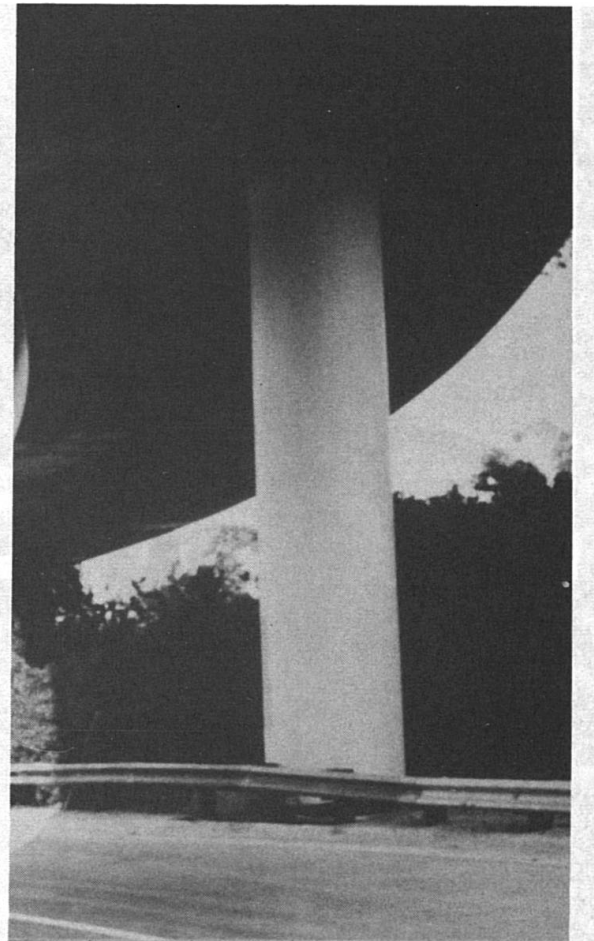


Figure 3 Epoxy-Fiberglass Column Wrap in Laboratory Test      Figure 4 Field Application

Figure 5 illustrates the application of pre-preg carbon fiber wrapping on bridge columns at the field test site. The wrapping machine does not require heavy lifting equipment and a later version now applies more strands simultaneously but can wrap a column of 20 foot height in two hours. The columns are heat cured under controlled conditions by electrically heated blankets or enclosures. The columns are painted concrete color for aesthetic purposes, but the coating does provide protection against the elements. This system has been developed by XXSys Technologies and a second, similar system is being tested by Mitsubishi Industries. The thickness can be varied as the ductility requirements dictate. In the field applications on the Santa Monica Freeway the white paint was also used for the same purposes as on the resin impregnated fiberglass wraps. Figure 6 shows the field application on a seismic retrofit project in San Diego. This material has the potential of becoming the most cost effective column wrapping system because of its high strength to weight ratio. The system does not require heavy lifting equipment and can generally compete favorably against the steel shell retrofit systems. Since it is not as labor intensive as some of the other systems being approved, it will ultimately be the system of choice for most contractors. The controlled heat curing system that is used by XXSys provides a material that is very reliable and has the best chance of guaranteeing the same properties as those of the laboratory samples. This reliability is more difficult to achieve with many of the other systems.

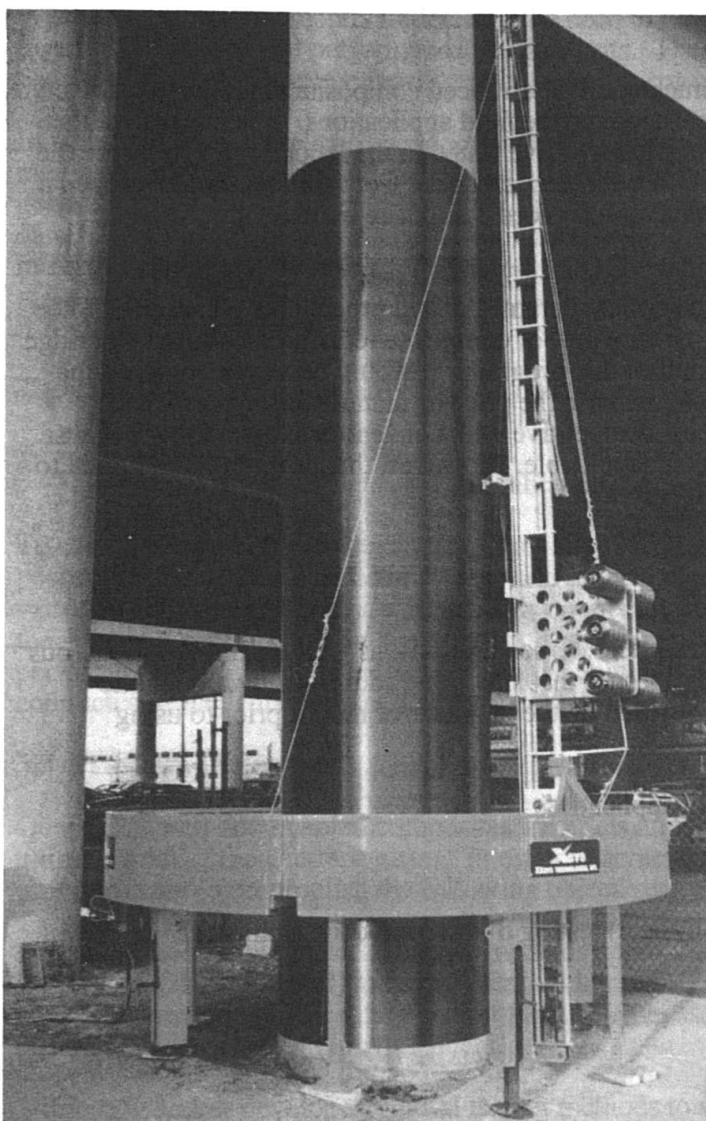


Figure 5 Application of Carbon Fiber ColumnWrap

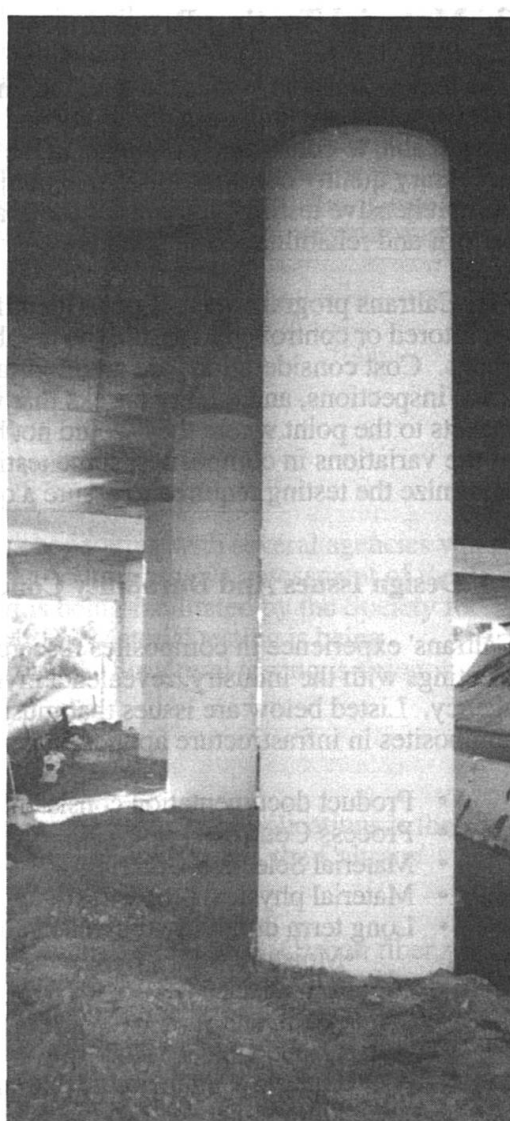


Figure 6 Completed Carbon Fiber Wrap

## 2. Strengthening Arch Ribs and Spandrel Columns

Analysis has shown that the typical arch bridge is extremely vulnerable to seismic forces in the transverse direction and, therefore, it is necessary to retrofit strengthen the main ribs and spandrel columns. Getting any type of erection and application equipment into these locations is very costly and difficult so Caltrans has developed retrofit solutions using carbon or fiberglass sheets. Portions of the arch ribs and the joint where spandrel columns frame into the ribs are being reinforced by wrapping with these sheets. Testing has also been conducted at UC San Diego to evaluate the various sheet systems over the past three years. Results show that the shear capacity increase and confinement can be achieved to the levels required. Full scale tests are being conducted during this summer (1997) on the column-rib joint to determine the material thickness needed to provide the required performance in a seismic event. Use of these materials on older arches is also important from a historical preservation perspective because the sheets do not significantly alter the appearance of the bridges.

Figure 5 shows the application of carbon fiber wraps to a bridge column. The wrap is being applied to the side of the column, and a worker is visible at the base of the column. The wrap is a thick, white material that covers the entire circumference of the column. Figure 6 shows the completed wrap, which appears as a smooth, white cylinder. The original concrete column is visible at the base and top of the wrap.

### 3. Material Testing Program

The major concerns associated with the implementation of advanced composite materials into the civil infrastructure are long term durability and consistency in the field applications. It is imperative that we are able to consistently replicate in the field what we have tested in the laboratory. To insure the necessary quality control Caltrans, in conjunction with the Aerospace Corporation, has developed a comprehensive testing program for the evaluation of advanced composite materials for seismic retrofit and rehabilitation of structures.

The Caltrans program was set up to identify the critical parameters and procedures which need to be monitored or controlled to assure the reliable performance of composite retrofitted columns or bridge decks. Cost considerations are an important part of this program. It would be very easy to define tests, inspections, and quality checks that would increase the price of manufacturing composite jackets to the point where they would not be cost competitive with conventional materials. Because of the variations in composites, some testing is unavoidable. However, this program is designed to minimize the testing required to assure a quality product.

#### 3.1 Design Issues And Durability Concerns

Caltrans' experience in composites research, trial field demonstrations, as well as through numerous meetings with the industry, revealed a myriad of issues that should be addressed by any public agency. Listed below are issues that must be verified by the engineer of record prior to using composites in infrastructure applications.

- Product documentation consistent with application
- Process Control
- Material Selection Criteria
- Material physical properties
- Long term durability (chemical and physical) testing of the composite against:
  - Moisture
  - Salt attack
  - Alkali attack
  - Ozone
  - High/low temperature extremes
  - Ultra violet
  - Other
- Quality control in manufacturing, mixing and applying
- Fiber content, voids, resin ratio
- Design guidelines for the specific composite
- Safety factors
- Damage and failure modes
- Adequate specifications
- Repeatability and consistency
- Acceptable field erection methods
- Effect of fatigue on bond behavior
- Performance under dynamic load
- Testing under sustained loading
- Qualifications of suppliers and product designers
- Cure temperature
- Transportation, handling
- Maintenance issues

Our experience has also revealed crucial issues that are unique to each fiber, resin, and equally important, the manufacturing process and application method. Composites material testing which was conducted by various research institutions show sensitivity to certain environmental factors and possible strength degradation. These results should not necessarily eliminate the use of composites

in infrastructure; they merely underscore the need to properly select all components of the composite to suit applications and performance requirements. These results further show the need for safety factors of such magnitude typically not common in conventional construction materials.

In addition to column retrofit concepts, some manufacturers have tested upgrading structural members, such as beams and slabs, using carbon fiber. However, only empirical data was generated, with no significant design or durability guidelines. Even though the industry is rich in data related to aerospace and marine applications, the data we need, relevant to civil engineering infrastructure applications, is very limited.

### **3.2 Program Overview**

The Caltrans program primarily focuses on two areas of applications:

- 1 - Seismic retrofit of bridges.
- 2 - Bridge strengthening and rehabilitation methods.

To ensure a sound objective technical evaluation, Caltrans is cooperating with several agencies which possess viable technologies, knowledge and tools to conduct a comprehensive assessment of the various systems under consideration. This cooperative effort is being facilitated by the Society for the Advancement of Material and Process Engineering (SAMPE). Material testing is being performed by the Aerospace Corporation (El Segundo, California). Structural testing is being conducted at the University of California at Irvine (UCI).

### **3.3 Program Objectives**

Qualifying well documented composites materials and processes for structural applications is the ultimate goal of the Caltrans effort. In order to achieve such level of confidence, the Caltrans' program is set to accomplish the following objectives:

- 1 -Identify acceptable material testing methods appropriate for each material type (Carbon fiber, E-Glass, S-Glass, Aramid) and consistent with intended applications. This item includes identifying environmental and physical factors that must be addressed. This objective has been accomplished through the pre-qualification document.
- 2 -Identify and/or develop structural testing methods to verify shear, confinement and flexural strength of the composite system. The goal is to develop test methods that are capable of demonstrating the structural performance of a given system, yet simple and inexpensive. This objective has been accomplished.
- 3 -Develop analysis and modeling techniques appropriate for the intended application. Such analysis should take into account the interaction between the composite material and the structure. Work in this area is in progress.
- 4 -Establish performance criteria for the various materials.
- 5 -Develop standard specifications and necessary special provisions for viable systems. These specifications should address material types, manufacturing process, mixing and curing, quality control, quality assurance and application methods. Where applicable, ASTM tests will be identified and used. Several projects have been advertised already. Specifications were developed for those contracts.
- 6 -Develop and adopt design guidelines taking into account environmental and physical factors. Current design guidelines incorporate environmental factor of safety. This factor will be re-examined at the conclusion of the program for any possible need to adjust.

### 3.4 Material Testing

Caltrans issued its pre-qualification requirements in April 1996 and later amended such requirements in January 1997. During the same period, Caltrans issued its Memo-to Designers, which states the conditions under which composite alternatives may be used. To help industry participants qualify, Caltrans is carrying out this program for qualifying composite jackets for seismic retrofit of bridge columns. The Aerospace Corporation is supporting Caltrans in the qualification program and is performing environmental durability qualification tests. Degradation of mechanical and physical properties of composite panels is being determined following exposure to various environmental conditions for periods up to 10,000 hours. Environmental exposures include 100% humidity at 100°F immersion in salt water, immersion in alkali solution, ultraviolet light, dry heat at 140°F, a freeze/thaw test, and immersion in diesel fuel. The effects of the environmental exposures are being quantified by measurements of the composite panel mass, tensile modulus, strength, and failure strain, interlaminar shear strength, and glass transition temperature. Property measurements are being made after exposure intervals of 1,000 hours, 3,000 hours and 10,000 hours to allow estimates of degradation over the projected service life. As of December 1996, property testing following the 1,000 hours and 3,000 hours exposure periods has been completed for three glass fiber/polymer resin systems and for four carbon fiber/polymer resin systems.

### 3.5 Structural Testing

All composite column casing systems are required to satisfy reduced scale cyclic column testing requirements to verify the casing constructability and effectiveness as a seismic retrofit measure. To qualify a system as an alternative column casing for seismic retrofit, a minimum of two types of retrofit enhancements must be demonstrated and tested in accordance with Caltrans requirements. Test results must satisfy Caltrans requirements relative to ductility performance, shear strength, and flexural enhancement. For each shape, cyclic tests must be conducted to demonstrate the performance of both retrofit enhancements and corresponding unretrofitted "As-Builts". Manufacturers may elect to qualify only one shape (circular or rectangular) by satisfying all tests requirements for either the circular tests or rectangular tests, thus limiting their qualifications to these systems.

For each geometrical shape, and for each corresponding enhancement, a minimum of one retrofitted "As-Built" column and one unretrofitted column shall be built and tested. For example, to qualify a system for circular column retrofit applications, the following four test specimens must be constructed and tested:

1. Circular Shear As-Built Column (Unretrofitted)
2. Circular Lap Splice As-Built Column (Unretrofitted)
3. Circular Shear Retrofitted Column subjected to double bending load
4. Circular Lap Splice Retrofitted Column subjected to single bending load.

All column details must conform to Caltrans requirements. Retrofit jacket thickness (or fiber ratio) must comply with the current Caltrans design criteria, with proper scaling factors when applicable, and shall satisfy the following:

1. Minimum confinement stress of 300 psi in the lap splice and/or plastic hinging zone
2. Maximum material elongation of 0.001 in/in in the lap splice zone and 0.004 in/in in the plastic hinging zone
3. Minimum confinement stress of 150 psi and material elongation of 0.004 must be maintained elsewhere in the column with appropriate transition
4. Minimum displacement ductility for the retrofitted column of 8 to 12 is to be expected.

An expected concrete strength of 5000 psi at the time of testing and Grade 60 reinforcing steel shall be used, although Grade 40 is preferable when available.

### 3.6 Summary Of Program Tasks

The following briefly summarizes tasks which are used to develop the information necessary to qualify vendors to wrap bridge columns with composites for the purpose of seismic retrofitting. All of the data will be cataloged and the program will be managed under one of the tasks. The proposed work includes an analysis of a variety of designs, materials and application techniques to determine the internal stresses in the composite and the strength of the jacket. Two of the tasks involve extensive testing of the composite materials, to fill holes in the database and, using materials from previously wrapped test columns, determine the effect of weathering/aging. Techniques and specifications will be defined under the quality assurance task to guarantee that the vendor's products are consistent and of sufficient quality to fulfill their function. Under the nondestructive evaluation task, techniques will be developed to verify the quality of the jacket as well as the health of the concrete itself.

#### Task 1: Analytical Design Verification - Modeling

**Objective:** Conduct analytical modeling of selected sub-scale tests and estimate a critical flaw size. Help develop a simplified guide for designing composite jackets.

**Deliverable:** Internal stress analysis of selected sub-scale tests and critical flaw size estimation.

#### Task 2: Composite Properties Characterization

**Objective:** Develop specific requirements for manufacturing and testing composite jackets. Identify limits (e.g., temperature and humidity) allowed during manufacture.

**Deliverables:** List of recommended test methods.  
Recommended manufacturing methods and placards.

#### Task 3: Reduced Scale Test Column Verification

**Objective:** Determine the quality of the wraps on the test specimens and the resolution of the nondestructive testing techniques.

**Deliverables:** Nondestructive evaluation maps of selected sub-scale columns both before and after testing.  
Comparison of test results to analytical models.

#### Task 4: Quality Assurance

**Objective:** Establish the basis for a plan to assure that composite retrofitted columns uniformly meet established performance requirements defined by Caltrans.

**Deliverables:** Define standard test procedures for incoming inspection and witness specimens.  
Specify/define minimum requirements for quality testing, e.g., number of witness specimens required.

#### Task 5: Non-Destructive Evaluation

**Objective:** Finalize and document column assessment techniques

**Deliverables:** Document the most effective NDE techniques.  
Demonstrate techniques on sub-scale columns.

#### Task 6: System Evaluation

**Objective:** Develop a manufacturing model to compare total costs of composite jackets with steel jackets.

**Deliverables:** Estimation of labor and material costs for composite jackets and steel jackets  
Life cycle cost estimates

**Task 7: Database Organization and Project Management**

**Objective:** Collect, assimilate, and store the generated data into a database. Manage tasks 1 through 6.

**Deliverables:** Management, schedule and cost reports  
Database generated by this and related programs including: material properties, NDE methods, manufacturing specifications, processes and modal studies.

Preliminary results are now available and are published in a report by Sultan of Caltrans and Steckel of Aerospace Corporation. More complete results will be available during the winter of 1997.

#### **4. Field Application Quality Control Specifications**

Caltrans has developed preliminary construction specifications to ensure quality control for the field applications of advanced composite materials. Separate specifications are available for the various materials but they are generic enough to allow the various vendors of each material to bid, assuming they have passed the qualification tests. Design guidelines are also available for determining the proper thickness of materials.

#### **5. Summary**

Caltrans has embarked on a program to utilize the advanced composite materials in seismic retrofit strengthening of bridge columns and other structural members. The goal is to increase the shear capacity and develop ductile performance in these members during a seismic event. It seems obvious that, in the current United States economy, these composite materials are not competitive with the more common bridge materials now being used, unless accurate life cycle costs are considered. We know the advantages of these advanced composite materials from the testing and field applications to date. We also know some of the obstacles to be overcome. These programs across the nation and especially the California program are designed to implement the use of these materials into the bridge and highway infrastructure as research and good engineering practice permit.

#### **References**

1. California Department of Transportation, Draft Special Provisions-Section 10-1.\_ Alternative Column Casing, June 1997
2. Priestley, M.J.N., Seible, F., and Calvi, G.M., "Seismic Design and Retrofit of Bridges" John Wiley & Sons, 1996, 686 pp.
3. Seible, F., "Advanced Composites for Bridge Infrastructure Rehabilitation and Renewal" International Conference on Composite Construction, Innsbruck, September 1997
4. Steckel, G.L., and Sultan, M., "Evaluating Advanced Composites For Application In Transportation Structures-A Program Overview" Second FHWA/Caltrans National Seismic Conference, Sacramento, CA, July 1997